

ULTRASONIC ABSORPTION IN  
SOLUTIONS OF PROTEINS AND PEPTIDES  
AND IN SUSPENSIONS OF LIPOSOMES

BY

PHILIP REED STROM-JENSEN

B.A., Pomona College, 1977

THESIS

Submitted in partial fulfillment of the requirements  
for the degree of Doctor of Philosophy in Biophysics  
in the Graduate College of the  
University of Illinois at Urbana-Champaign, 1983

Urbana, Illinois

## ACKNOWLEDGEMENT

The author would like to express gratitude to his adviser, professor Floyd Dunn, for suggesting the thesis topic and providing constant guidance and encouragement. Collaborative efforts of professor Richard Magin in studies on liposomes are also greatly appreciated. Thanks are due the following for assistance and helpful discussions in various phases of the work: Thomas Baldwin, Michael Borrelli, Robert Cicone, Joseph Cobb, David Duback, Wanda Elliott, Ronald Johnston, Valerie Maynard, Billy McNeil, Michael Niesman, and Robert White. Finally, the author wishes to thank his parents for their constant support throughout his educational career, and his wife, Lorrel, whose patience and suggestions sustained his progress in this project.

This work was supported by the following grants: 5 T32 CA09067 and CAL-1-20910-01 of the National Cancer Institute, DHHS; GM12281 of the National Institutes of Health; and 82-9 of the American Cancer Society, Illinois Division.

## TABLE OF CONTENTS

CHAPTER	
1	INTRODUCTION . . . . . 1
2	ACOUSTIC THEORY . . . . . 19
	2.1 WAVE PROPOGATION IN FLUIDS . . . . . 19
	2.2 THEORY OF THE CYLINDRICAL RESONATOR . . . . . 37
3	MATERIALS AND BIOCHEMICAL PREPARATIONS . . . . . 48
	3.1 MYOGLOBIN AND ITS DERIVATIVES . . . . . 48
	3.2 $\alpha$ -LACTALBUMIN . . . . . 53
	3.3 BACITRACIN . . . . . 55
	3.4 LIPOSOMES . . . . . 55
4	APPARATUS AND MEASUREMENT TECHNIQUES . . . . . 61
	4.1 CELL DESIGN . . . . . 61
	4.2 CELL ASSEMBLY AND DISASSEMBLY . . . . . 67
	4.3 CELL USE . . . . . 70
	4.4 DATA ACQUISITION AND CALCULATIONS . . . . . 78
	4.5 CELL PERFORMANCE AND ERROR ANALYSIS . . . . . 79
5	RESULTS AND DISCUSSION . . . . . 81
	5.1 ABSORPTION BY PROTEINS AND PEPTIDES . . . . . 81
	5.2 ULTRASONIC PROPERTIES OF LIPOSOMES . . . . . 110
6	CONCLUDING REMARKS . . . . . 133
	REFERENCES . . . . . 137
	VITA . . . . . 149

## CHAPTER 1

### INTRODUCTION

Ultrasound is presently an important tool in both diagnostic and therapeutic medicine. In both applications energy is transmitted into a body tissue by a wave process. Initially, the wave is in the form of mechanical energy, exhibiting, for example, pressure variations in time and space. As the wave propagates through the tissue, however, some of its energy is converted to heat through processes known collectively as absorptions, and deposited in the tissue. It is the aim of this investigation to pursue better understanding of the nature of energy transformation and absorption in tissues through the study of more elementary systems.

Aqueous solutions of biomolecules constitute such elementary systems since they lack the structural complexity of whole tissues. The ultrasonic properties of aqueous solutions of proteins and lipids presented in this study can be used to form models of absorption processes occurring in tissues. The study of such solutions has certain advantages. Environmental conditions, such as temperature, solvent composition and biomolecular concentration are easily controlled. This permits the isolation of certain ultrasonic phenomena for more detailed scrutiny and possibly better analysis. Also, measurement techniques can be employed which determine accurately the significant ultrasonic properties, *viz.*, velocity and absorption. Care must be taken, however,

in applying the deduced behavior of biomolecules in solution to the same molecules' behavior in situ. Nevertheless, the conclusions reached may be applied judiciously to the concerns of medical ultrasound.

The ultrasonic absorption coefficient (fully described in chapter 2) describes the extent to which sound energy is degraded to heat as a wave propagates through a medium. The absorption coefficients measured in soft tissues, such as liver, kidney, and brain, differ from each other by less than an order of magnitude (Dunn and O'Brien, 1978). It is reasonable, therefore, to suspect that similar mechanisms of absorption are involved in these tissues.

As an example of the magnitude of ultrasonic propagation properties, liver exhibits an absorption coefficient with an approximately linear frequency dependence in the medically relevant frequency range of 0.1 to 10 MHz. In this same frequency range the propagation velocity is close to that of a dilute salt solution. Pauly and Schwan (1971) investigated the origin of absorption in liver using tissue preparations in various degrees of structural integrity. They found that at least two thirds of the absorption in liver occurred at the level of constituent macromolecules. In particular, proteins were the primary contributors to absorption at the molecular level. Homogenization of various degrees resulted in a decrease in the absorption coefficient of twenty to thirty percent. As in whole liver, the frequency dependence was

roughly linear and so failed to yield clues that might lead to particular physical mechanisms of absorption.

Other molecular components have been found to contribute to the absorption in tissue to a lesser extent than the proteins. The absorption coefficient in fatty tissue is about half that in tissues such as liver (Dunn, 1975; Carstensen, 1979), and the presence of lipid containing red blood cell membranes accounts for only about ten percent of the total absorption in whole blood (Carstensen and Schwan, 1959a; Carstensen et al., 1953). Due to the lower specific absorption (absorption per unit weight) few ultrasonic measurements had been made on lipid systems until recently (Eggers and Funck, 1976; Mitaku et al., 1978,1981). Nucleic acids in aqueous solutions are characterized by a high specific absorption (Sturm et al., 1972), but do not cause an overwhelming contribution to the total absorption in tissue due to their scarcity relative to other molecular components. Approximate values of the specific absorption per wavelength for these materials are given in Table 1.1.

Table 1.1

Ultrasonic Absorption by some Cellular Components

Category	Specimen	$\alpha\lambda/c$ (ml/g)	Frequency (MHz)
Lipid	DPPC/DPPG (a) suspension	0.02	2
Protein	Hemoglobin (b)	0.024	2
DNA	calf thymus (c)	0.029	2.82

(a) this investigation

(b) O'Brien and Dunn, 1972

(c) Sturm et al., 1972

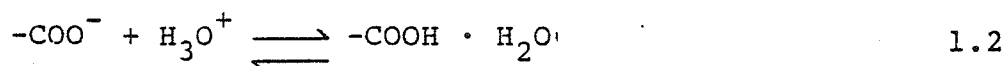
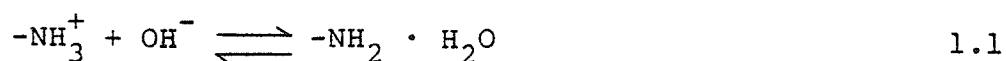
Early investigations of the ultrasonic properties of blood by Carstensen and coworkers also established the importance of proteins in determining ultrasonic absorption in biological systems (Carstensen *et al.*, 1953; Carstensen and Schwan, 1959b). These investigators varied specimen composition by resuspending red blood cells to selected volumes after centrifugation. The observed absorption was found to be linearly proportional to the protein content of the solution. In these same studies, aqueous solutions of hemoglobin and serum albumin exhibited specific absorption values which were linearly dependent upon the protein concentration. On the basis of this work attention has been given to the ultrasonic properties of proteins, and related compounds, in solution.

Amino acids, as the fundamental units of proteins, are appropriate subjects for study in attempting to understand the ultrasonic properties of protein solutions. Near neutral pH, aqueous solutions of amino acids exhibit an absorption only slightly greater than water itself. Accompanying the small absorption is an increase in the propagation velocity of the sound wave. These effects have been attributed to an alteration in the water structure caused by the amino acids (Hammes and Pace, 1968).

Absorption by amino acids can be considerably increased under conditions of low or high pH. Since amino acids exist as zwitterions, possessing amino and carboxyl groups capable of positive and negative ionization, respectively, they are

characterized by at least two pK values. Near these pK values an increased absorption coefficient is measured. It has been observed in glycine, for example, that a large increase in the absorption occurs in the vicinity of pH 11-12 where the  $\alpha$ -amino group titrates (Applegate *et al.*, 1968). An increase in absorption of glycine solutions has also been observed around pH 1 corresponding to titration of the  $\alpha$ -carboxyl group (Hussey and Edmonds, 1971a).

The anomolous absorption at these pH extremes has been treated theoretically as a relaxation process. In such a process, explained fully in chapter 2, energy is absorbed from the ultrasonic wave as its temperature or pressure fluctuations perturb an equilibrium. In the present case the perturbation affects the chemical equilibria represented in eqns. 1.1 and 1.2.



This mechanism is called proton transfer relaxation since the reactions involve the transfer of a proton from one molecular location to another. In addition to glycine, absorption maxima at high pH have been attributed to the reaction of eqn. 1.1 in solutions of serine and threonine (White *et al.*, 1971) and valine, leucine, isoleucine, alanine, phenlalanine and glutamic acid (Grimshaw *et al.*, 1973). The rates of the reactions in eqns. 1.1 and 1.2 determine characteristic relaxation frequencies. Measurements over a spectrum of



frequencies have characterized the reaction of eqn. 1.1 with relaxation frequencies in the range 5-15 MHz (Grimshaw *et al.*, 1973). The reaction of eqn. 1.2 is much faster and its relaxation frequency often falls near the upper limit of measurement but has been estimated from data on glycine to be between 80 and 160 MHz (Hussey and Edmonds, 1971a).

Ultrasonic measurements have also been made on the amino acids arginine and lysine which possess both  $\alpha$  and side chain amino groups (Hussey and Edmonds, 1971b). The theoretical analysis is necessarily more complex since interaction was possible between the two amino groups; a presumption of no interaction lead to an inadequate fit of the data. An optimal fit was obtained by assuming a degree of interaction somewhat less than total dependence (in which one reaction proceeds only at the termination of the other). The presence of intramolecular interactions in these simple molecules suggests the possibility of similar phenomena in more complex systems such as proteins.

Polyamino acids, being synthetic polymers of single amino acid residues, are model compounds for natural proteins. There is a definite influence on absorption by polymerization of amino acids. At neutral pH, poly-L-glutamic acid, for example, has a significantly higher absorption than an equal monomer concentration of glutamic acid (Dunn *et al.*, 1969). In addition to proton transfer, relaxational absorption may also be caused by solvation and helix-coil equilibria (Hammes and Roberts, 1969). As an example of the latter, polyglutamic

acid exhibits an increased absorption in the vicinity of pH 5-6 where it is known to undergo a helix-coil transition. Other studies have confirmed that this behavior is indeed due to a helix-coil relaxation rather than proton or ion transfer (Barksdale and Stuehr, 1972; Zana, 1972).

Similar experiments were conducted with polylysine, however, with the opposite conclusion resulting (Zana and Tondre, 1972a). Poly-L-lysine is known to undergo a helix-coil transition in the pH range 10-12. However, this is also the region in which amino groups are being titrated and thus some ambiguity is possible over the cause of an observed absorption increase in this pH range. Comparison was made to the pH dependent absorption in poly-D-L-lysine for which the helix-coil transition does not occur. Similar behavior of both polylysine isomers led to the conclusion that proton transfer relaxation was the dominant form of absorption. It is likely that the rate of the helix-coil transition is, in this case, too slow to cause appreciable absorption in the megahertz frequency range. However, while these investigators rejected relaxation absorption due to the helix-coil equilibrium, they considered the overall conformation of the polymer to have a measureable effect on its ultrasonic properties (Zana and Tondre, 1972b).

Natural proteins, as more complex structures, tend to present greater difficulties in interpretation of their ultrasonic behavior. The early work on blood prompted investigators to study other proteins in solution, most

extensively, hemoglobin. At present only about twelve different proteins have been studied ultrasonically in solution, due primarily to the large quantities required for most measurement techniques. Carstensen and Schwan found that the absorption in hemoglobin solutions was roughly independent of the species of origin and was linearly dependent on concentration up to 15 percent. Above that concentration the absorption increased at a greater than linear rate. (Goss and Dunn (1974) found absorption in bovine serum albumin (BSA) to depend on concentration to a power of 1.2.) Such behavior has been attributed to protein-protein interactions in solutions of BSA as well as hemoglobin (Kremkau, 1972). Later studies have extended the frequency range of measurement in the more dilute solutions of hemoglobin to span the interval 35 KHz to 1000 MHz (Edmonds et al., 1970; O'Brien and Dunn, 1972; Schneider et al., 1969). In all cases at least four discrete relaxation frequencies were necessary to fit the absorption spectrum. Such results indicate contributions from several absorption mechanisms or possibly a complex mechanism characterized by a distribution of relaxation frequencies.

Explaining the origin of these relaxation processes is a formidable task. The mechanisms generally suggested are the same as those cited for the polyamino acids (Kremkau, 1972). As might be expected, peaks in the absorption of most proteins occur at low and high pH extremes. In the cases of hemoglobin,  $\beta$ -lactoglobulin, and lysozyme, this behavior has been attributed to proton transfer equilibria occurring at

residues with high and low pK values (O'Brien and Dunn, 1972; Zana and Lang, 1970). Some disagreement has occurred over the application of this mechanism to BSA. Kessler and Dunn (1969) discovered a sharp increase in the absorption, as well as a minimum in the propagation velocity, around pH 4. They attributed this excess absorption to interaction of the sound wave with a structural transition in the albumin from the native state to a more expanded conformation. Zana and Lang (1970) preferred to attribute the low pH behavior to the proton transfer mechanism. As there is evidence to support both theories, no firm conclusion has been reached (Dunn and Kessler, 1970).

As well as the proton transfer theory provides an explanation for absorption in amino acids and proteins at pH extremes, it fails to do so under conditions close to physiological pH. Calculations of absorption due to proton exchange involving histidine (pK 6-7) and water show that this contributes insignificantly to overall absorption (Hussey and Edmonds, 1971a). Other mechanisms must therefore be involved.

The role of protein structure in ultrasonic absorption has been investigated for several proteins. This has particular application for conditions near neutral pH where contributions to the absorption by proton transfer with the solvent are theoretically negligible. Variation of solvent conditions can greatly alter the conformation of a protein. Yamanaka et al. (1978) examined the ultrasonic characteristics of lysozyme, a single chain enzyme possessing

four disulfide bonds. Upon denaturation with guanidine hydrochloride (GuHCl) absorption at 9 MHz increased. Subsequent reduction of the disulfide bonds with dithiothreitol caused a reduction in absorption to well below that in the native state. The increased absorption with denaturation may be related to an expansion of the molecule since the rate of this increase is in good agreement with the rate of structural change as measured by optical rotation.

The effect of GuHCl on hemoglobin has also been studied (O'Brien and Dunn, 1971). At low GuHCl concentrations hemoglobin exists in its native state of four non-covalently bonded peptide chains. As the concentration of GuHCl is raised, the hemoglobin molecule first splits into two compact dimers and at higher concentrations exists as four separate random coils. As in the case of polylysine there was little connection between the dynamics of the structural changes and the observed absorption. However the overall conformation had some effect as evidenced by the difference in absorption between the native molecule and the random coils present at high GuHCl concentration.

Lang *et al.* (1971) studied the effects of urea, formamide, dimethylformamide, dioxane, and ethylene glycol on solutions of BSA,  $\beta$ -lactoglobulin, and lysozyme. As with the case for hemoglobin in GuHCl, there was no convincing correlation between the absorption and the conformational equilibria. The majority of the absorption was attributed instead to various types of proton transfer equilibria. They

did believe, however, that while the excess absorption induced by the various solvents was not greatly affected by a conformational equilibrium, it was sensitive to the overall conformational state. This was supported by the difference in absorption between a solution at pH 7 (native protein) and a solution at pH 1 (unfolded protein). They suggest that a mechanism involving a protein-solvent interaction may have a different magnitude of effect depending upon the conformational state of the molecule.

Involvement of the hydrating water surrounding a protein as an absorption mechanism has been proposed in several ultrasonic studies of proteins (Dunn and O'Brien, 1978). That the structure of water is important in determining ultrasonic absorption has been shown by study of  $\text{GuHCl}$ , acetamide, sodium chloride, and ammonium chloride in water (Hammes and Swann, 1967). Each of these compounds decreases the ultrasonic absorption, presumably due to their tendency to decrease the structural order in liquid water.

Proteins, when dissolved in water, will accumulate a hydration shell of water molecules ordered in such a way as to constitute a separate phase from the bulk water (Dandliker and de Saussure, 1971). Through hydrophobic interactions with water, proteins are maintained in their native state, generally burying non-polar amino acids in their interior. Indeed, the water structure plays a crucial role in determining the conformation and activity of soluble enzymes. Ultrasonic absorption is thought to arise in this context

through a relaxation of the equilibrium between the bound, hydrating water and the bulk water. Perturbation of the hydrating water has been suggested as an absorption mechanism at neutral pH in the proteins hemoglobin (O'Brien and Dunn, 1972), BSA (Kessler and Dunn, 1969), and gelatin (Dunn and O'Brien, 1978). In most of these cases several relaxation frequencies were necessary to fit the data. Such behavior is expected from the structural relaxation of a hydration layer as various sites are subject to slightly different local environments. Perturbation of the water of hydration remains an important consideration among mechanisms possibly active at physiological pH.

A mechanism involving solvent-solute interactions is also supported in studies of non-protein, linear polymers. In particular, dextran (1-6 polyanhydroglucose) has been the subject of several studies. Hawley *et al.* (1965) found dextran to possess an absorption spectrum very similar to that of hemoglobin. Further study showed that the absorption increased with molecular weight from the monomer value and reached a plateau around 100 monomer units (Hawley and Dunn, 1969). These investigators suggested that this behavior might be explained by a coupling of the normal mode motion of the polymer chain to changes in the bound water structure. This speculation was substantiated in a more recent study by Kato *et al.* (1980). An excellent correlation was found between the relaxational absorption amplitude in dextran solutions and the degree of hydration as measured at various temperatures by

an independent method (Gekko and Noguchi, 1971). Similar mechanisms have been proposed in studies of polyethylene glycol (PEG) (Hammes and Lewis, 1966; Hammes and Schimmel, 1967; Kessler et al., 1970).

To this point, each of the absorption mechanisms discussed has involved an interaction of the solvent with the solute surface. Some studies support the notion that part of the absorption arises from phenomena occurring independent of the solvent, possibly in the interior of a globular molecule. White and Slutsky (1971, 1972) have developed a model in which proton transfer can occur at appreciable rates under physiological conditions by virtue of internal proton exchange between histidine and carboxyl residues. Proton exchange between such neighbors in hemoglobin was judged as significant if the residues were within 5 to 10  $\text{\AA}$  of each other. Estimating kinetic parameters from studies on O-aminobenzoic acid, White and Slutsky concluded that such internal proton exchange could make a significant contribution to the acoustic relaxation spectrum of hemoglobin near neutral pH.

Comparison of absorption in lysozyme and hemoglobin led Kanda et al. (1976) to the conclusion that the neutral pH absorption of these proteins is due to some bulk property of the molecules rather than a surface property. They suggest that this may involve a motion of amino acid side groups. Indeed, molecular motion between isomeric forms has been indicated as an absorption mechanism in other systems. For example, rotational isomers cause absorption in polystyrene



(Nomura et al., 1975), liquid alkanes (Cochran et al., 1972), and alkylammonium salts (Blandamer et al., 1968). Also, interchange between the axial and equatorial isomers of methylcyclohexane causes an absorption spectrum which can be fit by a single relaxation frequency (Piercy and Subrahmanyam, 1965). Based on these studies it is possible to propose that internal motion in a protein could contribute to the observed ultrasonic absorption.

From the forgoing discussion it is apparent that a complete understanding has not been reached regarding the cause of the relatively high absorption in proteinaceous solutions. The experiments undertaken in this investigation have been aimed at gaining a better understanding of the mechanisms of absorption by proteins at physiological conditions. To this end, study has been made on proteins and peptides which fall in a molecular weight range generally below those previously studied. This molecular weight range corresponds to that in which absorption is a strong function of molecular weight in the polymers dextran and PEG. In an analogous manner, some transition must occur between the low absorption of amino acids and the high absorption of proteins.

Results on the proteins and peptides in this study lend support for a mechanism involving perturbation of the hydration layer surrounding these molecules. Also, such a mechanism appears to make a greater contribution in the cases where the molecule exists more as a random coil than a compact globular protein. These conclusions are supported by the

molecular weight dependence of the absorption, and by the effect of phosphate ions on the absorption.

As mentioned above, few ultrasonic studies have been made on lipids. However, the importance of these systems, especially bilayer aqueous suspensions, as models for biological membranes has prompted several such studies recently. Hopefully, this line of inquiry will contribute to an understanding of the role that membranes play in absorption of ultrasound in tissue.

The types of lipids used to create model membranes are amphiphilic phospholipids, generally composed of two hydrocarbon chains attached to a glycerol backbone and a polar headgroup. When the phospholipids are suspended in water, lamellar structures are formed whose structures depend on the method of suspension. For example, when dipalmitoyl phosphatidylcholine (DPPC) is agitated by a vortex mixer in an aqueous carrier, multilamellar vesicles (MLVs) are formed. These consist of concentric phospholipid bilayers having diameters in the range 1-10  $\mu\text{m}$ . DPPC MLVs have been found to undergo a crystalline to liquid-crystalline phase transition at 41-42 $^{\circ}\text{C}$  (Chapman *et al.*, 1974). If a suspension of MLVs is irradiated with intense, cavitating ultrasound for 15 min to 1 hr, small unilamellar vesicles (SUVs) are formed, having diameters of 20-50 nm and are composed only of single bilayers. (The energy delivered by this ultrasound is more than  $10^6$  times as great as that used in the analytic experiments of this investigation and so their effects bear

virtually no similarity.) SUVs undergo a phase transition, but at 4-5°C lower than the phase change in MLVs of the same constituent phospholipids (Melchior and Steim, 1976). SUVs also exhibit a transition much broader in temperature than that for MLVs. In the present investigation, measurements have been made on large unilamellar vesicles (LUVs) having diameters in the range 0.1 to 0.4  $\mu\text{m}$  and whose method of preparation is described in chapter 3.

Of primary interest in most ultrasonic investigations of liposomes has been their behavior in the vicinity of the crystalline to liquid-crystalline phase transition. Measurements on MLVs and SUVs reveal a significant increase in ultrasonic absorption as the transition temperature is approached. The absorption per wavelength shows a temperature dependence for both of these types of liposomes which agrees qualitatively with calorimetric measurements. That is, a sharp (1-2°C half-width), tall peak for MLVs and a broad (5-7°C half-width), short (about 1/2 that in MLVs) peak in SUVs. In addition, the temperatures of peak absorption in MLVs and SUVs agree well with the transition temperatures measured calorimetrically. Evidently, the increase in absorption is directly related to some process occurring at the phase transition.

In order to study the ultrasonic properties of membrane bound proteins and to further elucidate the phenomena described in the preceding paragraph, measurements have been made (primarily of ultrasonic absorption) in this

investigation on LUVs of various compositions. The results indicate, as expected from calorimetry (Melchior and Steim, 1976), that the behavior of LUVs is very similar to that of MLVs. Incorporation of cholesterol into the bilayer of the liposomes tends to diminish the effect of the transition, also as expected from calorimetry. Pure lipid LUVs exhibit, near the transition temperature, a narrow distribution of relaxation frequencies centered at about 2.1 MHz. This is interpreted as a perturbation by the ultrasound of the equilibrium between trans and gauche bonds of the hydrocarbon chains. Incorporating the peptide gramicidin into the liposome bilayer, while having some effects in common with cholesterol, lowers the mean relaxation frequency from 2.1 MHz to 0.75 MHz. This is attributed to close, hydrophobic interactions of the gramicidin with adjacent phospholipids thus restricting the trans-gauche isomerization of the hydrocarbon chains.

The thesis is organized as follows. Chapter 2 presents the acoustic theory of propagation and absorption of sound in fluids. Also in this chapter is the theory of operation of a cylindrical resonator, the instrument used to make ultrasonic measurements in this study. Biochemical methods for preparation of the specimens under study are presented in chapter 3. Chapter 4 details the design and operation of the cylindrical resonator which was constructed for the purpose of this investigation. Results and their discussion are

presented in chapter 5. Chapter 6 concludes the thesis with a summary and speculations on future directions in the field.

CHAPTER 2  
ACOUSTIC THEORY

2.1 WAVE PROPOGATION IN FLUIDS

2.1.1 Basic Equations. The equations governing wave motion in fluids are derived from three fundamental equations: the equation of continuity, the equation of motion, and the equation of state. These equations are presented first in general form, and then simplified using approximations to facilitate their simultaneous solution. Further details of the solution can be found in Temkin (1981).

The continuity equation is based on the principle of conservation of mass. It is obtained by considering an arbitrary volume of fluid, fixed in space, and relating the change in mass within the volume to the mass flux through the surface enclosing the volume. The result is

$$\frac{\partial \rho}{\partial t} + \nabla \cdot (\rho \vec{u}) = 0 \quad 2.1$$

where  $\rho$  is the fluid density and  $\vec{u}$  is the particle velocity.

The equation of motion is an application of Newton's second law of motion to a volume of fluid. The volume is specified to move with a velocity such that it will always contain the same material elements. The equation derived in this way is

$$\rho \frac{D\vec{u}}{Dt} = \rho \vec{F} + \nabla \cdot \vec{\sigma} \quad 2.2$$

The notation  $D/Dt$ , known as the material derivative, is used instead of the the conventional symbol since the frame of

reference moves with the fluid. The quantity  $\vec{F}$  represents all of the body forces acting on the volume, including gravity, and  $\nabla \cdot \vec{\sigma}$  represents the surface forces resulting from the local stress,  $\vec{\sigma}$ .

As can be shown from thermodynamics, it is possible to specify the physical state of the system with two independent variables. For the purpose of this development the pressure,  $p$ , is written as a function of the density,  $\rho$ , and the entropy,  $s$ .

$$p = p(\rho, s) \quad 2.3$$

The particular form of this function depends on the system under consideration.

The form of the equation of state is quite simple for an ideal fluid, since there is no viscosity or heat conduction and all changes occur adiabatically so that  $Ds/Dt=0$ . From eqn. 2.3

$$dp = \left(\frac{\partial p}{\partial \rho}\right)_s d\rho + \left(\frac{\partial p}{\partial s}\right)_\rho ds \quad 2.4$$

$$\frac{Dp}{Dt} = \left(\frac{\partial p}{\partial \rho}\right)_s \frac{D\rho}{Dt} + \left(\frac{\partial p}{\partial s}\right)_\rho \frac{Ds}{Dt} = \left(\frac{\partial p}{\partial \rho}\right)_s \frac{D\rho}{Dt} \quad 2.5$$

If the adiabatic compressibility is defined as

$$K_s = -\frac{1}{v} \left(\frac{\partial v}{\partial p}\right)_s \quad 2.6$$

where  $v=1/\rho$  is the specific molar volume, then

$$\left(\frac{\partial p}{\partial \rho}\right)_s = \frac{1}{\rho K_s} \quad 2.7$$

and the equation of state is

$$\frac{Dp}{Dt} = \frac{1}{\rho K_s} \frac{D\rho}{Dt} \quad 2.8$$

It is apparent that in an ideal fluid the pressure changes occur in phase with density changes.

The consideration of an ideal fluid allows some simplification of eqn. 2.2. In such a fluid there are no tangential stresses on a fluid element. Thus, the stress tensor can be expressed simply as a diagonal matrix whose non-zero elements are equal to the negative of the mechanical pressure. Equation 2.2 then becomes

$$\rho \frac{D\vec{u}}{Dt} = \rho \vec{F} - \nabla p \quad 2.9$$

The three equations can be combined, to eliminate  $u$  or  $p$ , if approximations, known collectively as linearization, are made. These approximations assume that the changes in  $u$  and  $p$  due to an acoustic wave are small so that all terms of second order or higher in these parameters can be ignored. The resulting linearized constitutive equations for an ideal fluid are

$$\frac{\partial \rho}{\partial t} + \rho_0 \nabla \cdot \vec{u} = 0 \quad 2.10$$

$$\rho_0 \frac{\partial \vec{u}}{\partial t} = -\nabla p \quad 2.11$$

$$\frac{\partial p}{\partial t} = \frac{1}{\rho_0 K_s} \frac{\partial \rho}{\partial t} \quad 2.12$$



where  $\rho_0$  is the undisturbed density of the medium and  $p$  now represents the change in pressure from that at equilibrium, i.e., the acoustic pressure.

**2.1.2 Wave Equation in an Ideal Fluid.** Equations 2.10 and 2.12 can be combined to give

$$\rho_0 K_s \frac{\partial p}{\partial t} + \rho_0 \nabla \cdot \vec{u} = 0 \quad 2.13$$

Taking the spatial derivative of eqn. 2.11 and the time derivative of eqn. 2.13 yields, respectively,

$$\rho_0 \nabla \cdot \frac{\partial \vec{u}}{\partial t} = -\nabla^2 p \quad 2.14$$

$$\rho_0 K_s \frac{\partial^2 p}{\partial t^2} + \rho_0 \nabla \cdot \frac{\partial \vec{u}}{\partial t} = 0 \quad 2.15$$

which, upon combination, give

$$\frac{\partial^2 p}{\partial t^2} = \frac{1}{\rho_0 K_s} \nabla^2 p \quad 2.16$$

This is the acoustic wave equation for an ideal fluid having a propagation velocity  $c = (1/\rho_0 K_s)^{1/2}$ . Since most of the work discussed in this thesis deals with plane, longitudinal waves, the simpler case of a one-dimensional equation will be adequate, i.e.,

$$\frac{\partial^2 p}{\partial t^2} = \frac{1}{\rho_0 K_s} \frac{\partial^2 p}{\partial x^2} \quad 2.17$$

where changes in the pressure, and other acoustic parameters, occur only in the  $x$  direction. An appropriate particular solution to eqn. 2.17 is that of a sinusoidal wave propagating in the  $+x$ -direction.

$$p = p e^{i(kx - \omega t)}$$

2.18

where  $P$  is the pressure amplitude,  $k$  is the wave constant,  $2\pi/\lambda$ ,  $\omega$  is the angular frequency,  $ck=2\pi f$ , and  $f$  is the frequency. Thus, the wave is periodic in time and space and, for the ideal lossless fluid, maintains a constant amplitude.

2.1.3 Classical Absorption Mechanisms. Real media for the propagation of sound are not ideal and, as such, are not described completely by the preceding analysis. In particular, sound does not travel through real media with a constant pressure amplitude. This effect is known as attenuation. Attenuation describes the decrease in the amplitude of the wave as it propagates, irrespective of the mechanism. The mechanisms of attenuation fall into two categories: redirection of the wave out of its original propagation direction, and absorption of the sound wave in the body of the propagating medium. Absorption refers to any process by which the acoustic energy contained in the periodic condensations and rarefactions is degraded to heat. As absorption constitutes the primary contribution to the attenuation in the specimens of this investigation, the mechanisms of absorption are discussed in some depth.

In the ideal fluid the properties of viscosity and thermal conductivity, present in all real fluids, were ignored. Each of these properties makes a contribution to the absorption which occurs in real fluids. When the constitutive equations are written to include the effects of viscosity and

heat conduction, the results, after linearization are, respectively, (Temkin, 1981)

$$\frac{\partial \rho}{\partial t} + \rho_0 \nabla \cdot \vec{u} = 0 \quad 2.19$$

$$\rho_0 \frac{\partial \vec{u}}{\partial t} + \nabla p = \mu \nabla^2 \vec{u} + (\mu_v + \mu/3) \nabla (\nabla \cdot \vec{u}) \quad 2.20$$

$$\rho_0 T_0 \frac{Ds}{Dt} = \rho_0 c_p \frac{DT}{Dt} - T_0 \beta \frac{Dp}{Dt} = k_0 \nabla^2 T \quad 2.21$$

$$\frac{Dp}{Dt} = c_0^2 \frac{D\rho}{Dt} + \left( \frac{\partial p}{\partial s} \right)_\rho \frac{Ds}{Dt} \quad 2.22$$

where the subscript zero refers to equilibrium values and  $\mu$  is the coefficient of shear viscosity,  $\mu_v$  is the coefficient of volume viscosity,  $T$  is the absolute temperature,  $c_p$  is the specific heat at constant pressure,  $\beta$  is the coefficient of thermal expansion,  $k_0$  is the coefficient of thermal conductivity, and  $c_0$  is the ideal propagation velocity. For an understanding of the effects of viscosity and thermal conductivity on wave propagation, the one dimensional equations are solved, first considering viscosity only, and then incorporating thermal conductivity.

To consider only the effects of viscosity,  $k_0$  is set equal to zero. As a result, entropy is conserved and eqn. 2.22 can be written as

$$\frac{\partial p}{\partial t} = c_0^2 \frac{\partial \rho}{\partial t} \quad 2.23$$

Combining this with eqn. 2.19 yields

$$\frac{\partial p}{\partial t} + \rho_0 c_0^2 \frac{\partial u}{\partial x} \quad 2.24$$

Equation 2.20, which is a form of the Navier-Stokes equation, can be written as

$$\rho_0 \frac{\partial u}{\partial t} + \frac{\partial p}{\partial x} = \frac{4}{3} \mu' \frac{\partial^2 u}{\partial x^2} \quad 2.25$$

where  $\mu' = \mu(1 + 3\mu_v/4\mu)$ . Combining the time derivative of eqn. 2.24 and the space derivative of eqn. 2.25 and eliminating  $u$  gives

$$\frac{\partial^2 p}{\partial t^2} = c_0^2 \left(1 + \frac{4}{3} \frac{v}{c_0} \frac{\partial}{\partial t}\right) \frac{\partial^2 p}{\partial x^2} \quad 2.26$$

where  $v$  is  $\mu'/\rho_0$ . A steady state solution to this equation for waves travelling in the +  $x$ -direction can be written as

$$p = P e^{i(Kx - \omega t)} \quad 2.27$$

where  $K$  is, in general, complex and can therefore be written as

$$K = k + i\alpha \quad 2.28$$

Using this harmonic solution in eqn. 2.26 yields

$$K^2 = \frac{(\omega/c_0)^2}{1 - i \frac{4}{3} (\omega v/c_0)^2} \quad 2.29$$

Equation 2.27 thus has the form

$$p = P e^{-\alpha x} e^{i(kx - \omega t)} \quad 2.30$$

where the quantity  $\alpha$  will here be called the absorption coefficient which describes an exponential decay of the amplitude as the wave propagates in the +  $x$ -direction. The viscous medium, therefore, supports a damped harmonic wave.

Dispersion, a frequency dependence of the phase velocity of the wave, will also occur since the value of  $k$  is frequency dependent, cf., eqn. 2.29. These two effects, viz., dispersion and absorption, relate to the real and imaginary parts of the complex wave constant, respectively. To obtain quantitative relations describing the dispersion and attenuation, the real and imaginary parts of eqns. 2.28 and 2.29 are set equal to each other, and yield

$$\left(\frac{\alpha c_0}{\omega}\right)^2 = \frac{1}{2} \left\{ \frac{1}{(1 + \omega^2 \tau_v^2)^{1/2}} - \frac{1}{1 + \omega^2 \tau_v^2} \right\} \quad 2.31$$

$$\left(\frac{k c_0}{\omega}\right)^2 = \frac{1}{2} \left\{ \frac{1}{(1 + \omega^2 \tau_v^2)^{1/2}} + \frac{1}{1 + \omega^2 \tau_v^2} \right\} \quad 2.32$$

where  $\tau_v = 4\nu/3c_0^2$ . The quantity  $\tau_v$  is known as the viscous relaxation time. Its meaning can best be understood by examining the product  $\omega\tau_v$ , which is a measure of the rate of momentum transfer in the real fluid as compared with that in the ideal fluid. Thus, when viscosity is included, the propagation velocity increases due to an increased momentum transfer rate.

At the ultrasonic frequencies employed in this investigation, the quantity  $(\omega\tau_v)^2$  is much less than one and incorporation of this approximation into eqn. 2.31 yields

$$\alpha \approx \frac{\omega^2 \tau_v}{2c_0} = \frac{2}{3} \frac{\omega^2 \nu}{c_0^3} \quad 2.33$$

viz., the viscous contribution to classical absorption.

If the finite thermal conductivity of the medium is included as a loss mechanism, the development of a solution

proceeds in much the same manner as for viscous effects occurring alone and results in an analogous relaxation time for the thermal conductivity. Again, it is sufficient to suppose that a harmonic solution with a complex wave constant,  $K$ , adequately describes the situation. The relation between  $K$  and the physical parameters is then given by

$$K_n^2 = \frac{(1 + i\gamma\omega\tau_K K_n^2)(1 + i\omega\tau_V K_n^2)}{(1 + i\omega\tau_K K_n^2)} \quad 2.34$$

where  $K_n$  is  $Kc/\omega$ , and  $\gamma$  is  $c_p/c_v$ ,  $\tau_K = k_0/\rho c_0^2 c_p$  is the thermal relaxation time, and  $c_p$  is the specific heat at constant pressure. It is clear from eqn. 2.34 that when viscosity and thermal conductivity are not included,  $\tau_V$  and  $\tau_K$  are zero, and  $K$  is one. Generally the absorption due to viscosity and thermal conductivity in fluids is very small and  $\alpha \ll k$ . This allows an approximation in which  $K_n$ , on the right hand side of eqn. 2.34., can be given a value of one. The resulting equation is

$$K_n^2 \approx \frac{(1 + i\gamma\omega\tau_K)(1 + i\omega\tau_V)(1 - i\omega\tau_K)}{1 + \omega^2\tau_K^2} \quad 2.35$$

The same order of approximation is made if terms of order higher than  $\omega\tau$  are ignored. In this case, the relation for  $K_n$  reduces to

$$K_n \approx 1 + \frac{1}{2} i\{(\gamma - 1)\omega\tau_K + \omega\tau_V\} \quad 2.36$$

Since  $\alpha c_0/\omega = \text{Im}(K_n)$ , the absorption coefficient is

$$\alpha = \frac{\omega}{2c_0} \{(\gamma - 1)\omega\tau_K + \omega\tau_V\} \quad 2.37$$

This is known as the classical absorption coefficient and it is important to note several of its characteristic features. Since the assumption has been made that  $\omega\tau$  is small compared to unity, eqn. 2.37 is applicable only in a frequency range where the period of the wave is long compared to the viscous and thermal relaxation times. This condition exists for most fluids below a frequency of 1 GHz, and applies, in particular, to all the experiments described in this investigation. Thus, the absorption coefficient is seen from eqn. 2.37 to vary as the square of the frequency. This classical theory is in agreement with empirical values for the absorption coefficient in monatomic fluids. As part of the approximations for the solution, it was implicitly assumed that the contributions to the absorption by viscosity and thermal conductivity were additive. Based on the agreement of experimental and theoretical results, there is a negligible interaction between these two mechanisms and the assumption of additivity is correct.

Measurements on more complex fluids indicate that the absorption coefficient is greater than that predicted by the classical theory. Water, for example, exhibits an absorption coefficient proportional to the square of the frequency, as expected from the classical equation, but with a magnitude approximately three times that expected from the classical theory (Kinsler & Frey, 1962). This discrepancy has been attributed to a perturbation by the sound wave <sup>on</sup> of the water structure and intermolecular hydrogen bonds. This

perturbation causes an absorption in addition to the classical contribution. Since it is modelled by incorporating into the system other relaxing elements, such anomolous absorption is referred to as relaxational absorption. Some of these relaxation processes occur at experimentally attainable frequencies, while others, like the classical mechanisms, occur well beyond this frequency range. In the case of water, the relaxation frequencies characterizing the structural equilibrium are above the experimentally accesable range.

2.1.4 Relaxational Absorption Mechanisms. Relaxational absorption will occur whenever a physical or chemical equilibrium exists which can be perturbed by a change in environmental conditions, such as pressure or temperature. In the simplest case, the equilibrium can be formulated as



This is a reaction in which the states, A and B, can be interpreted in the most general sense, for example, as the reactant and product in a simple chemical equilibrium, or as two structural states in a physical rearrangement equilibrium. Here,  $k_f$  and  $k_b$  are the forward and backward rate constants, respectively.

The linear rate equation governing such a reaction is

$$-\frac{dc_A}{dt} = \frac{dc_B}{dt} = k_f c_A - k_c c_B \quad 2.39$$



where  $c_A$  and  $c_B$  are the concentrations of particular states A and B, respectively. This has the solution, for small perturbations from equilibrium (Eigen & deMaeyer, 1963)

$$x = x_0 e^{-t/\tau} \quad ; \quad 1/\tau = k_f + k_b \quad 2.40$$

where  $x$  is the difference between the instantaneous concentration and a new equilibrium concentration. The value of  $x_0$  is the same difference at the onset of the perturbation. Thus, if a static perturbation is imposed, the system will approach a new equilibrium state exponentially with time constant,  $\tau$ .

In general, if the time course of the perturbation is given by a forcing function,  $f(t)$ , then the response of the system parameter,  $x$ , can be written as (Ilgenfritz, 1977)

$$x(t) = \frac{e^{-t/\tau}}{\tau} \int_0^t e^{t'/\tau} f(t') dt' \quad 2.41$$

When  $f(t)$  is the harmonic function  $Ge^{i\omega t}$ , then the solution of the integral is

$$x(t) = \frac{Ge^{i\omega t}}{1 + i\omega\tau} = f(t) \frac{1}{1 + i\omega\tau} \quad 2.42$$

and the quantity  $1/(1+i\omega\tau)$  is in the form of a transfer function, here denoted by  $F$ , as

$$F = F_{\text{real}} + F_{\text{imag}} = \frac{1}{1 + \omega^2\tau^2} + i \frac{-\omega\tau}{1 + \omega^2\tau^2} \quad 2.43$$

Following the development by Eigen and deMaeyer (1963), it is possible to write the wave equation as in eqn. 2.17,

provided the adiabatic compressibility can be complex and written as

$$K_S = K_S^\infty + K_S' F \quad 2.44$$

where  $K_S'$  is complex and corresponds to the portion relating to effects of the reaction in eqn. 2.38.  $K_S^\infty$  is real and corresponds to relaxations occurring at frequencies much greater than those under consideration as in this investigation. This implies a complex propagation velocity, expressed as follows.

$$\frac{1}{c} = \frac{1}{c_{re}} - \frac{i\alpha}{\omega} \quad 2.45$$

Here  $c_{re}$  is the real phase velocity and  $\alpha$  is the absorption coefficient. The relation between  $K_S$  and  $\alpha$  is, since  $c = (\rho_0 K_S)^{1/2}$ ,

$$\rho_0 K_S = \left\{ \left( \frac{1}{c_{re}} \right)^2 - \left( \frac{\alpha}{\omega} \right)^2 \right\} - i \left( \frac{2\alpha}{\omega c_{re}} \right) \quad 2.46$$

The real and imaginary parts of  $K_S$  are related to the velocity and absorption as

$$c_{re}^2 = \frac{-2 \operatorname{Re}(K_S)}{\rho \left[ \operatorname{Im}(K_S)^2 \right] \left\{ 1 - \left[ 1 + \left( \operatorname{Im}(K_S) / \operatorname{Re}(K_S) \right)^2 \right]^{1/2} \right\}} \quad 2.47$$

$$\frac{\alpha c_{re}}{\omega} = \frac{\operatorname{Re}(K_S)}{\operatorname{Im}(K_S) \left\{ 1 - \left[ 1 + \left( \operatorname{Im}(K_S) / \operatorname{Re}(K_S) \right)^2 \right]^{1/2} \right\}} \quad 2.48$$

If the assumption is made that the imaginary part of  $K_S$ , i.e. the contribution from the reaction of eqn. 2.38, is small compared to the real part of  $K_S$ , then

$$c_{re} \approx [\rho \text{Re}(K_s)]^{1/2} \quad 2.49$$

$$\frac{\alpha c_{re}}{\omega} \approx -\frac{1}{2} [\text{Im}(K_s) / \text{Re}(K_s)] \quad 2.50$$

which results in

$$c_{re} \approx (\rho_0 K_s^\infty)^{-1/2} \left\{ 1 - \frac{K'_s}{2K_s^\infty} \cdot \frac{1}{1 + \omega^2 \tau^2} \right\} \quad 2.51$$

$$\frac{\alpha c_{re}}{\omega} = \frac{K'_s}{2K_s^\infty} \frac{\omega \tau}{1 + \omega^2 \tau^2} \quad 2.52$$

Equation 2.52 expresses the frequency dependent absorption due to the reaction of eqn. 2.38. When this absorption is assumed to be algebraically additive to the classical absorption, which is always present, eqn. 2.52 becomes the more commonly seen form, *viz.*, the absorption per wavelength,

$$\alpha \lambda = \frac{A \omega \tau}{1 + \omega^2 \tau^2} + B \omega \quad 2.53$$

where A and B are amplitude coefficients for the relaxational and classical absorption processes, respectively. This can also be written in terms of the real frequency, f, and the relaxation frequency,  $f_r = 1/2 \pi \tau$ , as

$$\frac{\alpha}{f^2} = \frac{A' \tau}{1 + (f/f_r)^2} + B' \quad 2.54$$

where  $A' = A/2 \pi c$  and  $B' = B/2 \pi c$ . Figure 2.1 is a graphical representation of eqn. 2.53, where A is one and B is zero. Note that a maximum in the absorption per wavelength occurs at the relaxation frequency. The width of this spectrum is determined by the form of eqn. 2.53 and spans about one decade

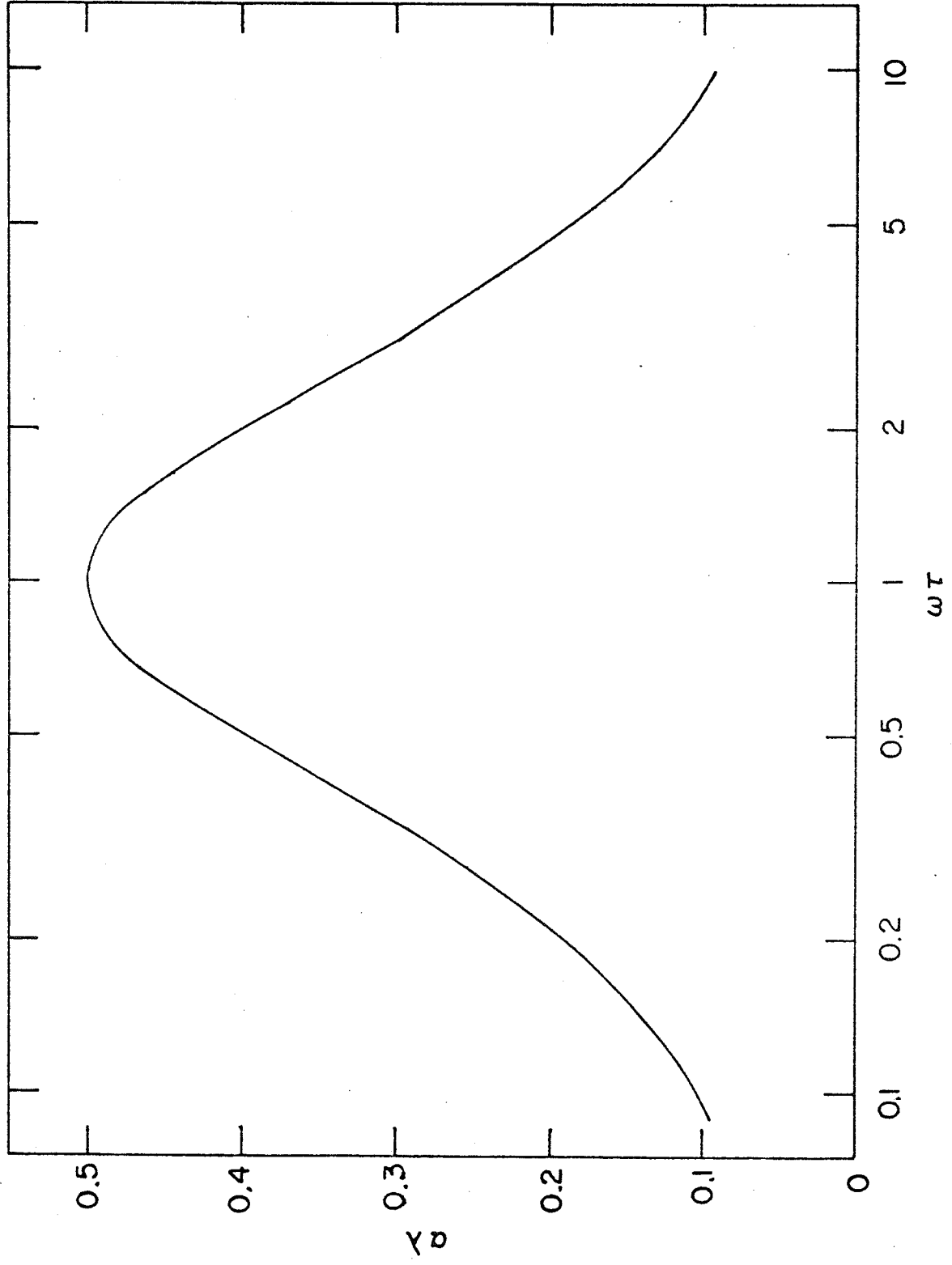


Figure 2.1 Theoretical absorption per wavelength due to single relaxation process.

in frequency at half maximum. The parameter  $\alpha/f^2$  is plotted in Figs. 2.2 and 2.3 where  $A'\tau$  is one and  $B'$  is zero. In the double logarithmic presentation, the curve decreases monotonically with a limiting slope of -2 at high frequency. The appearance of the same parameter in a semi-logarithmic plot is rather different, levelling off at high frequencies. Such levelling off occurs in a semi-logarithmic plot regardless of the  $B'$  value and is only seen in a double logarithmic plot if  $B'$  is comparable in magnitude to  $A'\tau$ .

The sigmoidal shape in Fig. 2.3 is suggestive of the manner in which relaxational absorption takes place. As a wave propagates through a fluid, all of its energy is initially in a mechanical form, i.e., the kinetic and potential energy of the vibrating, compressed fluid particles. When relaxational absorption occurs, there is a flow of energy from the mechanical mode to the internal energy of whatever equilibrium is being perturbed by the variations in pressure or temperature. This flow of energy will be significant when the period of the wave is on the order of or longer than the time required for the perturbed process to relax to a new equilibrium. Thus, the sound wave cannot cause a change which would not also occur by a static change in pressure or temperature, and no energy transfer will occur if the frequency of the perturbations is too great (Herzfeld & Litovitz, 1959).

In the case that eqn. 2.38 specifies a chemical reaction characterized by an enthalpy change,  $\Delta H$ , and a volume change,

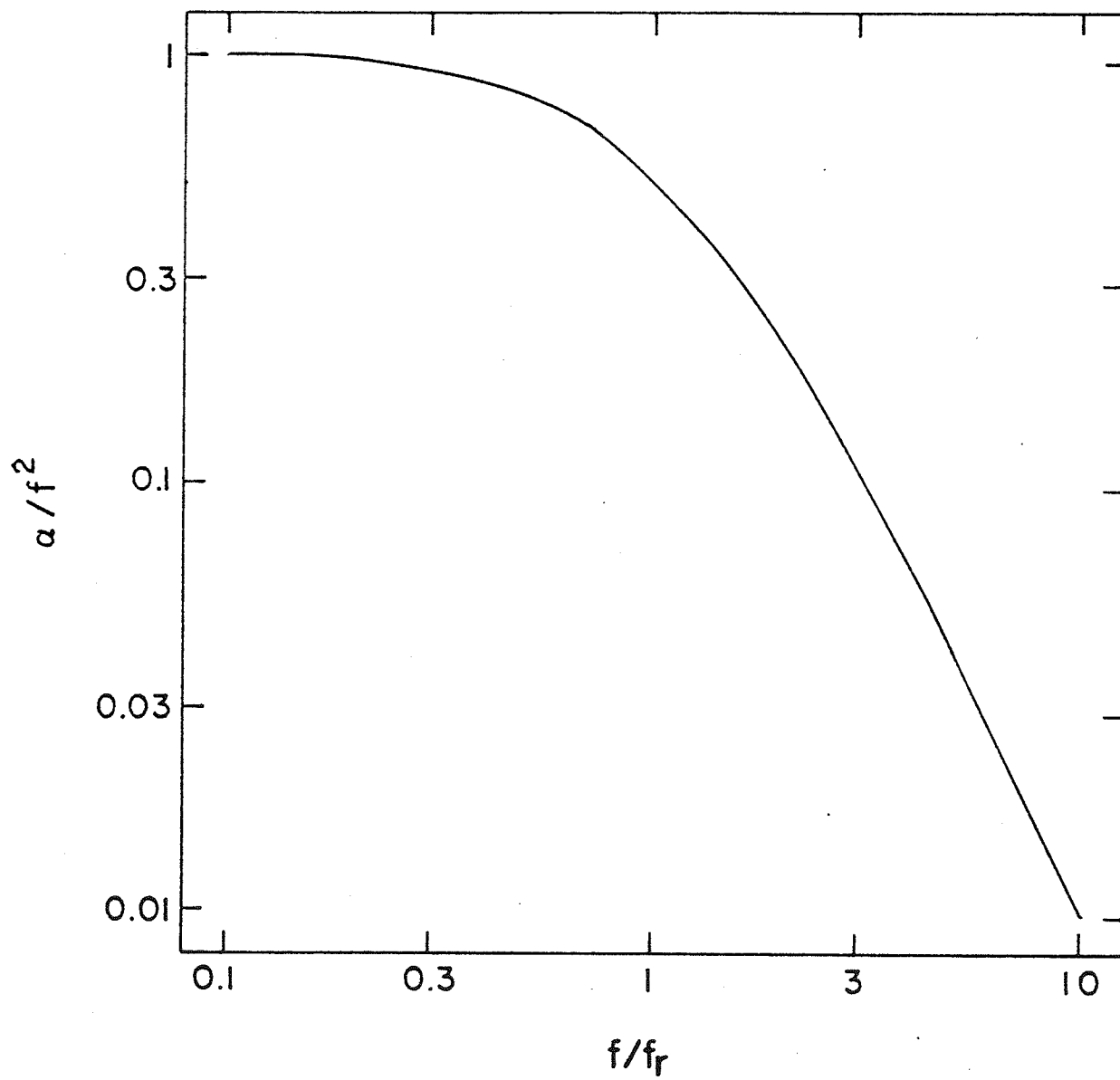


Figure 2.2 Theoretical frequency-free absorption due to single relaxation process, double logarithmic plot.

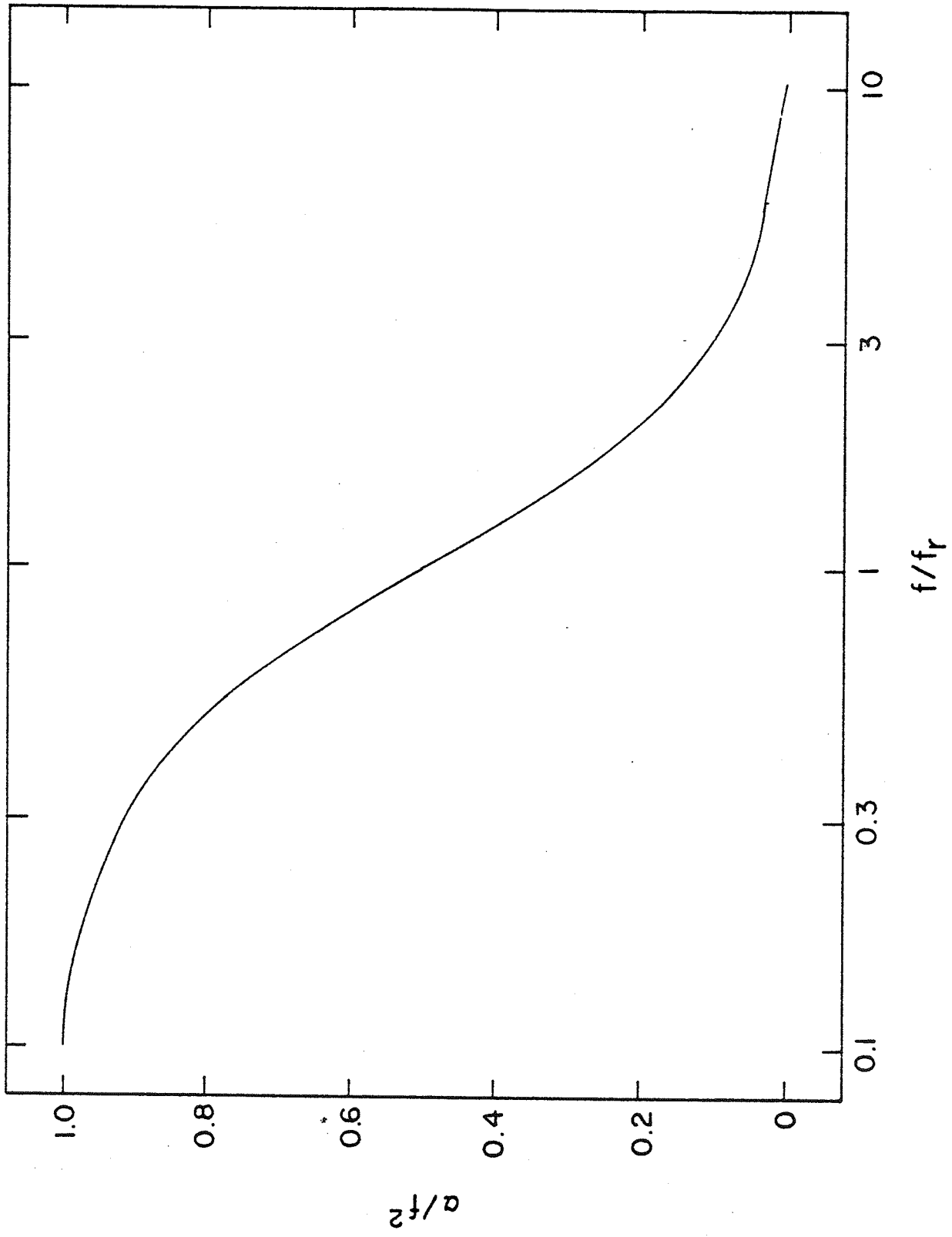


Figure 2.3 As in Fig. 2.2, semi-logarithmic plot.

$\Delta V$ , then the coefficient,  $A'$ , in eqn. 2.54 has been shown to be given by (Slutsky *et al.*, 1980)

$$A' = \frac{2\pi^2 \rho_o c_o \Gamma}{RT} \left\{ \frac{\beta \Delta H}{c_p} - \Delta V \right\} \quad 2.55$$

where  $R$  is the gas constant and  $\Gamma$  is a factor which depends upon the specific reaction and its ionic environment.

## 2.2 THEORY OF THE CYLINDRICAL RESONATOR

**2.2.1 Physical Description.** Resonators and resonance measurement techniques have been used in acoustics for many years. One common design for the study of chemical systems is the spherical resonator. Such an apparatus is capable of yielding highly accurate values for the absorption in the contained fluid. From the standpoint of biochemical studies, however, this type of resonator has a limited applicability due to its large volume, viz., one to one hundred liters. The introduction of the low volume cylindrical resonator (Eggers and Funck, 1973), therefore, permitted the ultrasonic study of many systems whose investigation had previously been impractical due to material availability limitations.

The cylindrical resonator consists of a column of fluid, contained at the ends by quartz crystal plates, and on the side walls by an inert solid material. The quartz crystals serve as piezoelectric transducers which transmit and receive the ultrasonic waves. In the ideal theory, the side wall does not interact with the fluid or the sound wave. Figure 2.4 is a schematic cross-sectional drawing of this part of the resonator, which is a figure of revolution about the axis



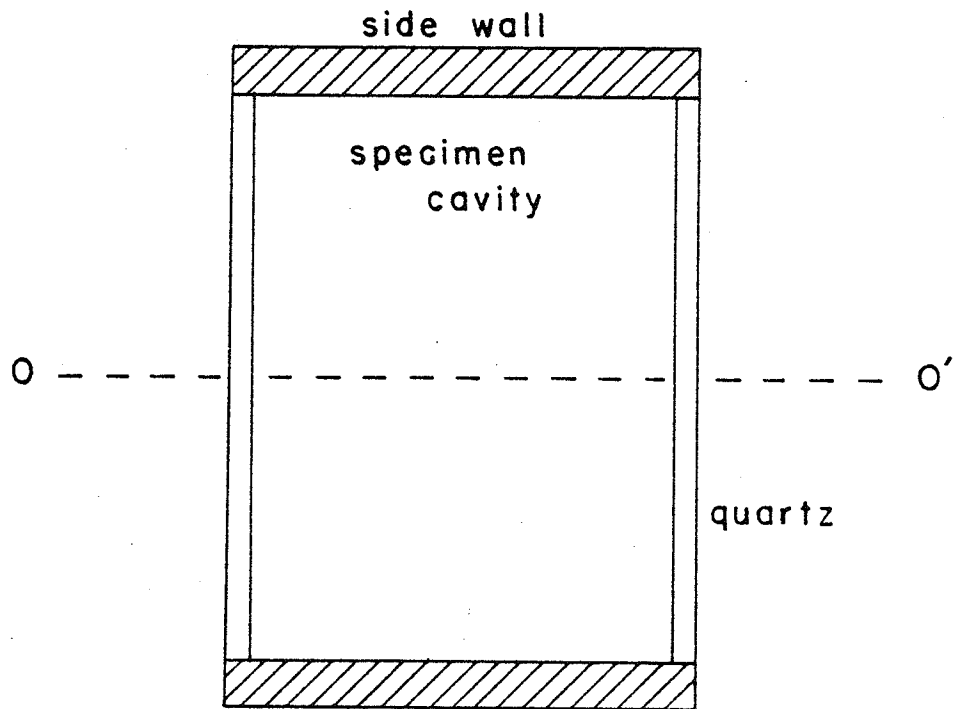


Figure 2.4 Resonator for ideal theory.

O-O'. Resonant cells, as they are called, have been constructed which contain volumes in the range of one to 40 ml. The cell employed in this investigation requires 4 to 12 ml for operation.

2.2.2 The Ideal Resonator. The theory supporting the measurements in this investigation is based upon the assumption of an ideal resonator characterized by lossless reflection at the transducers and by plane wave propagation. One of the transducers is driven by a sinusoidally varying voltage which excites sound waves and establishes a standing wave pattern in the fluid. Resonances, maxima in the standing wave amplitude, will occur at frequencies such that an integral number of half-wavelengths are fit between the quartz plates. If  $m$  half-wavelengths are contained in a distance  $h$ , then this resonance condition can be expressed as

$$h = \frac{m\lambda}{2} = \frac{mc}{2f_m} \quad 2.56$$

and for a higher frequency,  $f_{m+1}$ , fitting  $m+1$  half wavelengths

$$h = \frac{(m+1)c}{2f_{m+1}} \quad 2.57$$

Combining these relations and solving for the velocity of the wave in the fluid under study in the cell yields

$$c = 2h(f_{m+1} - f_m) \quad 2.58$$

Equation 2.58 can be used to determine the sound velocity provided the cavity length,  $h$ , is known. However, sufficiently accurate determination of  $h$  is often difficult

and it is preferable to determine the sound velocity in comparison to a reference specimen solution of known velocity by using the relation (Eggers and Funck, 1973).

$$\frac{\delta c}{c} = \frac{\delta f_m}{f_m} \quad 2.59$$

where  $c$  is the velocity in the reference fluid,  $\delta c$  is the difference between  $c$  and the unknown velocity,  $f_m$  is the  $m$ th resonance frequency of the reference-fluid-filled cavity and  $\delta f_m$  is the difference between  $f_m$  and the frequency of the  $m$ th resonance in the specimen-fluid-filled cavity. The approximation of eqn. 2.59 is most accurate when  $\delta c$  is much less than  $c$ ; under most experimental conditions of this investigation, an error is incurred of a few tenths of a percent.

While the relative positions of the resonance frequencies can be used to determine the sound velocity, the width of each resonance curve is related to the absorption occurring in the liquid containing cavity. All types of resonance phenomena, including those in the cylindrical resonator, can be characterized by a quality factor, generally denoted by  $Q$ , and defined as

$$Q = \frac{2\pi(\text{Energy stored in the system})}{(\text{Energy dissipated per cycle})} \quad 2.60$$

To derive an expression for  $Q$  in terms of measurable quantities, it is first necessary to relate the energy associated with a wave to the acoustic parameters. The energy transported by an acoustic wave is described in terms of the

energy per unit volume, or energy density. In terms of the equilibrium density and the positive and negative particle velocities, the energy density is given by

$$E = \rho_0 (U_+^2 + U_-^2) \quad 2.61$$

Another useful quantity is the intensity or energy flux. The energy transported by the wave process across a unit area in a unit time, *viz.*, the intensity, is equal to the energy density times the propagation velocity and is given by

$$I = cE = \rho_0 c (U_+^2 + U_-^2) \quad 2.62$$

or, in terms of the acoustic pressure

$$I = \frac{p^2}{\rho_0 c} \quad 2.63$$

It has been shown that the absorption of sound is manifested spatially by an exponential decay of the pressure amplitude (eqn. 2.30). From eqn. 2.63 it is therefore possible to write the intensity at  $x=x$  as

$$I = I_0 e^{-2\alpha x} \quad 2.64$$

where  $I_0$  is the intensity at the position  $x = 0$ . To arrive at an expression for the energy dissipated per cycle, the quantity  $\partial I / \partial x$  is first calculated, which will yield an energy loss per volume per unit time.

$$\frac{\partial I}{\partial x} = -2\alpha I_0 e^{-2\alpha x} = -2\alpha I \quad 2.65$$

If the energy dissipated per cycle is much less than the total energy of the wave, then the intensity is not significantly changed in one period. When such a restriction is imposed, eqn. 2.65 becomes

$$\frac{\partial I}{\partial x} \approx -2\alpha I_0 \quad 2.66$$

The energy dissipated per cycle is given by the quantity in eqn. 2.66 multiplied by the resonator volume,  $V$ , and the wave period,  $1/f$ . The quality factor can therefore be written as

$$Q = \frac{2\pi\rho_0 (U_+^2 + U_-^2) \cdot V}{2\alpha\rho_0 c (U_+^2 + U_-^2) \cdot V \cdot 1/f} \quad 2.67$$

which reduces to

$$Q = \frac{\pi f}{\alpha c} \quad \text{or} \quad \alpha\lambda = \frac{\pi}{Q} \quad 2.68$$

If the assumption is again made that the energy dissipated per cycle is much less than the total stored energy, then the quality factor of a resonance can be approximated as

$$Q \approx \frac{f_0}{\Delta f} \quad 2.69$$

where  $f_0$  is the center frequency of the resonance and  $\Delta f$  is the half-power bandwidth of the resonance. Combination of this approximation with eqn. 2.68 gives

$$\alpha\lambda = \frac{\pi\Delta f}{f_0} \quad 2.70$$

This is the fundamental equation used to determine absorption coefficient values by the resonance method.

In the actual use of the resonator, the parameter  $\alpha$ , given in eqn. 2.70, is the result of many absorption and other attenuation mechanisms. In addition to the absorption attributable to the solute, which is of primary interest in this investigation, the mechanisms of diffraction, scattering from the side walls, imperfect reflection at the transducer surfaces, and absorption by the solvent, all contribute to the measured resonance bandwidth. If these modes of attenuation can be assumed to be algebraically additive, it is possible to isolate the absorption due to the solute by making measurements in the system with a reference liquid whose absorption and other physical and acoustical properties are known. The absorption due to the solute is then given by

$$(\alpha\lambda)_{\text{ex}} = \frac{\pi(\Delta f_S - \Delta f_R)}{f_0} \quad 2.71$$

where the subscripts S and R denote measurements made in the specimen solution and in the reference solution, respectively. Application of this equation presumes that all non-solute contributions to the attenuation remain the same during the specimen and reference measurements. This is a valid presumption when a reference liquid is chosen which has acoustic properties similar to those of the specimen solution. The subtraction of the reference values will then eliminate any non-ideal effects of the resonator as well as absorption due to the solvent.

Proper operation of the cylindrical resonator requires a high degree of planarity and parallelism of the transducer

surfaces. This is due to the large number of reflections that a partial wave must undergo before being damped to  $1/e$  of its original value. Propagation of the wave out of the resonator axis direction results in an energy loss so large that absorption by the fluid is obscured. The number of reflections is given by (Eggers & Funck, 1973)

$$m = \frac{l}{\alpha h} = \frac{Q\lambda}{\pi h} \quad 2.72$$

When the specimen is water, the value of  $m$  calculated using eqn. 2.72 is about  $2 \times 10^3$  at a frequency of 1 MHz.

Another requirement for accurate resonator measurements is temperature stability. The effect of a temperature change,  $\Delta T$ , on the position of a resonance frequency can be estimated from eqn. 2.73, which follows from eqn. 2.59 (Eggers & Funck, 1973).

$$\Delta f(T) = \frac{f_o}{c_o} \frac{\partial c}{\partial T} \Delta T \quad 2.73$$

In aqueous solutions, at 5 MHz, a change in temperature of  $0.001^\circ\text{C}$  will result in a shift in a resonance frequency of 9 Hz. Significant error in absorption measurement will therefore result if a temperature change of a few thousandths of a degree occurs during the measurement of the half-power bandwidth.

**2.2.3 The Non-Ideal Resonator.** In actual operation, a cylindrical resonator does not exhibit ideal behavior. Some of the deviations from ideality in the cylindrical resonator have been explained in a theory developed by Labhardt and

Schwartz (1976). Figure 2.5 is a diagram of the coordinates used in this theory. The quartz crystals each have radius  $R_q$  and are placed concentrically at the ends of a right circular cylinder of radius  $R$  and length  $h$ . Position within the cylinder is described by the cylindrical coordinates,  $r$  and  $z$ . Since symmetry is presumed about the  $z$  axis, no angular dependence is included in the following equations.

The necessary boundary conditions are obtained by assuming that the normal particle velocity and pressure are continuous across the cylinder walls and ends. The three dimensional propagation inside the cylinder is obtained by first calculating the Green's function,  $G$ , satisfying the Helmholtz equation.

$$\{\nabla^2 + k^2\} G(r, z; r_0, z_0) = -\frac{1}{r} \delta(r - r_0) \delta(z - z_0) \quad 2.74$$

Here,  $\delta$  denotes the Dirac delta function. The solution takes the form

$$G = \{ae^{i\epsilon z} + be^{i\epsilon z}\} J_0(er) \quad 2.75$$

where  $\epsilon^2 + e^2 = k^2$  and  $J_0$  is the zeroth order cylindrical Bessel function. Application of the boundary conditions yields

$$-eR J_1(eR) - i\beta_2 k J_0(eR) = 0 \quad 2.76$$

where  $\beta_2$  is the admittance of the side wall material. The values of  $e$  which provide solutions to this equation form an infinite set of discrete complex values. The lowest order



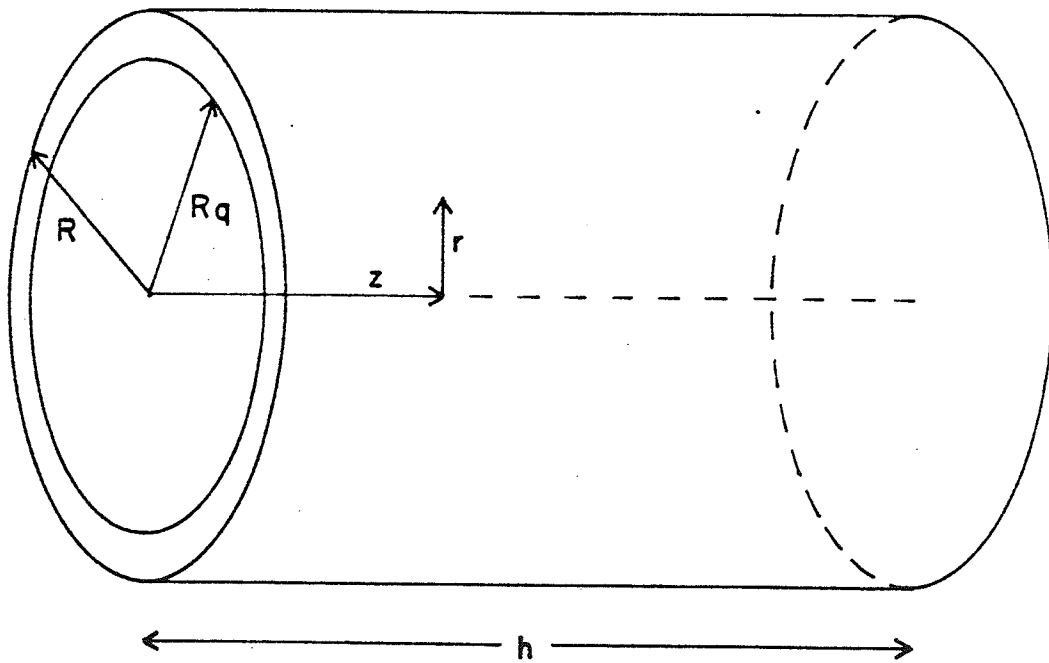


Figure 2.5 Resonator coordinates for non-ideal theory.

solution is the longitudinal cavity resonance which has been predicted by the classical theory. Higher order solutions, corresponding to radial modes of resonance, occur at frequencies slightly higher than each longitudinal resonance. The radial modes predicted by this theory correspond to the "satellite" peaks observed in actual cell operation. Since the satellite peaks often interfere with proper observation of the longitudinal resonance, it is interesting to note that the theory predicts a dependence of their relative amplitudes on the resonator radii  $R$  and  $R_q$ . Examples calculated by Labhardt and Schartz are shown in Table 2.1.

Table 2.1

## Relative Intensities of First Five Resonance Modes

order	$R = R$	$R = 0.8R$	$R_q = 0.7R$
1	100	100	100
2	3.6	0.28	0.00
3	0.60	0.00	0.43
4	0.17	0.10	0.17
5	0.09	0.15	0.00

Attempts to minimize the unwanted satellite peaks are discussed in chapter 4.

## CHAPTER 3

## MATERIALS AND BIOCHEMICAL PREPARATIONS

## 3.1 MYOGLOBIN AND ITS DERIVATIVES

Sperm whale myoglobin was purchased from U. S. Biochemical Corp. (Lot # 9825 and 44121). It was specified by the manufacturer to be salt free and was used without further purification. It dissolved readily in water for direct ultrasonic measurement or biochemical treatment.

Apomyoglobin was produced in the laboratory by the acid methylethyl ketone method (Teale, 1959). Myoglobin was dissolved in distilled water (2 g in 800 ml) and the pH decreased to 2.0 with 5N HCl. After cooling to 5°C, 200 ml of this solution was added to an equal volume of methylethyl ketone at the same temperature, in a separatory funnel. The mixture was gently agitated for one minute and allowed to stand at 5°C until separation of the phases had taken place. At this point the upper, ketonic, phase contained all the heme and the lower, aqueous, phase contained all the apomyoglobin. The lower phase also contained some methylethyl ketone which had dissolved into the water. After phase separation, most of the methylethyl ketone which had dissolved in the aqueous phase was removed by direction of a stream of dry air onto the surface of the mixture for three to four hours. Residual ketone was removed by dialysis against distilled water. A dry product was then obtained by lyophilization.

For production of smaller peptides, the apomyoglobin was cleaved using cyanogen bromide. This reagent cleaves

exclusively at methionine residues by the reaction shown Fig. 3.1. Myoglobin contains two methionine residues so this reaction should be expected to generate three peptides. The amino acid sequences of these peptides is shown in Fig. 3.2.

The cleavage reaction was carried out at concentrations of apomyoglobin and cyanogen bromide of 20 and 8 mg/ml, respectively, in 70 percent formic acid. The reaction proceeded at room temperature for 24 hours after which the excess cyanogen bromide was removed to a cold trap by rotary evaporation at 25°C. A dry product was then obtained by lyophilization.

The method of isolation of the peptides was adapted from Edmundson (1963) and Marshall *et al.* (1974). After lyophilization, the material was dissolved in 10 percent acetic acid at a concentration of 50 mg/ml. The sample was then applied in 10 ml quantities to a column (4 x 180 cm) of Sephadex G-50-fine (Pharmacia Fine Chemicals) equilibrated with 10 percent acetic acid and eluted with this solvent at a rate of 60 ml/hr. Fractions were collected by a Gilson Micro Fractionator. The fractional positions of the peptides were identified using a Beckman DB-G spectrophotometer modified for flow through operation and interfaced with a computer to monitor absorption at 276 nm continuously during the separation process. A typical recording of the absorption against fraction number is shown in Fig. 3.3.

Three main peaks were always observed and are here labeled P1, P2, and P3. The first peak contained unreacted

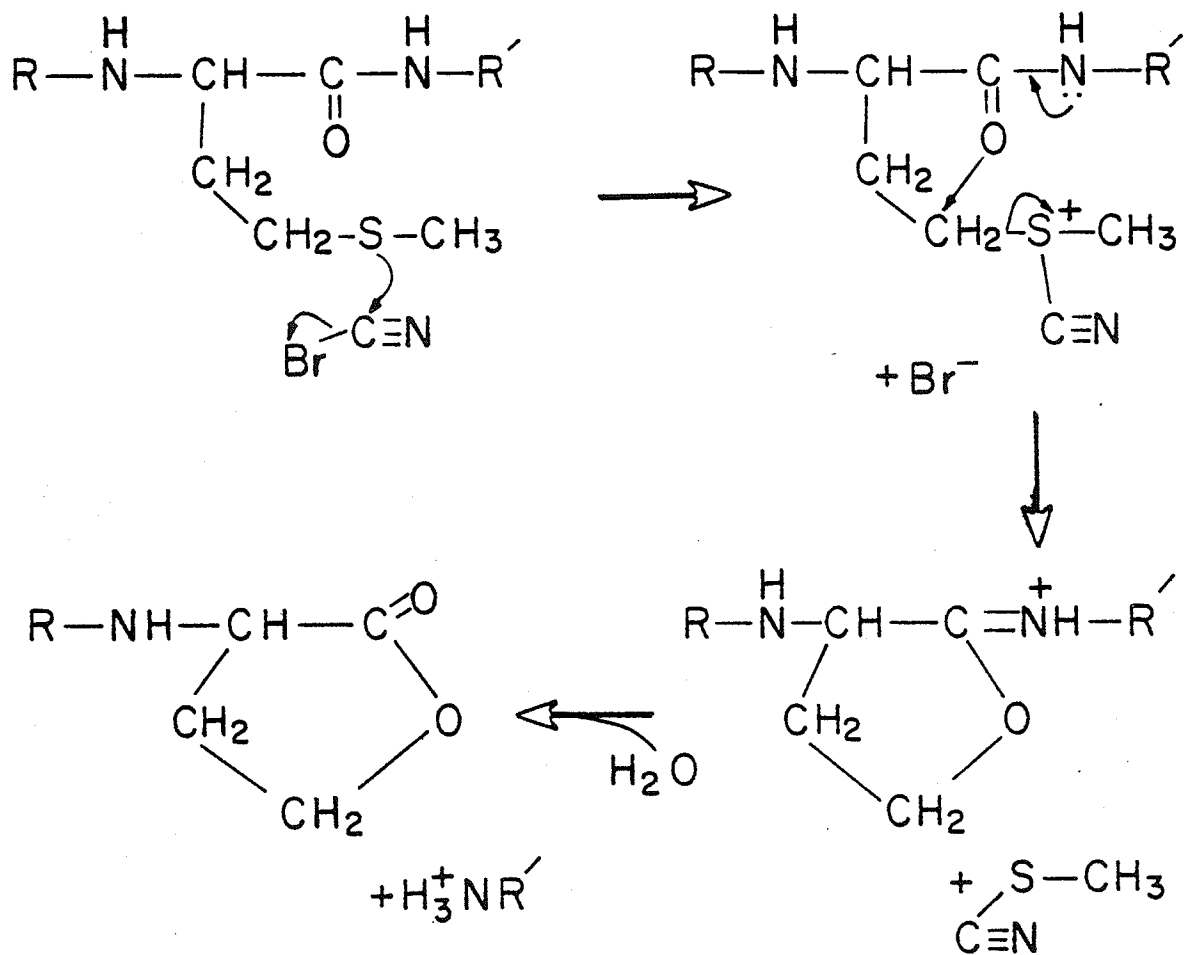


Figure 3.1 Cleavage by cyanogen bromide. R and R' represent continuation of the peptide chain on either side of the methionine residue and the solid arrows represent movements of electrons.

MW = 6388 (P2)

VAL LEU SER GLY GLY GLU TRP GLN LEU VAL LEU HIS VAL TRP  
ALA LYS VAL GLY ALA ASP VAL ALA GLY HIS GLY GLN ASP ILU  
LEU ILU ARG LEU PHE LYS SER HIS PRO GLU THR LEU GLU LYS  
PHE ASP ARG PHE LYS HIS LEU LYS THR GLU ALA GLU MET

MW = 8238

LYS ALA SER GLU ASP LEU LYS LYS HIS GLY VAL THR VAL LEU  
THR ALA LEU GLY ALA ILU LEU LYS LYS LYS GLY HIS HIS GLU  
ALA GLU LEU LYS PRO LEU ALA GLN SER HIS ALA THR LYS HIS  
LYS ILU PRO ILU LYS TYR LEU GLU PHE ILU SER GLU ALA ILU  
ILU HIS VAL LEU HIS SER ARG HIS PRO GLY LEU PHE GLY ALA  
ASP ALA GLN GLY ALA MET

MW = 2535 (P3)

ASN LYS ALA LEU GLU LEU PHE ARG LYS ASP ILU ALA ALA LYS  
TYR LYS GLU LEU GLY TYR GLN GLY

Figure 3.2 Amino acid sequence of myoglobin peptides  
(from Dayhoff and Eck, 1965).

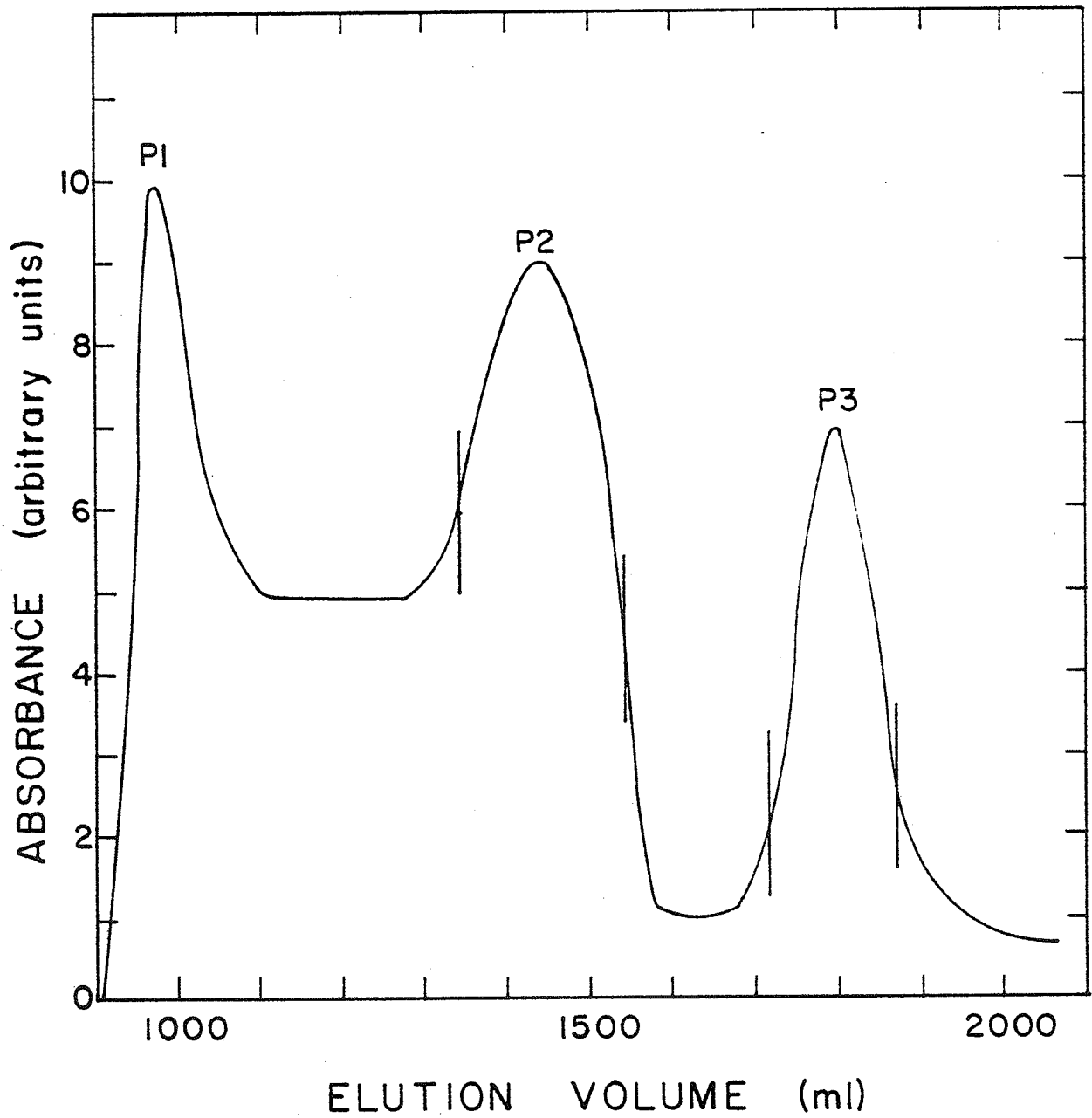


Figure 3.3 Chromatographic separation of myoglobin peptides.

myoglobin. The second and third peaks correspond to the N-terminal and C-terminal peptides, respectively. In some column runs a small peak was observed between P1 and P2 containing the central myoglobin peptide. However, the recovery of this peptide was always too low to allow sufficient accumulation for ultrasonic study. Scarcity of this component is probably due to the necessity for two successful cleavage reactions on a single myoglobin molecule as opposed to one for the peptides in P2 and in P3.

The volumes enclosed in the vertical lines were pooled to isolate the peptides, designated hereafter as peptide P2 and peptide P3. These were initially concentrated by rotary evaporation at 32°C and then lyophilized to a dry product. About thirty runs of the column as described above were necessary to accumulate the one to two grams of each product necessary for ultrasonic absorption measurements.

### 3.2 $\alpha$ -LACTALBUMIN

The milk protein  $\alpha$ -lactalbumin has a structure and amino acid sequence very nearly that of lysozyme. The  $\alpha$ -lactalbumin used in this investigation was isolated from a crude lactalbumin product purchased from U. S. Biochemical Corp. (Lot # 19371). The crude lactalbumin is an acid precipitate from bovine milk and contains the protein  $\alpha$ -lactalbumin as a minor component. The method of isolation, described below, was adapted from that of Robbins and Kronman (1964).



Approximately thirty grams of crude lactalbumin was added to 500 ml of distilled water with vigorous magnetic stirring. Sufficient 1N  $\text{NH}_4\text{OH}$  was added simultaneously with the lactalbumin to maintain the pH at 6.7, insuring maximum solubility of the  $\alpha$ -lactalbumin fraction. Upon standing, an insoluble material would sediment and the supernatant could be poured off. A similar addition of lactalbumin and  $\text{NH}_4\text{OH}$  was repeated twice more using the supernatant as solvent. After a final removal of undissolved material by filtration through cheesecloth, the pH was decreased to 4.0 (1N HCl) and the solution stored overnight at  $5^\circ\text{C}$ , causing precipitation of  $\alpha$ -lactalbumin. The precipitate, isolated by centrifugation, was redissolved in 50 ml of distilled water and brought to pH 6.7 with  $\text{NH}_4\text{OH}$ . This solution was clarified by centrifugation and the supernatant retained. The  $\alpha$ -lactalbumin was again precipitated at pH 4.0 with HCl and redissolved in 25 ml of distilled water as above. After filtration of the resulting solution through a glass fiber filter,  $\alpha$ -lactalbumin was once again precipitated and redissolved in 25 ml of distilled water.

The protein was then salted out with saturated  $(\text{NH}_4)_2\text{SO}_4$  (43 g salt/100 g saturated solution) previously adjusted to pH 6.7 with 1N  $\text{NH}_4\text{OH}$ . The salt solution was added, one drop at a time, to the protein solution with very slow stirring (50 rev/min). When an equal amount of salt solution had been added, an amorphous precipitate was removed and discarded. Seed crystals of  $\alpha$ -lactalbumin were then added

to the solution to promote crystallization. A volume of  $(\text{NH}_4)_2\text{SO}_4$  solution equal to that added previously was then added in the same manner as before. When this procedure was completed, the mixture was at 2/3 saturation of  $(\text{NH}_4)_2\text{SO}_4$  and crystallization was complete.

The crystals were isolated by centrifugation and redissolved in a minimum of distilled water. The  $\alpha$ -lactalbumin was again precipitated with acid, this time using 0.5N  $\text{H}_2\text{SO}_4$ . The precipitate was redissolved in distilled water and salted out once more as described above. A salt free dry product was obtained by passage of an  $\alpha$ -lactalbumin solution through a column of Sephadex G-10 followed by lyophilization. The recovered material produced a single band on SDS gel electrophoresis.

### 3.3 BACITRACIN

The antibiotic bacitracin was purchased from U. S. Biochemical Corp. (Lot # 26581) and used without further purification. Its structure is shown in Fig. 3.4 where the arrows represent peptide bonds proceeding from carboxyl to amine groups.

### 3.4 LIPOSOMES

The LUVs used in this investigation were prepared by the following method. DPPC and dipalmitoyl phosphatidylglycerol (DPPG) were purchased from Avanti Biochemical Co. (Birmingham, Ala.). These are synthetic products, not derived from natural sources. Samples of 100  $\mu\text{g}$  gave single spots on thin layer

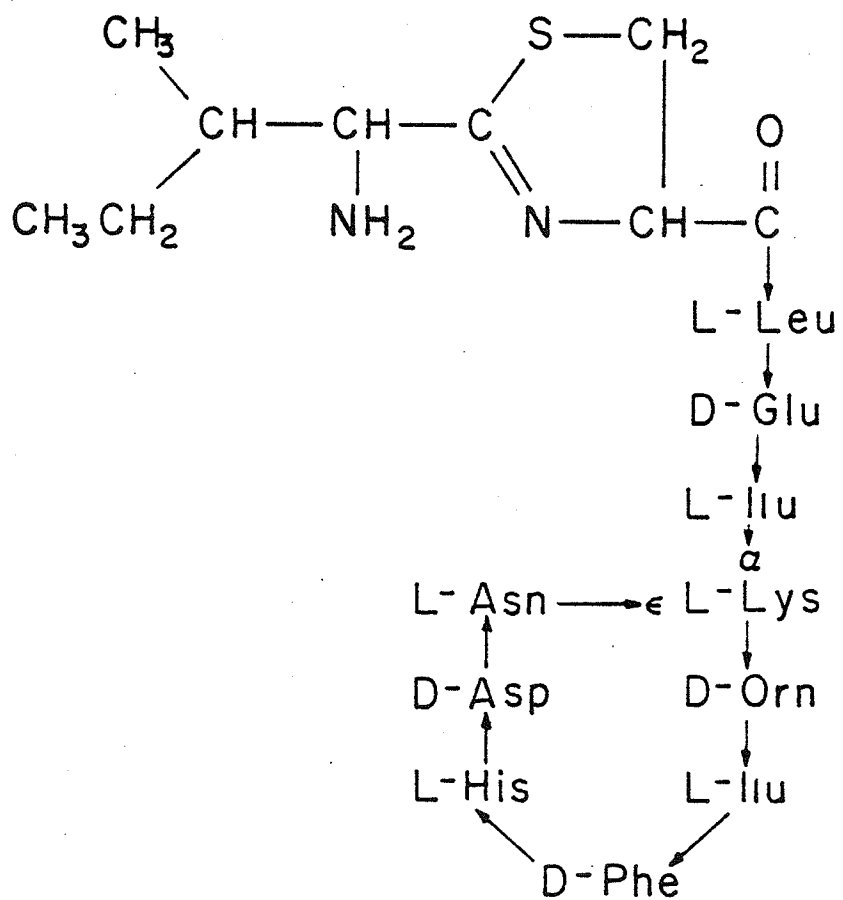


Figure 3.4 Bacitracin (after Galardy et al., 1971).

chromatograms (silica gel G; developed with  $\text{CHCl}_3:\text{CH}_2\text{OH}:\text{H}_2\text{O}$  64:24:4, visualized with  $\text{I}_2$  vapor). Tritiated cytosine 1- $\beta$ -D arabino furanoside (ara-C) was purchased from Amersham (Arlington Heights, IL.).

LUVs were made by evaporating to dryness 125 mg of lipids, as a mixture of DPPC and DPPG in the ratio 4:1 on a rotary evaporator. (DPPG was used in all LUV preparations. The net negative charge of its head group acts to prevent aggregation of the liposomes which occurs in LUVs composed entirely of DPPC.) The dried lipids were redissolved in 8 ml isopropyl ether, freshly washed with 10 percent sodium bisulfite, and 4 ml of chloroform. This was combined, at  $50^\circ\text{C}$ , with 4 ml of an aqueous phase consisting of 10 percent HEPES buffer (pH 7.4) and 72.9 mg/ml ara-C and the flask evacuated with nitrogen gas and sealed. The mixture was sonicated, 80 KHz at cavitating intensity, (Laboratories Supplies Co., Hicksville, NY.) for five minutes at  $45\text{--}50^\circ\text{C}$  producing a homogeneous, white emulsion. LUVs were then formed by reverse evaporation in which the organic phase is preferentially removed in a rotary evaporator. With the temperature of the emulsion maintained at  $50^\circ\text{C}$ , foaming and organic phase evaporation was accomplished by reduction of the pressure to a vacuum of 400 mm Hg. Controlled foaming action during this step, without loss of product, was essential to proper formation of the LUVs. After 10-20 minutes of this condition, 2 ml of HEPES buffer was added to replace that portion of the aqueous phase which had also evaporated.

Reduced pressure was again applied to induce foaming and continued until foaming ceased. The liposomes were then allowed to anneal at 50°C for 30 min. The temperature was then decreased rapidly to room temperature in an ice bath and the liposome suspension dialysed against HEPES buffer until use, always within 1-3 days.

Cholesterol was purchased from Nu Chek Prep., Inc. (Elysian, MN) and gramicidin from Sigma Chemical Co. (St. Louis, MO). Gramicidin is a peptide consisting of 15 amino acids and such commercial products are actually composed of four different peptides known as gramicidins A, B, C, and D. These are present in the percentages 85, 9, 6, and <1, respectively (Hunter and Schwartz, 1967). The first three differ only at position eleven with the following residues being present, A:L-trp, B:L-phe, C:L-tyr. Such differences are expected to have no effect on the ultrasonic properties studied here. To make liposomes incorporating cholesterol or gramicidin, these materials were added to the initial, dried lipids and dissolved together in the organic phase. Both cholesterol and gramicidin are therefore contained within the bilayer structure. Attempts to incorporate gramicidin at mole percentages much greater than 10 percent failed as these mixtures were not soluble in the organic phase.

The size distribution of LUVs prepared in the manner described above has been measured by negative stain electron microscopy. The results of these measurements are shown in Fig. 3.5, where it is seen that they are rather uniform in

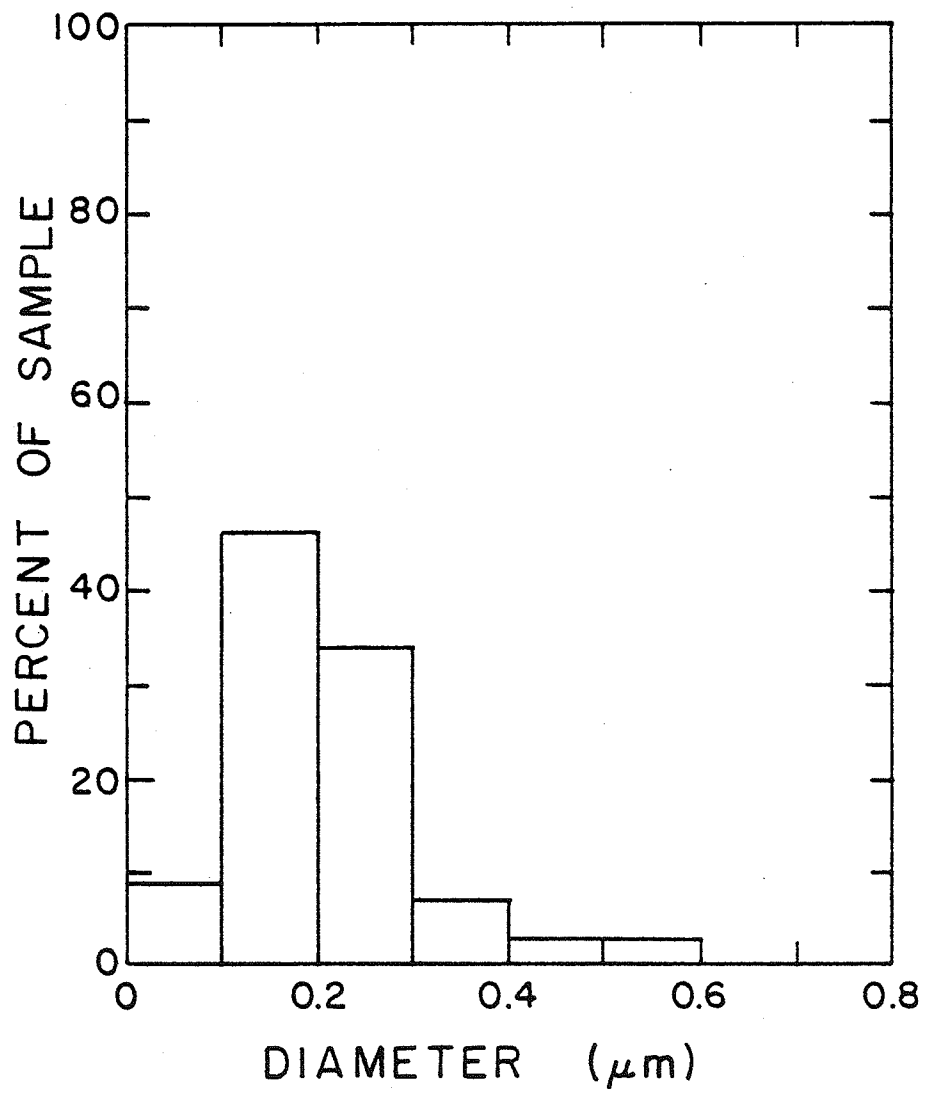


Figure 3.5 LUV size distribution.

size, with approximately 80 percent falling in the diameter range of 0.1 to 0.3  $\mu\text{m}$ .

## CHAPTER 4

## APPARATUS AND MEASUREMENT TECHNIQUES

## 4.1 CELL DESIGN

The development of the resonant cell used in this study was guided by the design of Labhardt and Schwartz (1976) as well as by previous work in this laboratory. The cell was designed to operate with small sample volumes, *viz.*, less than 20 ml, in a frequency range of 0.1 to 10 MHz. The cell was purposefully designed with very few parts in order to achieve the high degree of mechanical stability necessary for the desired operation.

Figure 4.1 is a cross-sectional view of the assembled cell, which is a figure of revolution about the axis O-O'. The frame, F, is stainless steel and forms the supporting structure for the rest of the cell parts. The two sections of F are held together by four stainless steel bolts, B, and associated nuts, N, which were machined to have 64 threads per inch on a 9/16 in. diameter. This thread size allows fine adjustment to achieve the degree of parallelism of the quartz transducers, Q, required for proper resonator operation. The quartz crystal transducers are held within an accurately machined recess in F by high vacuum grease (Dow-Corning) and they form the ends of the resonating cylindrical cavity. The wall of the cylindrical cavity is formed by a plexiglas spacer, S, which is fitted with rubber O-rings, O, to make a liquid tight seal against F. Also on the spacer are ports, P, which are used to fill and empty the cavity with specimen



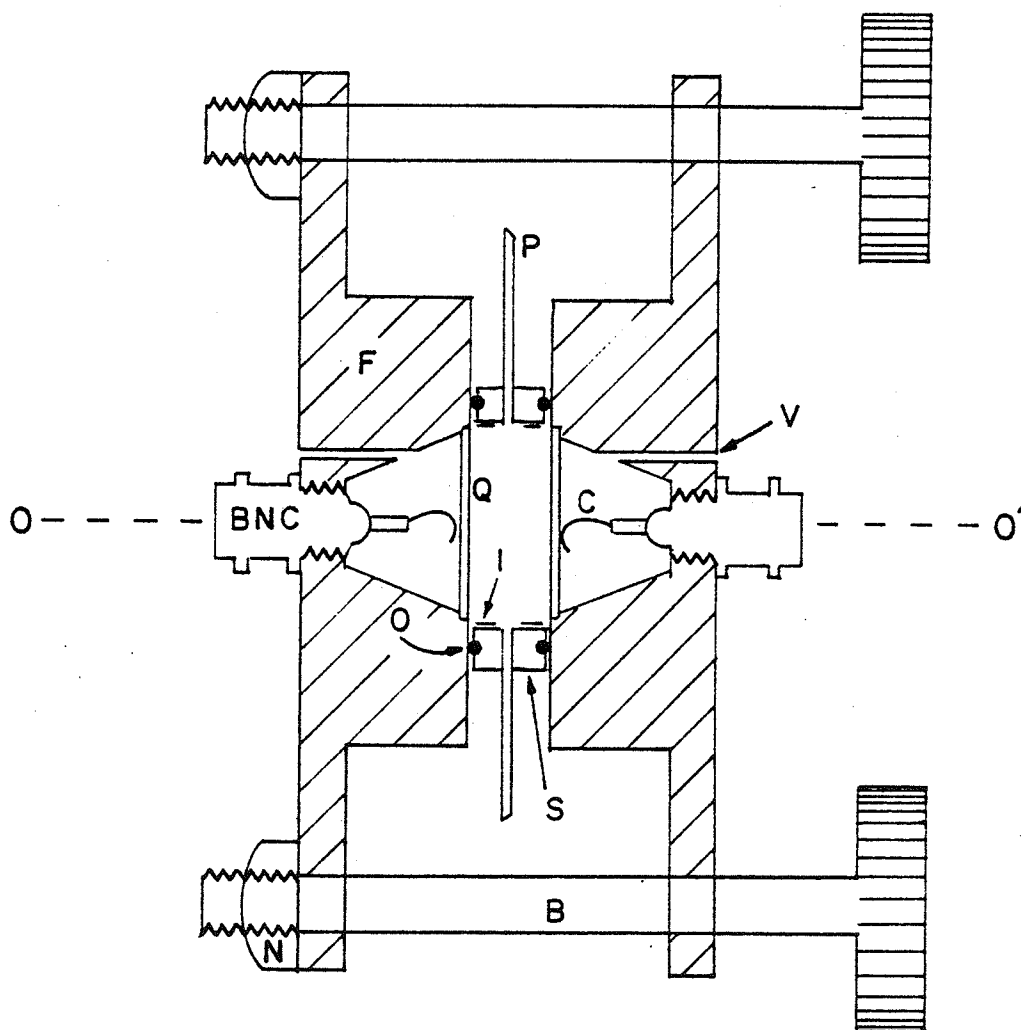


Figure 4.1 Cross-section of cylindrical resonator.

material. A standard male BNC connector is threaded into the frame and, with a light pressure from the spring contact, C, makes electrical connection to the hot electrode of the quartz crystal.

The 1 in. diameter, X-cut quartz crystals were purchased from Valpey-Fisher Corporation (Hopkinton, MA) with highly polished surfaces. These surfaces provide the necessary smoothness and flatness to maintain the multiple reflections which must take place without significant beam spreading. The electrodes, applied by the supplier, were composed of a layer of chromium covered by a layer of gold. The ground electrode, in contact with the specimen solution, covered the entire face of a crystal, while the hot electrode was a 7/8 in. diameter concentric spot. Crystal pairs with fundamental resonance frequencies of 4 and 8 MHz were employed in this study.

A persistent problem attending the operation of such small volume resonance cells is the phenomenon of unwanted resonances, or so called "satellite" peaks. Such phenomena determine the high frequency limit of operation of these cells, and so the measurements to be presented in this thesis. In an attempt to combat the problem of satellite peaks, the radius of the frame surface which is in contact with the spacer O-rings was made rather large. The theory of Labhardt and Schwartz (1976) predicts a complex behavior of satellite peaks as a function of the ratio  $R_q/R$ , where  $R_q$  is the radius of the quartz transducer and  $R$  is the effective radius of the cylindrical cavity. Theoretically, as shown in Table 2.1,

decreasing  $R_q/R$  should decrease the amplitude of the unwanted resonances, with respect to the principal longitudinal resonance. However, experimental trials using  $R_q/R$  values of 0.89, 0.72, 0.57 and 0.44 showed no significant difference in the high frequency limit imposed by these satellite peaks.

Another technique for reducing the interference of satellite peaks has been employed by Eggers et al. (1978). This technique consists of lining the inside surface of the spacer with a sound absorbing "inlay", presumably decreasing the side wall reflections that lead to radial mode resonances. The effects of 1/32 in. thick neoprene rubber and 1/8 in. thick silicone rubber inlays were tested with plexiglas spacers and Fig. 4.1 shows such a covering on the inside of the plexiglas surface, I, except for openings to accommodate the ports. Spacers of different diameter were used for the two material inlays to maintain a constant effective radius, R. Even though both inlays proved beneficial, the best results were obtained using the neoprene inlay, which extended the frequency limit from 5 MHz to 7 MHz. Figure 4.2 shows the effect of the neoprene inlay on the cell response in the vicinity of four resonance frequencies, where the amplitude response has been normalized to that of the principal longitudinal resonance and the frequency measured from the center of that resonance. The changes that occurred at the higher frequencies are easily seen and greatly facilitate measurement in that region. Even at low frequencies there was

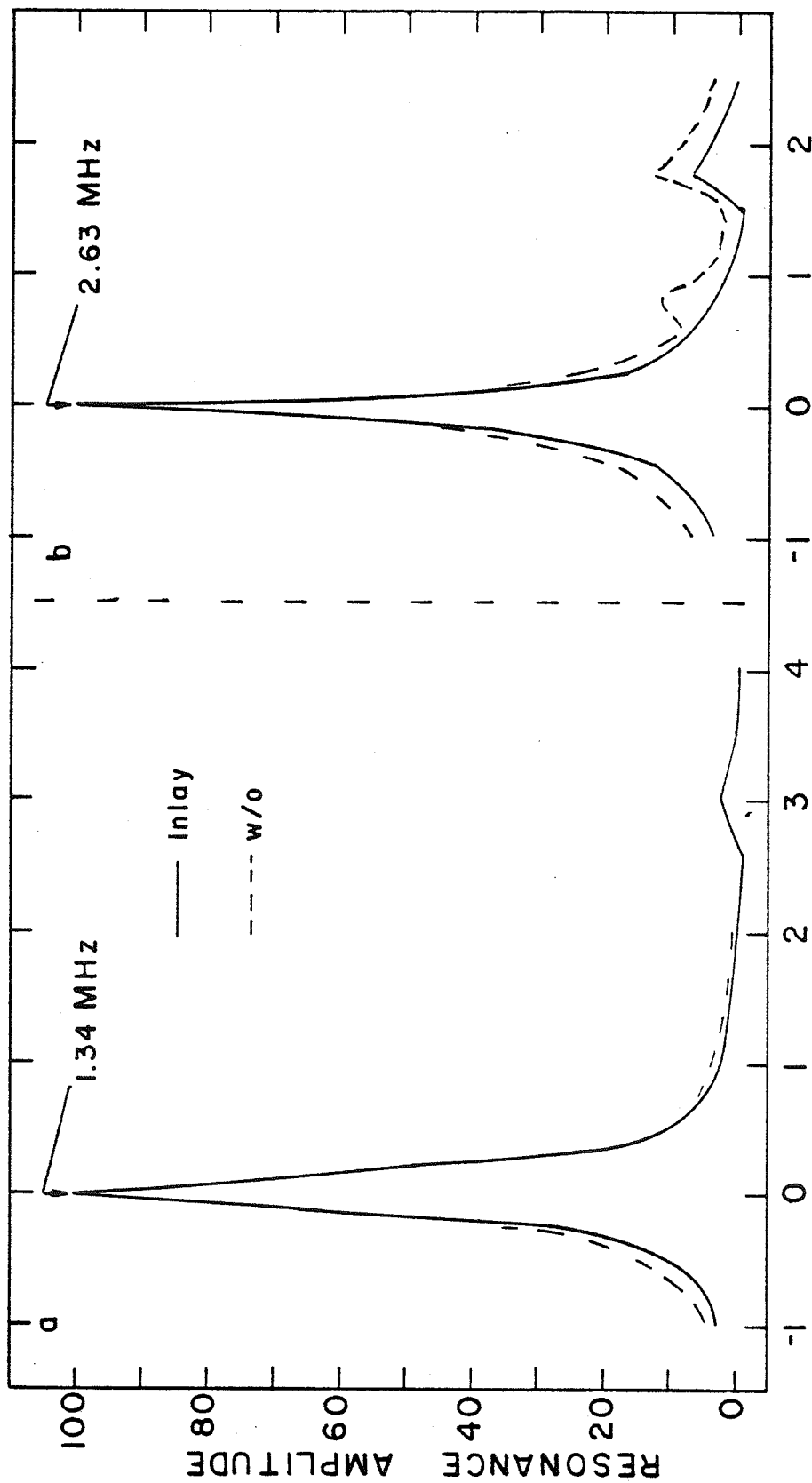


Figure 4.2 a,b Effect of neoprene inlay on satellite resonances.

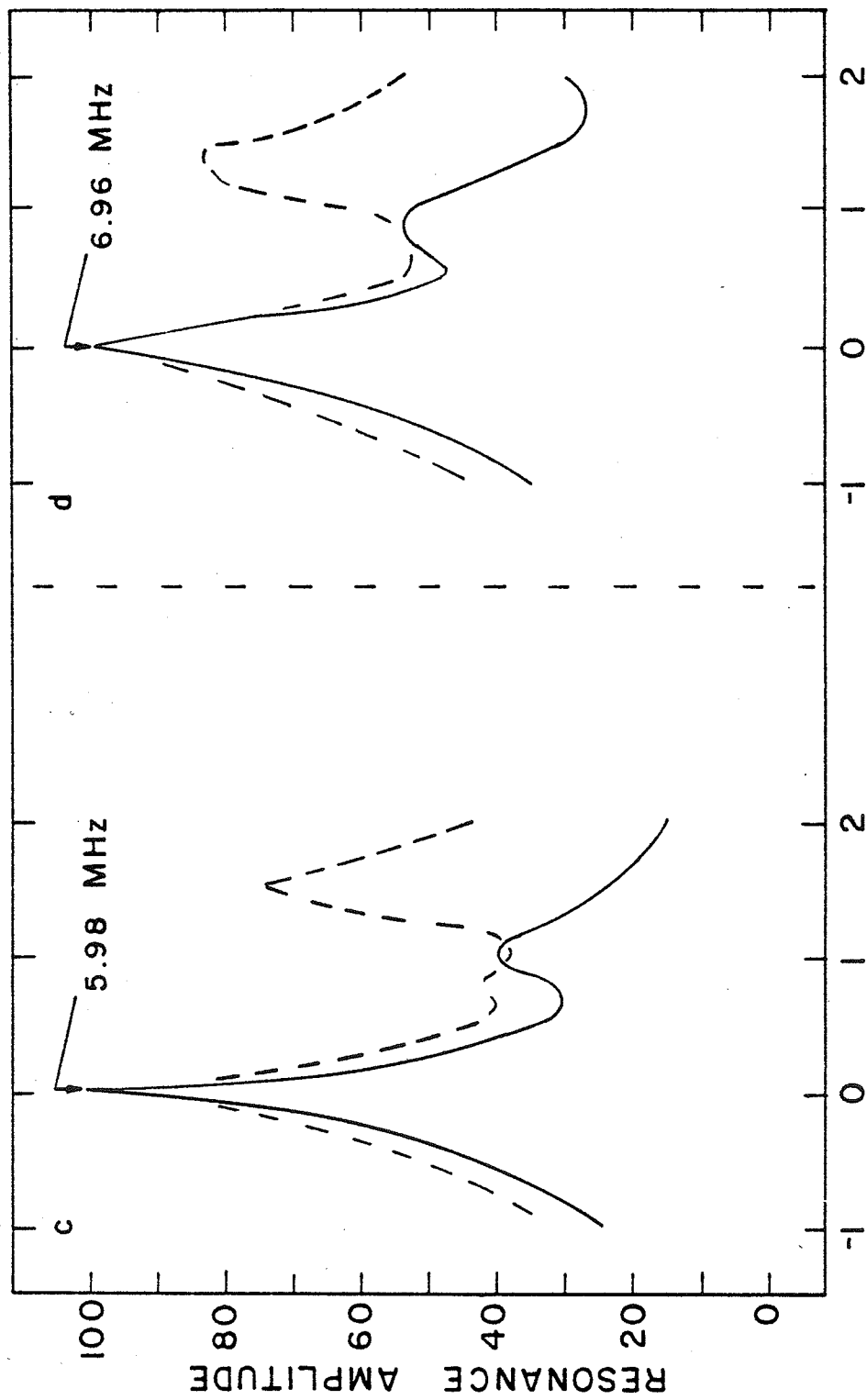


Figure 4.2 c,d Effect of neoprene inlay on satellite resonances.

a noticeable effect, such as the virtual disappearance of the first satellite peak at 2.63 MHz, when using the inlay.

Figure 4.3 illustrates the sample handling equipment peripheral to the resonant cell. Mounted on a plexiglas chasis are a piston in a cylinder for filling and pressurizing the cell, a pressure gauge for monitoring the pressure within the cell, and a regulated compressed air supply. Connections were made to the cell ports by polyethylene tubing (1.19 mm i.d., 1.70 mm o.d.).

#### 4.2 CELL ASSEMBLY AND DISASSEMBLY

The resonance cell consists of only a few parts and assembly is simple, but great care must be exercised during assembly to obtain optimum performance. A most important prerequisite is that all surfaces exposed to the sample solution, or making electrical contact, be free of grease or particulate films. Any residual silicone grease, from prior use, is removed from the frame and the quartz crystals by CEE-BEE C-105 HF silicone remover (McGean Chemical Co. Inc., Cleveland, Ohio). The frame surfaces were swabbed with this solvent while the crystals, wrapped in optical lens paper for protection, were allowed to soak in the silicone remover, usually overnight. The solvent was removed in both cases by a rinse of acetone followed by one of ethanol. The quartz crystals were further cleaned by soaking in Micro detergent (International Products Corporation, Trenton, NJ) from eight hours to overnight (approx. 12 hours). They were then rinsed thoroughly with tap water first and then with distilled water,

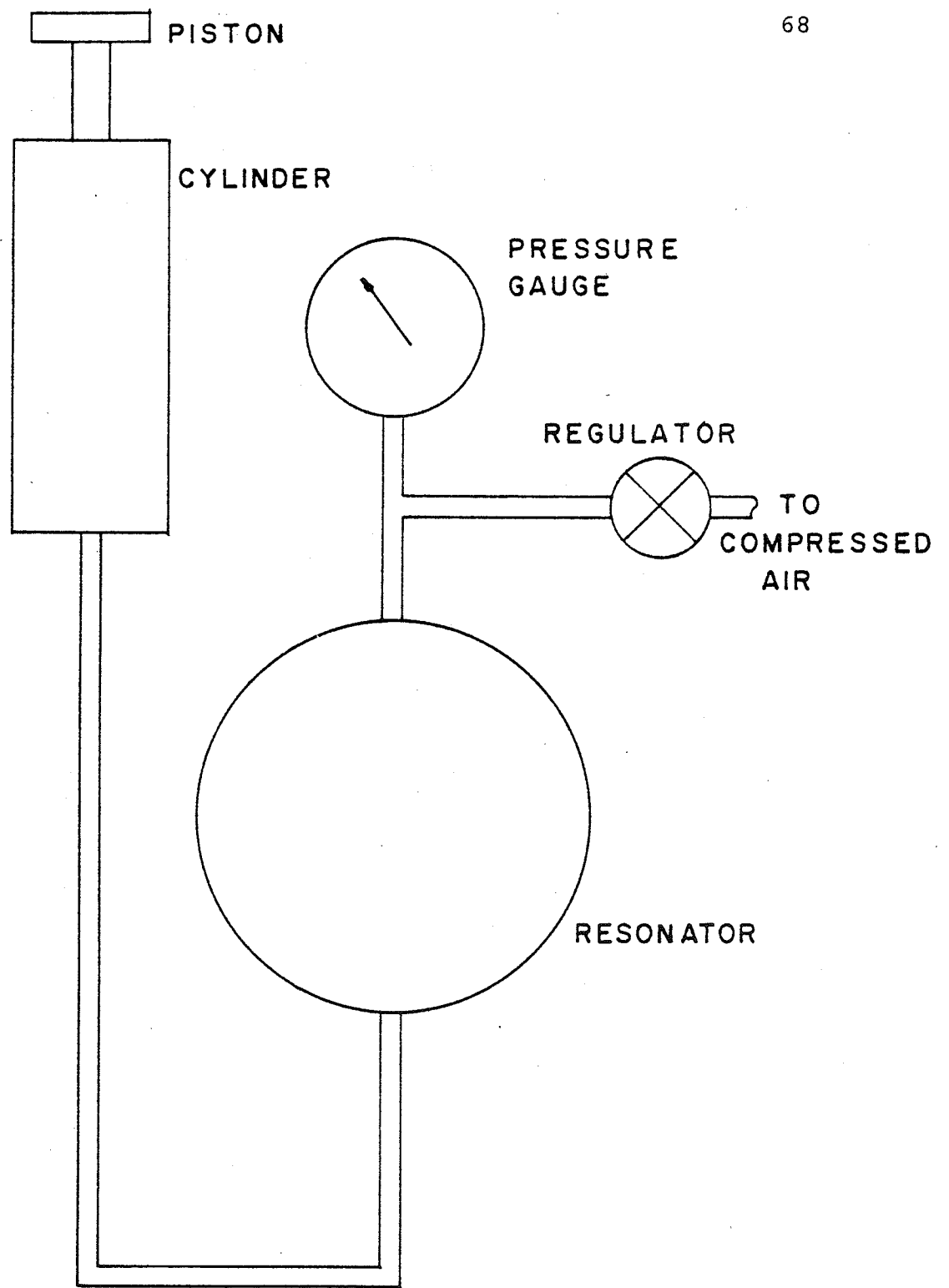


Figure 4.3 Pressurizing apparatus.

and dried in a stream of dry nitrogen gas. All other parts of the system which came in contact with the sample solutions were rinsed thoroughly with distilled water and allowed to air dry.

A crystal was installed into the frame by first applying a thin ribbon (approx. 1 mm wide) of Dow-Corning silicone high vacuum grease to the non-electroded rim of the hot side of the quartz plate, being careful not to involve more grease than necessary. This side was then placed gently against the frame recess. The liquid-tight seal was obtained by applying, with a 1 in. diameter rubber cylinder, a downward force simultaneously with a rotation through about 90 degrees. Considerable force can be exerted in this manner, even on the thin (about 0.34 mm) 8 MHz crystals without any fear of breakage. This procedure "rings-on" the crystal, forming a thin continuous adhesive layer of grease between the quartz and the frame.

Electrical ground contacts to the quartz transducers were then made with conductive silver paint, (G C Electronics, Rockford, IL). This was applied sparingly with a thin wire (approx. 0.3 mm diameter) to four spots on the periphery of each crystal. When dry, this resulted in a crystal face to frame dc resistance of 0.3 to 0.8 ohms. As discussed above, the electrical connection to the hot side of the crystal was made by spring contact from the BNC connector.

The assembly of the frame was accomplished by supporting one half of the unit so that the cell axis was vertical and



the bolts inserted from below. The spacer was then centered on top of the frame, and the other half of the frame was lowered onto it while being centered by the bolts. The nuts were then screwed on, and the bolts tightened gradually and sequentially to maintain approximate parallelism until the bolts had been rotated about three complete revolutions. The cell was then supported on a wooden frame with its axis horizontal, as shown in Fig. 4.1. At this point, the cell was ready to be filled for tuning, i.e., adjustment of parallelism.

Disassembly of the cell proceeded as follows. After measurements were completed, the sample cavity was emptied of the specimen and flushed thoroughly with distilled water. The securing bolts were then removed while the cell was supported with its axis vertical. The top half of the frame was lifted off and the spacer removed and dried. A small wooden stick (approx. 1.5 mm diameter) was then inserted through the vent holes and a light force applied to each crystal, to break the grease seal, until they were released from the frame. The excess silver paint was removed from the crystals and the silicone grease dissolved as described earlier. All the remaining parts of the cell were then rinsed with distilled water and allowed to air dry.

#### 4.3 CELL USE

The theory describing the functioning of the cell assumes the quartz transducers to be perfectly parallel. Thus, a high degree of parallelism must be achieved in order to obtain

useful results. Some investigators have employed elaborate means for establishing this parallelism, in particular optical schemes (Eggers and Funck, 1973). However, the cell used in this study always performed well when aligned by tuning for optimum resonance, and this technique was employed throughout. During assembly of the cell, the securing bolts were tightened uniformly, thus providing a first approximation of transducer parallelism. Tuning was always performed with the cell containing non-degassed distilled water at room temperature. Using a resonance frequency nearest 2 MHz, the bolts were turned by small amounts and the amplitude of the resonance was compared to the prior observed amplitude. From this procedure a general scheme of adjustment could be deduced for turning the bolts and this was continued until no further amplitude increase could be achieved. This procedure was then repeated at a resonance frequency near 4 MHz. Generally, the cell was in near perfect tuning after the procedure at 2 MHz and only small adjustments were necessary at 4 MHz. The tuning process could be completed in about twenty minutes.

There was some initial concern that since the cell was generally used at temperatures different from that at which it was tuned, that it would not remain well aligned at the various operating temperatures. To investigate this potential problem the cell was charged with degassed distilled water and absorption measurements were made over the range of temperatures used; the lowest being 4°C and the highest 51°C. The data obtained in this manner showed that, in this

temperature range, alignment was sufficiently maintained that any changes in measured absorption were within the inherent uncertainty in such measurements, about five percent.

The resonant cell required five to twelve milliliters of solution to make the measurements as described later in this chapter. The protein and peptide solutions were prepared for measurement as follows. An amount of dry powder chemical was weighed to the nearest 0.1 mg using an Ainsworth Type 10 analytical balance. This was placed in a 13 x 125 mm test tube to which 10 ml of distilled water was added. The test tube was covered with Parafilm M (American Can Co., Greenwich, CT) and agitated by a vortex mixer. The sample was completely dissolved by two to three minutes of vortex mixing, as judged by visual inspection. The solution was then filtered, to remove any undissolved residue, using a 20 ml disposable syringe and a Millex-HA syringe filter, pore size 0.45  $\mu\text{m}$  (Millipore Corp., Bedford, MA). The solution was stored in a flask overnight at 5°C.

To prepare for the ultrasonic measurements, i.e., to eliminate micro-bubbles which could interfere with the sound wave propagation, the solution was degassed under a reduced pressure (about 5 mm Hg) in a rotary evaporator (Pope Scientific Inc., Menomonee Falls, Wisc). As these solutions tend to foam when degassed, the pressure was reduced slowly to avoid any loss of product. The solution was maintained at the final reduced pressure for two to three minutes after all bubbling ceased. The degassing process took approximately ten

to fifteen minutes to complete. Concentrations of the specimen solutions were determined after the ultrasonic measurements by dry weight of two 3 ml aliquots after lyophilization.

The cell was filled using a 25 ml glass syringe body supported vertically with its outlet connected to the filling cylinder by polyethylene tubing. The solution was then carefully pipetted into the syringe body and drawn into the cylinder by retracting the piston slowly. When all of the solution had been withdrawn from the syringe, the tubing was reconnected to the lower port of the spacer and the cell filled by advancing the piston in the cylinder. Slow introduction of the fluid into the sample chamber is necessary (Eggers, personal communication) as any turbulence can cause bubbles to form. The bubbles, which also tend to form if the crystal faces are not adequately cleansed, will reduce the  $Q$  of the resonances and lead to significant errors in absorption measurements. Once the cell was filled, the upper port was connected to the pressure gauge assembly.

Since the frequency position of a cell resonance is highly temperature dependent, accurate absorption measurements can only be made if the cell's temperature is accurately maintained. Temperature control in this study was provided by a Neslab Exacal 500 constant temperature bath circulator and an accompanying Endocal 350 refrigeration unit (Neslab, Portsmouth, NH). The bath chamber, with a volume of 45 liters, was filled with a mixture of distilled water and

ethylene glycol, 50:50 by volume. This equipment is capable of maintaining the bath temperature constant to within less than  $0.01^{\circ}\text{C}$  during the 5-10 hours necessary to accomplish a set of absorption measurements. After the cell had been filled and the electrical connections made by attaching BNC 50 ohm coaxial cables, the cell and its wooden base were put into two plastic bags and the assembly submerged in the bath so that all of the cell was in the water-ethylene glycol mixture. This arrangement provided excellent temperature stability, as judged by the frequency stability of cell resonances, and a constant cell temperature was always reached within one hour.

Eggers et al. (1976) have shown that applying an overpressure to the specimen cavity of a resonant cell can improve the  $Q$  of the cell and extend the usable lower frequency range. The cell used in this study was pressurized by application of regulated, compressed air to the upper port. Generally an overpressure of 12 psi was used while making measurements in the frequency range 0.4-1.5 MHz. Above this frequency range the overpressure caused increased problems with satellite peaks and so measurements were made from 1.5-7 MHz at the prevailing ambient pressure. Figure 4.4 shows the effect, on the bandwidth, of increasing the static pressure, in distilled water at  $20^{\circ}\text{C}$ . The bandwidth values which would be expected if absorption by water was the only mode of energy loss in the resonator, are represented by the straight line which is based on absolute measurements of absorption in water (Fry and Dunn, 1962). An overpressure of 12 psi extends the

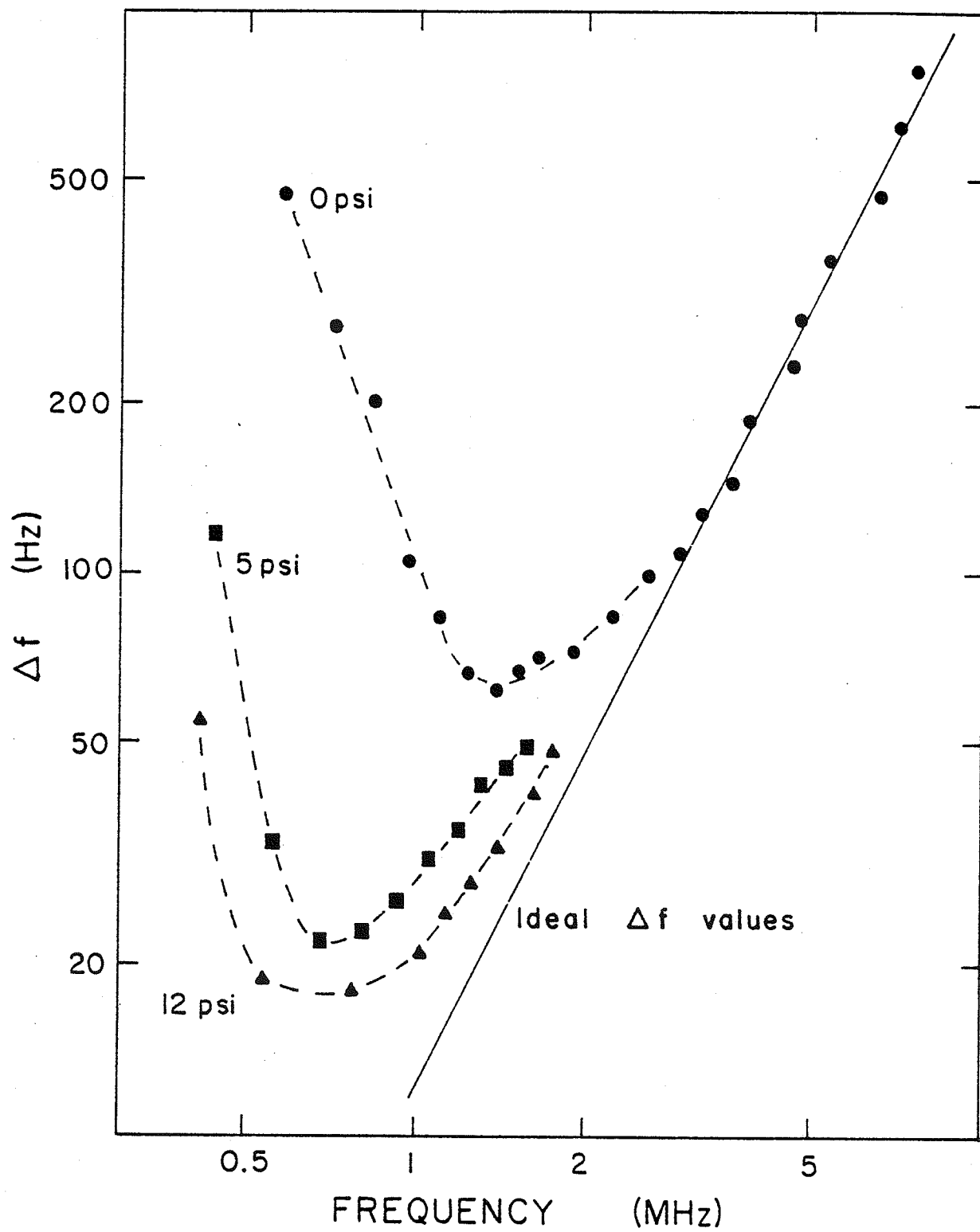


Figure 4.4 Effect of overpressure on resonance bandwidth.

lower limit to 0.4 MHz from a value of about 1 MHz at atmospheric pressure or 0 psi. The pressure was increased slowly, to avoid leakage, viz., about 1 psi/min, until a value of 12 psi was reached. As noted by others (Eggers et al., 1976), pressure equilibrium is reached in about one hour. Attainment of equilibrium was judged by stability of the pressure gauge reading and of the resonance frequencies. This system maintained the pressure to better than 1% over the period during which the absorption measurements were made.

Figure 4.5 is a block diagram showing the components used to measure ultrasonic absorption in the resonance cell. The frequency synthesizer, Hewlett-Packard 8660B, provided the voltage for the transmitting transducer and displayed the driving frequency to the nearest hertz. The output voltage from the receiving transducer was normally connected directly to the spectrum analyser, Hewlett-Packard 8552A, 8553B, which was used to measure the amplitude of the received signal. When the output voltage was too low to be displayed adequately by the spectrum analyser alone, a wideband preamplifier, Hewlett-Packard 461-A, was inserted between the resonant cell and the analyser. The 3 dB points of a resonance were determined by adjusting the synthesizer frequency above and below the resonant frequency to the points where the output voltage fell to a value  $1/\sqrt{2}$  of that at the resonance frequency.

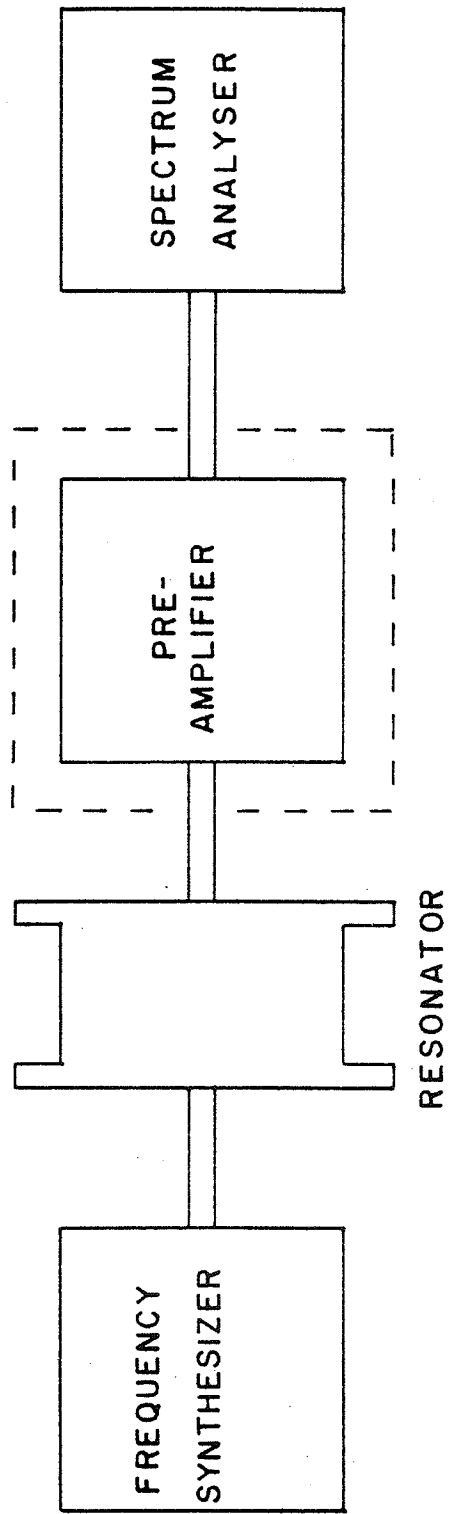


Figure 4.5 Electronic instrumentation.



#### 4.4 DATA ACQUISITION AND CALCULATIONS

As mentioned above, experimental measurement at a particular frequency yields a 3 dB bandwidth of the resonance, here referred to as  $\Delta f$ . This bandwidth is related to the absorption coefficient as in eqn. 2.70. In this study the  $\Delta f$  measured in a reference solution was subtracted from the  $\Delta f$  measured in a sample solution, as in eqn. 2.71, and the resulting  $\Delta f$  used to calculate  $\alpha_{ex}$  and other related parameters. In the cases where the solvent was essentially distilled water, the reference solution used was a NaCl solution whose concentration was chosen to match, as closely as possible, the velocity of sound in the specimen solution. Generally the velocity in the specimen solution is different from that in distilled water due to the presence of the protein or other solutes. NaCl provides a convenient reference solution since the propagation velocity in such solutions is a well known function of the salt concentration while the absorption is nearly identical to that in plain water. A reference solution which matches the velocity of the sample solution is preferred to one of distilled water since this produces identical waveform patterns within the resonant cavity during the specimen and reference measurements. This is particularly important at frequencies below 1.5 MHz where the significant diffraction effects should be identical in the reference and in the specimen measurements.

Most of the absorption data in this thesis is presented as the specific frequency-free absorption coefficient, defined

as  $\alpha/f^2c$ , here denoted as  $A$ , where  $c$  is the solute concentration in g/ml. Dividing by the square of the frequency has the advantage of providing a parameter in which the contribution from classical absorption is independent of frequency. Also, since the ultrasonic absorption coefficient of virtually all aqueous protein and peptide solutions of low concentration are nearly proportional to the concentration, division by the concentration provides for elementary comparison among specimens. Some absorption data is presented as the specific absorption per wavelength,  $\alpha\lambda/c$ . The behavior of both of these parameters in the vicinity of a relaxation has been described in chapter 2.

#### 4.5 CELL PERFORMANCE AND ERROR ANALYSIS

To test the cell performance and arrive at an estimate of measurement accuracy, numerous measurements were made on solutions of bovine serum albumin. In Fig. 4.6 comparison is made between data from these measurements (circles) and those of Kessler and Dunn (1969) (straight line). Agreement is quite good throughout the frequency range with slightly greater discrepancy occurring at low frequencies. Almost all points are within  $\pm 5\%$  of the previously measured values.

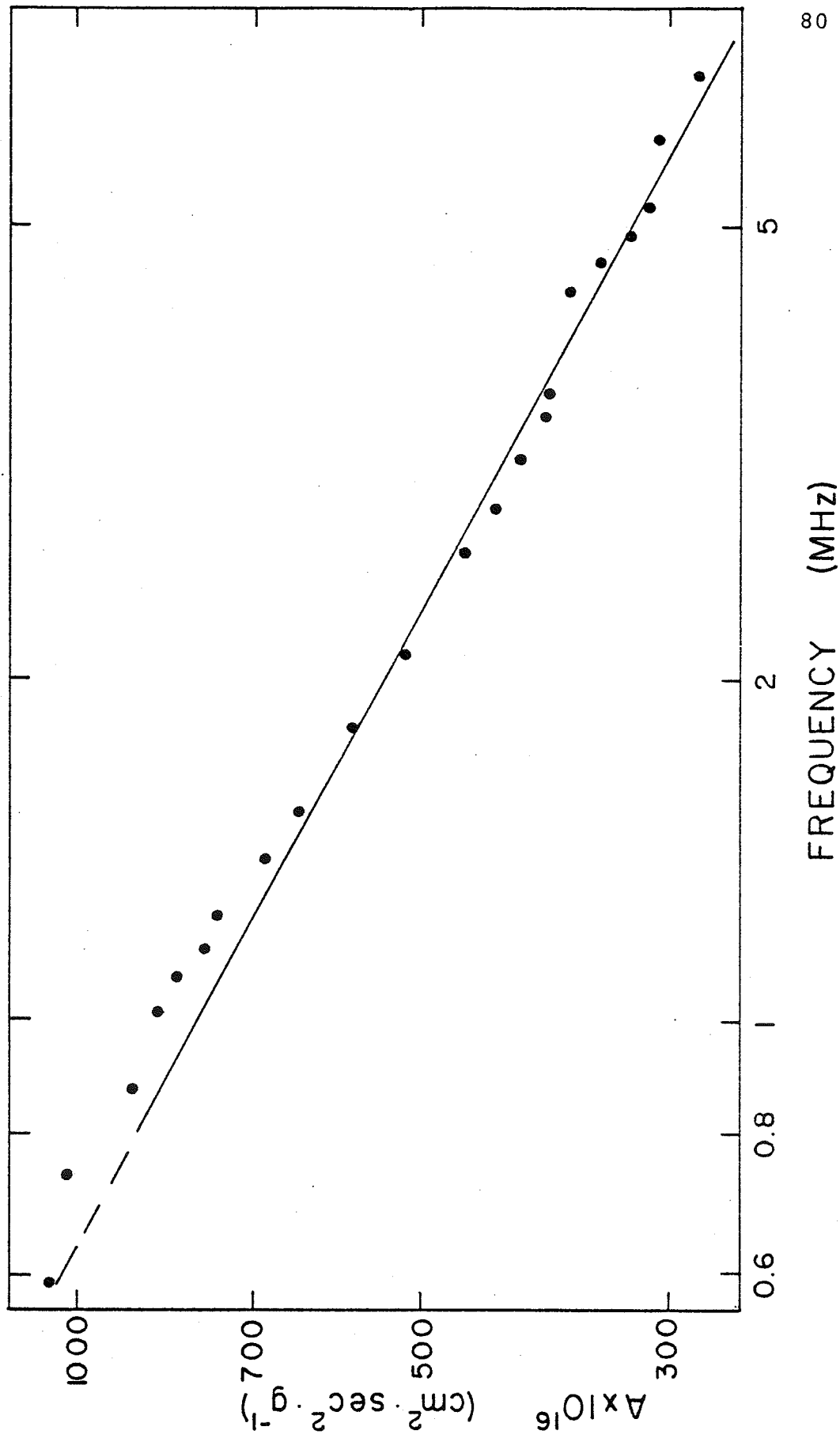


Figure 4.6 Absorption in solutions of bovine serum albumin.

CHAPTER 5  
RESULTS AND DISCUSSION

5.1 ABSORPTION BY PROTEINS AND PEPTIDES

5.1.1 Dependence on Frequency. Absorption measurements have been made on the proteins and peptides listed in Table 4.1.

Table 4.1

<u>Material</u>	<u>Molecular Weight</u>
Myoglobin	16,900
Apomyoglobin	16,280
$\alpha$ -Lactalbumin	14,000
Peptide P2	6320
Peptide P3	2570
Bacitracin	1420

Measurements were first made on aqueous solutions of these materials and, with the exception of apomyoglobin and peptide P2, all at pH 7.0. In all cases the concentrations of these solutions were below three percent by weight, a range in which absorption was found to be very nearly linear with concentration. Unless otherwise specified all measurements were carried out at 20.0°C.

Figure 5.1 is a plot of the specific frequency-free absorption,  $A$ , against frequency for sperm whale myoglobin and its biochemical derivatives. Each curve resembles, in a general way, the upper frequency portion of a relaxation spectrum. Unfortunately, the frequency range available did

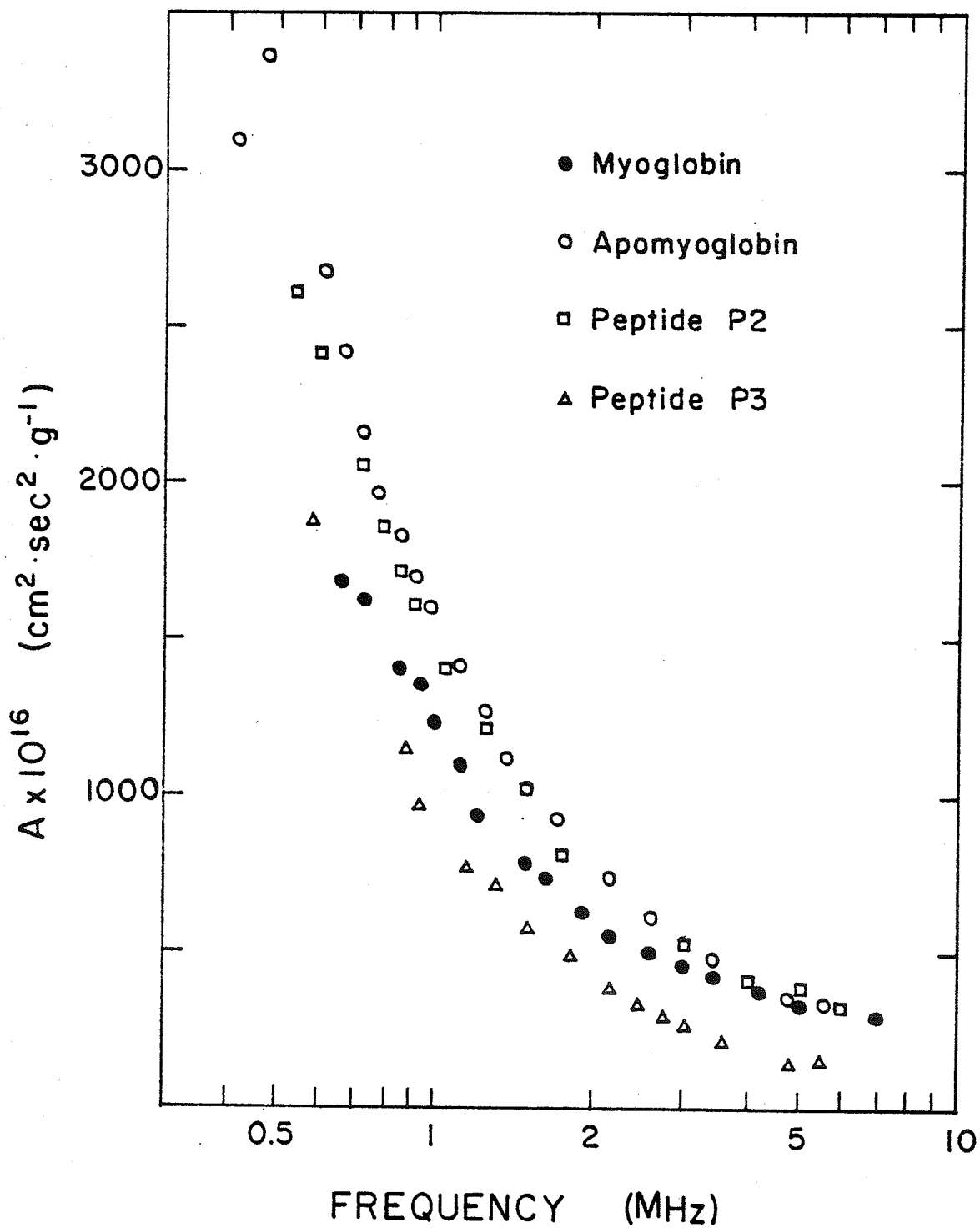


Figure 5.1 Absorption in solutions of myoglobin, apomyoglobin and peptides P2 and P3.

not allow the complete relaxation curve to be determined for these materials. Extension of the lower frequency limit attainable in the cylindrical resonator would necessitate the use of much larger volumes (>40 ml) of specimen solution and thus negate the low volume advantage of the current resonator design. However, it is apparent that some sort of relaxational absorption is occurring, probably a distribution of relaxations owing to the complexity of the molecules involved. These curves also bear a resemblance to those obtained for other proteins. Comparison can be made with the curve shown in Fig. 5.2, after O'Brien and Dunn (1972), which represents data for hemoglobin over a slightly greater frequency range than used in this study. In the case of hemoglobin, a reasonable fit to the data was made by using four discrete relaxation frequencies. Again, the similarities in these curves suggest that more than one relaxation is contributing to the absorption by materials represented in Fig. 5.1

Absorption values for  $\alpha$ -lactalbumin and bacitracin are plotted in the same manner in Fig. 5.3. These curves have an appearance much like those in Fig. 5.1 and a similar interpretation may be applied to them. Measurements on bacitracin have been made over the wider frequency range, 0.2 to 150 MHz (Slutsky *et al.*, 1977). A reasonable fit to the data was obtained by assuming relaxations occurred at 0.33 MHz and 7.3 MHz. The suggestion was made that the relaxation

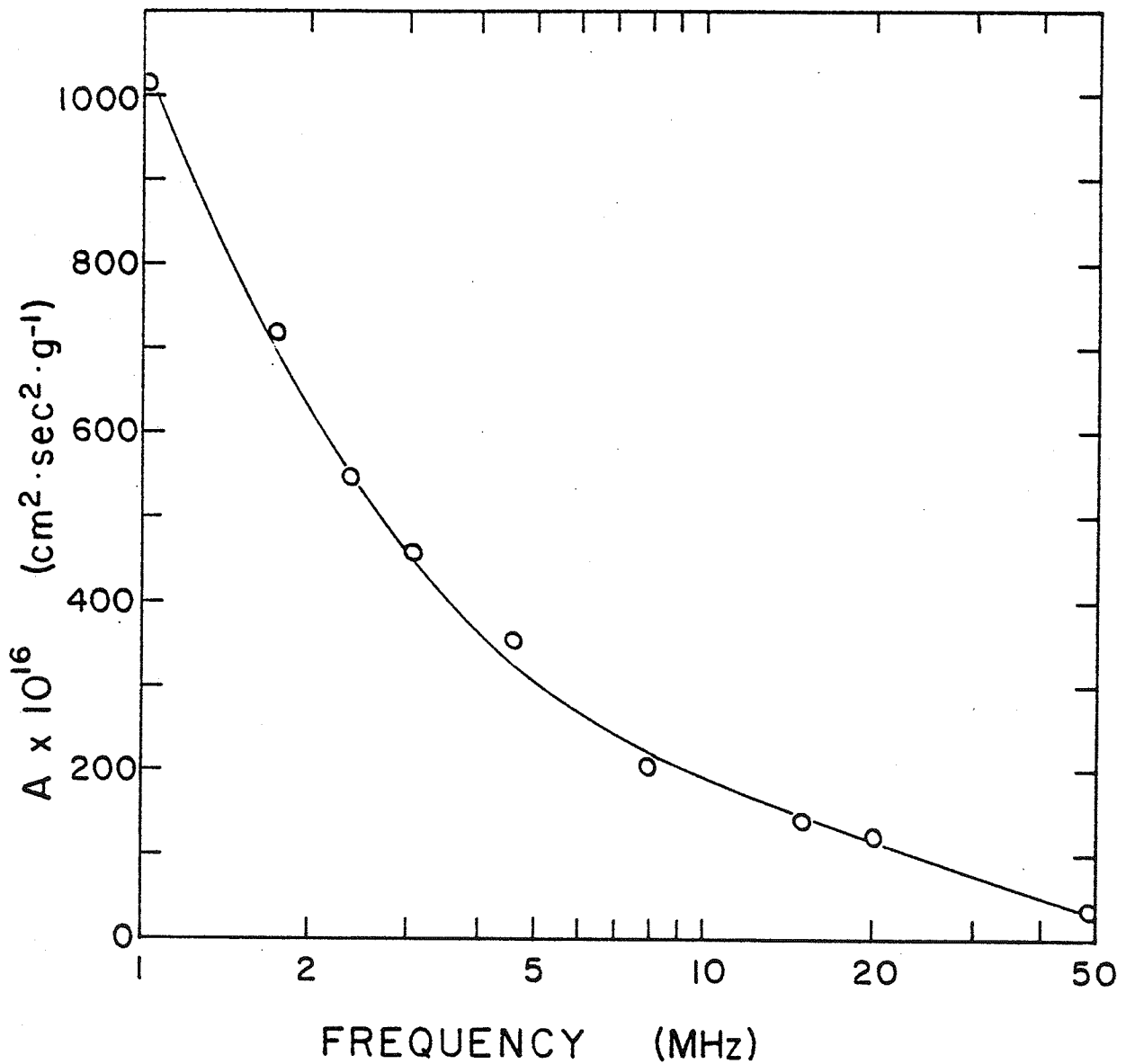


Figure 5.2 Absorption in solutions of hemoglobin  
(after O'Brien and Dunn, 1972).

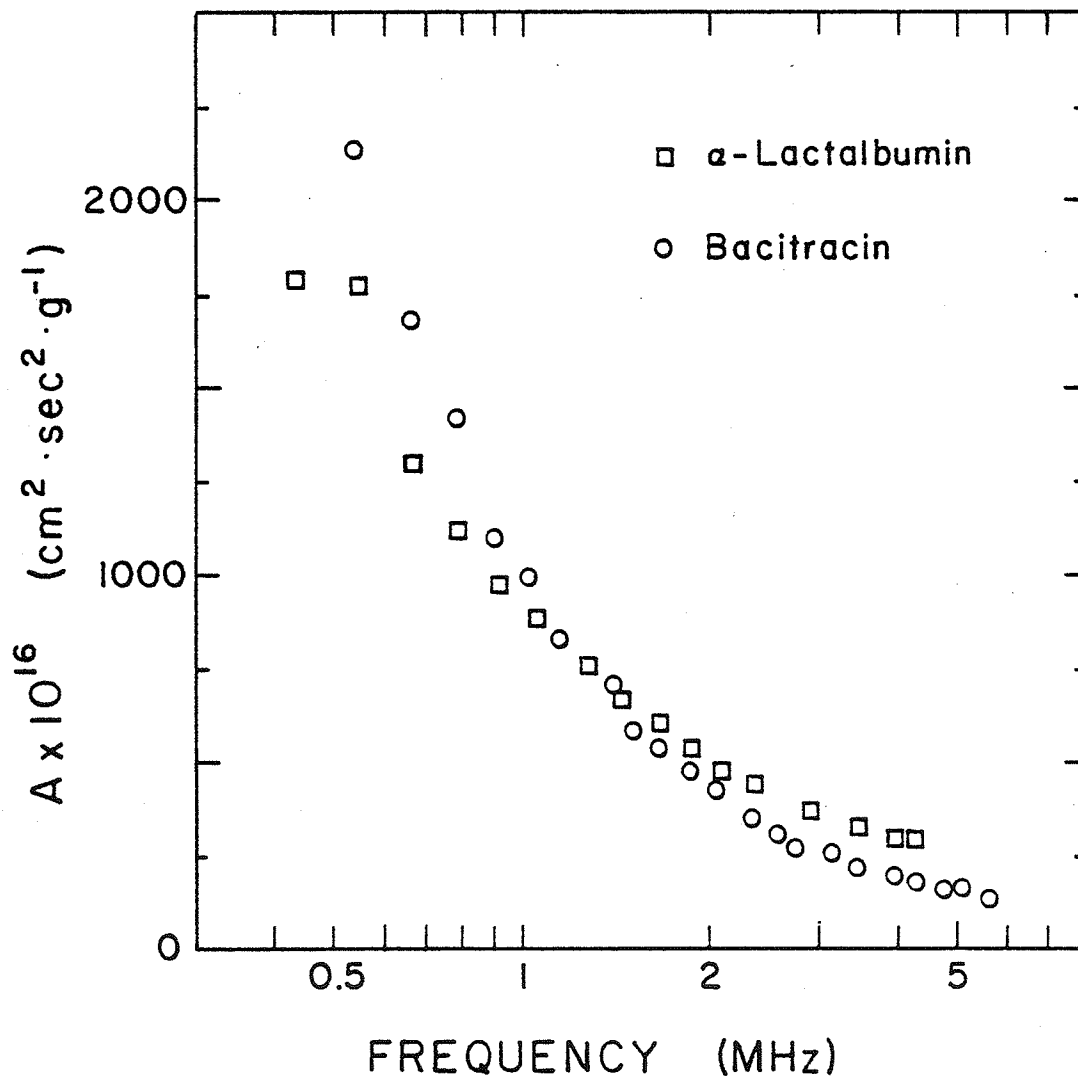


Figure 5.3 Absorption in solutions of  $\alpha$ -lactalbumin and bacitracin.



frequency of 7.3 MHz may be associated with a perturbation of solvation equilibrium around isoleucine residues.

Based on the discussion of relaxational data presentation in chapter 2, it may be possible to gain some information by comparing the semi-logarithmic plots of frequency-free absorption with the same data in a double logarithmic presentation. Figure 5.4 is such a plot for myoglobin and peptides P2 and P3. Notice that while the curve for myoglobin shows a definite tendency toward levelling off at the higher frequencies, such is not the case for the curves representing the peptides. A double logarithmic plot of frequency-free absorption will not level off at high frequency when no relaxation occurs at a still higher frequency. The straight line curves for peptides P2 and P3 in Fig. 5.4 indicate that no relaxations are associated with these specimens at higher frequencies, or that if any such relaxations exist, their magnitudes are much smaller than the magnitudes of those occurring in the frequency range of this investigation. The data for myoglobin, however, show a definite levelling off, indicating the presence of significant relaxational absorption at higher frequencies.

In general, these higher frequency relaxations may be related to the degree of structural complexity in the molecule. Optical measurements by Hermans and Puett (1971) show that the peptides P2 and P3 contain 15 and 8 percent helical structure, respectively, under the conditions present during these measurements. Myoglobin, on the other hand,

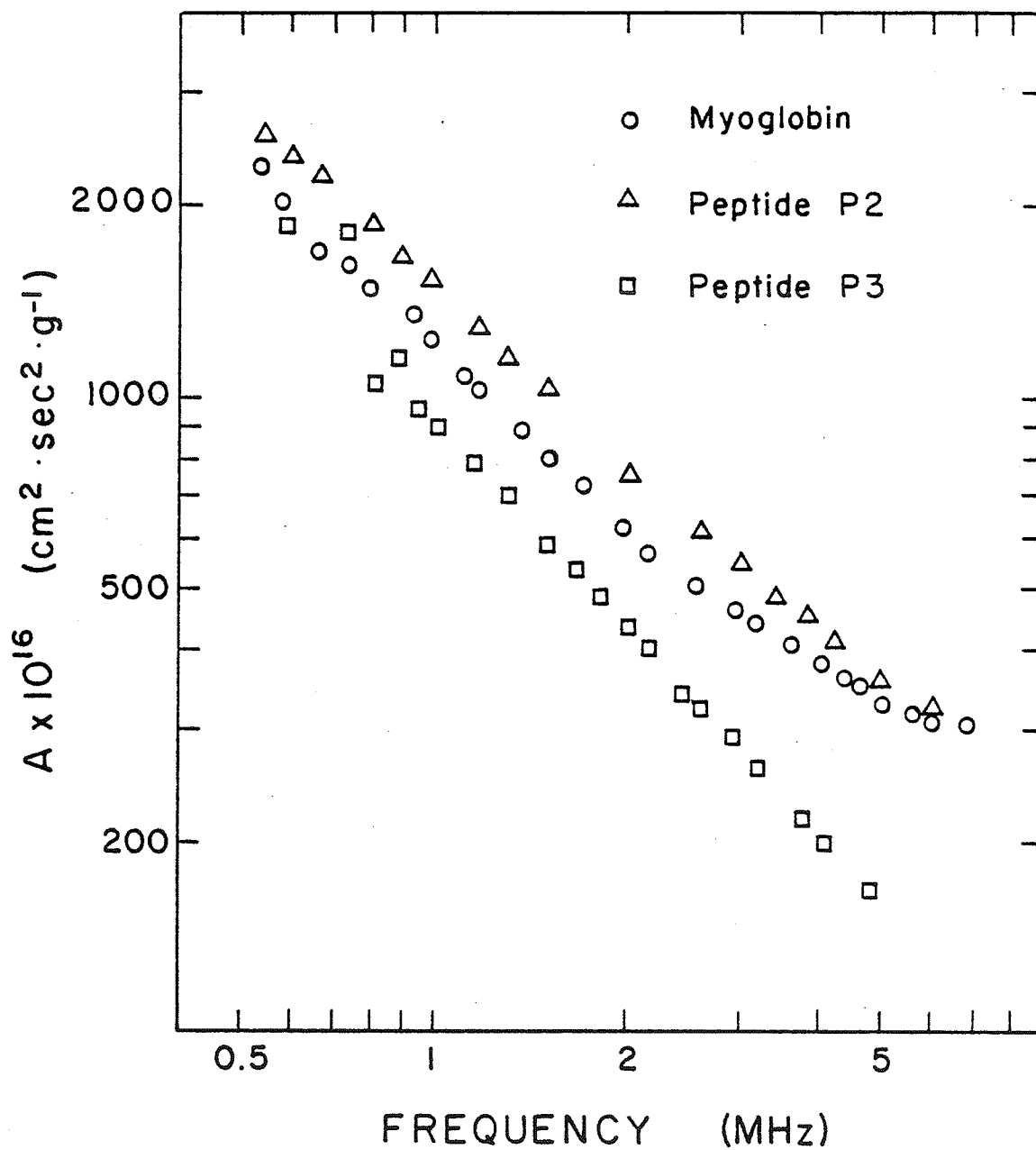


Figure 5.4 Double logarithmic presentation of absorption in solutions of myoglobin and peptides P2 and P3.

consists of a great deal more helical structure and a complex tertiary structure. Like myoglobin,  $\alpha$ -lactalbumin is a complex structure (very similar to lysozyme). A double logarithmic plot of the data for  $\alpha$ -lactalbumin and bacitracin is given in Fig. 5.5 where the appearance of the  $\alpha$ -lactalbumin curve is much like that of myoglobin and that of bacitracin is similar to those of the peptides. Thus, the higher order structure present in myoglobin and  $\alpha$ -lactalbumin seems to cause a significant relaxation at frequencies higher than those employed in this study. The lack of such structure in bacitracin and the peptides P2 and P3 may account for the lack of significant higher frequency contribution to the relaxation spectrum of these materials.

5.1.2 Effect of pH. The ultrasonic absorption of solutions of apomyoglobin and peptide P2 was not determined at pH 7 due to their insolubility at that pH. As both of these products were obtained from an acidic solution, their pH upon solution in distilled water was about 4.5. The pH could be raised to about 5.8 at which point the solution took on a cloudy appearance. This turbidity increased with pH until, near pH 7, a precipitous mass was produced.

Absorption measurements were made at several pH values below 5.8 for peptide P2. Figure 5.6 is a plot of A against frequency for three pH values. The general effect of a decrease in pH is to reduce the overall absorption.

Since the absorption changed as a function of pH, the possibility of proton transfer as the cause was investigated.

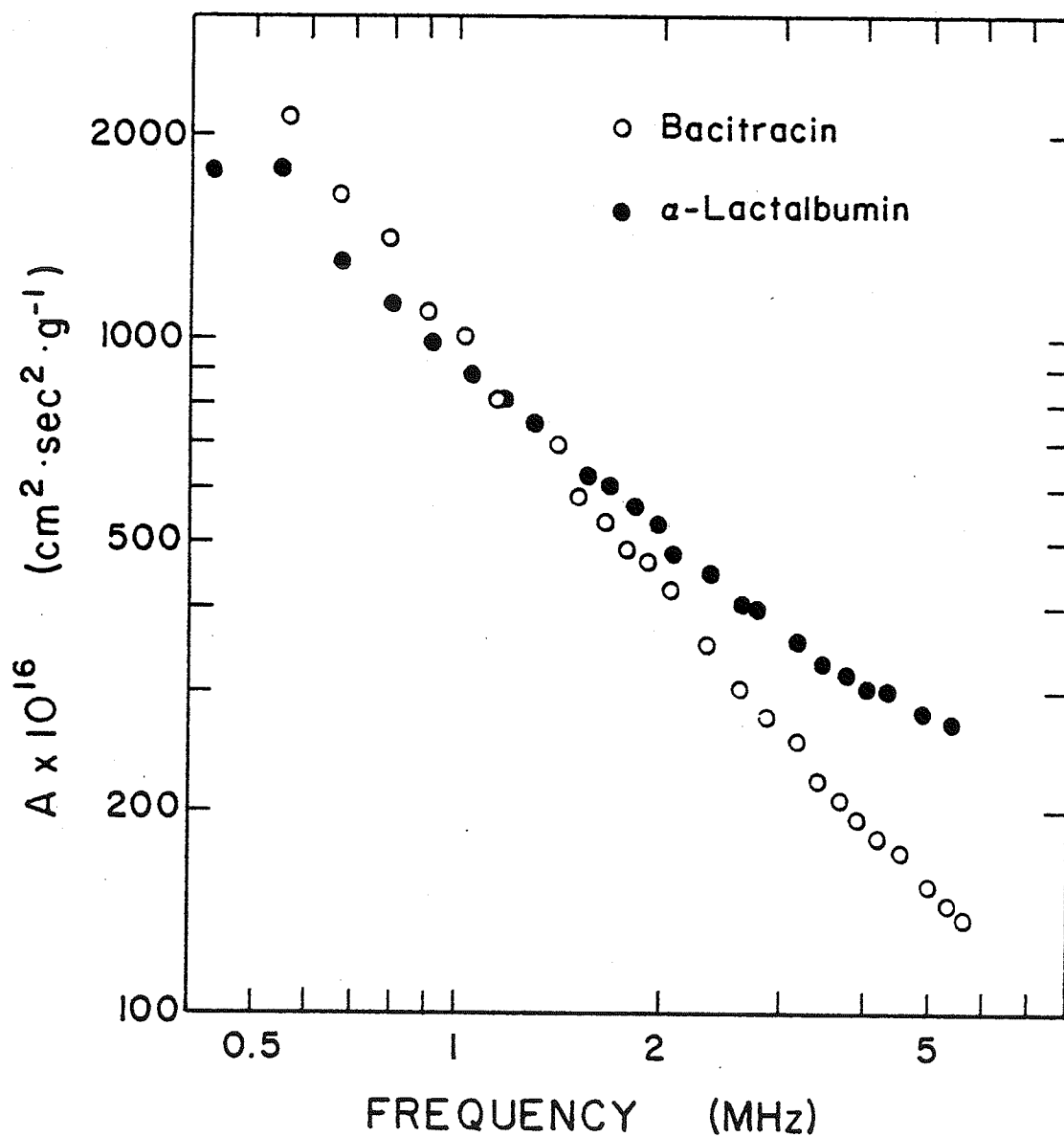


Figure 5.5 Double logarithmic presentation of absorption in  $\alpha$ -lactalbumin and bacitracin.

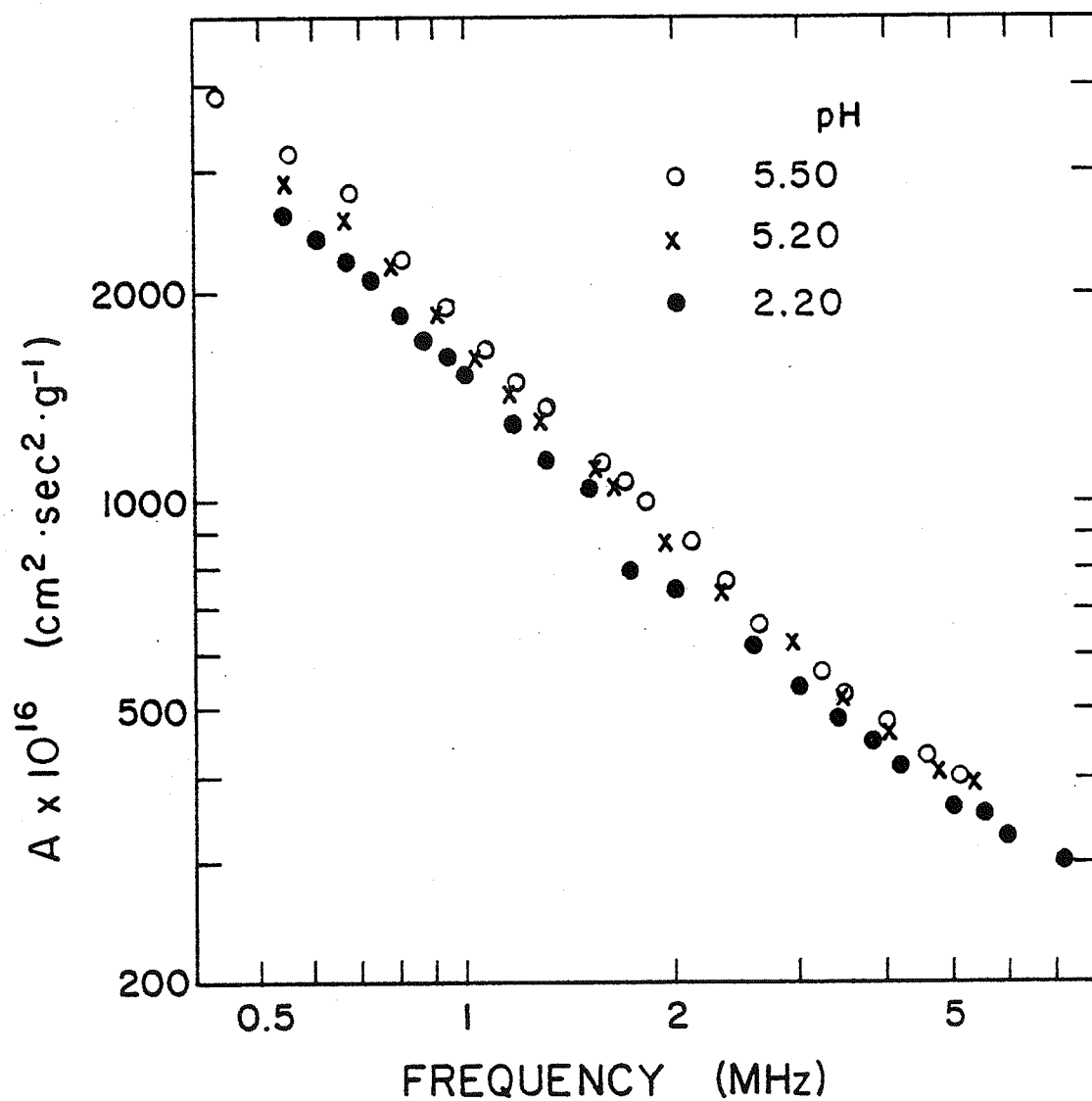


Figure 5.6 Dependence of absorption in solutions of peptide P2 on pH.

The only residue which might titrate near pH 5.8 is histidine. The pK values of all the histidine residues in sperm whale myoglobin have been measured using NMR techniques (Botelho and Gurd, 1976), and are listed in Table 5.2

Table 5.2

Observed Histidine pK Values in Sperm Whale Myoglobin				
5.33	5.53	6.34	6.65	7.97
5.37	6.21	6.44	6.72	8.05
5.39	6.31	6.55	6.83	

Peptide P2 contains four histidine residues and it is possible that one or more of these may possess a pK in the vicinity of 5.8. A calculation of absorption due to proton transfer has been made using eqn. 2.55 and assuming a pK of 5.5. Even for a relatively large associated volume change of  $30 \text{ cm}^3/\text{mol}$  (Hussey and Edmonds, 1971c), this contribution is still about  $10^4$  times too small to account for the difference in absorption between pH 2.2 and pH 5.5.

It is more likely, therefore, that the increase in absorption seen with pH for this peptide is associated with its solubility properties. Polystyrene and DNA both show an increased absorption when conditions are such that insolubility is being approached (Sturm *et al.*, 1972). Thus, the increase in absorption with pH in solutions of P2 is probably due to some manner of association between peptide molecules which is favored as residues (histidines) are neutralized. In fact, examination of the amino acid

composition of peptide P2 reveals that a type of balance between polar, charged, and non-polar amino acids exists which could be shifted toward insolubility as histidines are deprotonated. That is, deprotonation of a histidine residue produces an uncharged amino acid which then interacts less favorably with the polar water molecules and therefore tends to be insoluble.

Peptide P3 exhibits a different behavior. The absorption by this material is shown at pH 7.0 and 5.2 in Fig. 5.7. It is soluble throughout the pH range 2 to 9 but was found to be unstable at pH 2.2. In any case, it is evident that the absorption by peptide P3 is independent of pH within the accuracy of these measurements. This is consistent with histidine/solubility related absorption in peptide P2 since peptide P3 contains no histidine residues.

5.1.3 Dependence on Molecular Weight. One of the primary goals of this investigation was to examine the molecular weight dependence of absorption in solutions of small proteins and peptides. Figure 5.8 is a plot of the specific frequency-free absorption against molecular weight for the materials under study at three frequencies. Also included are values for diglycine and triglycine at a higher frequency (Hammes and Pace, 1968). This plot can be compared to similar ones for the polymers dextran and PEG, shown in Figs. 5.9 and 5.10 (Hawley and Dunn, 1969; Kessler *et al.*, 1970). In all cases the dependence of absorption on molecular weight exists only below a particular molecular weight. This dependence is

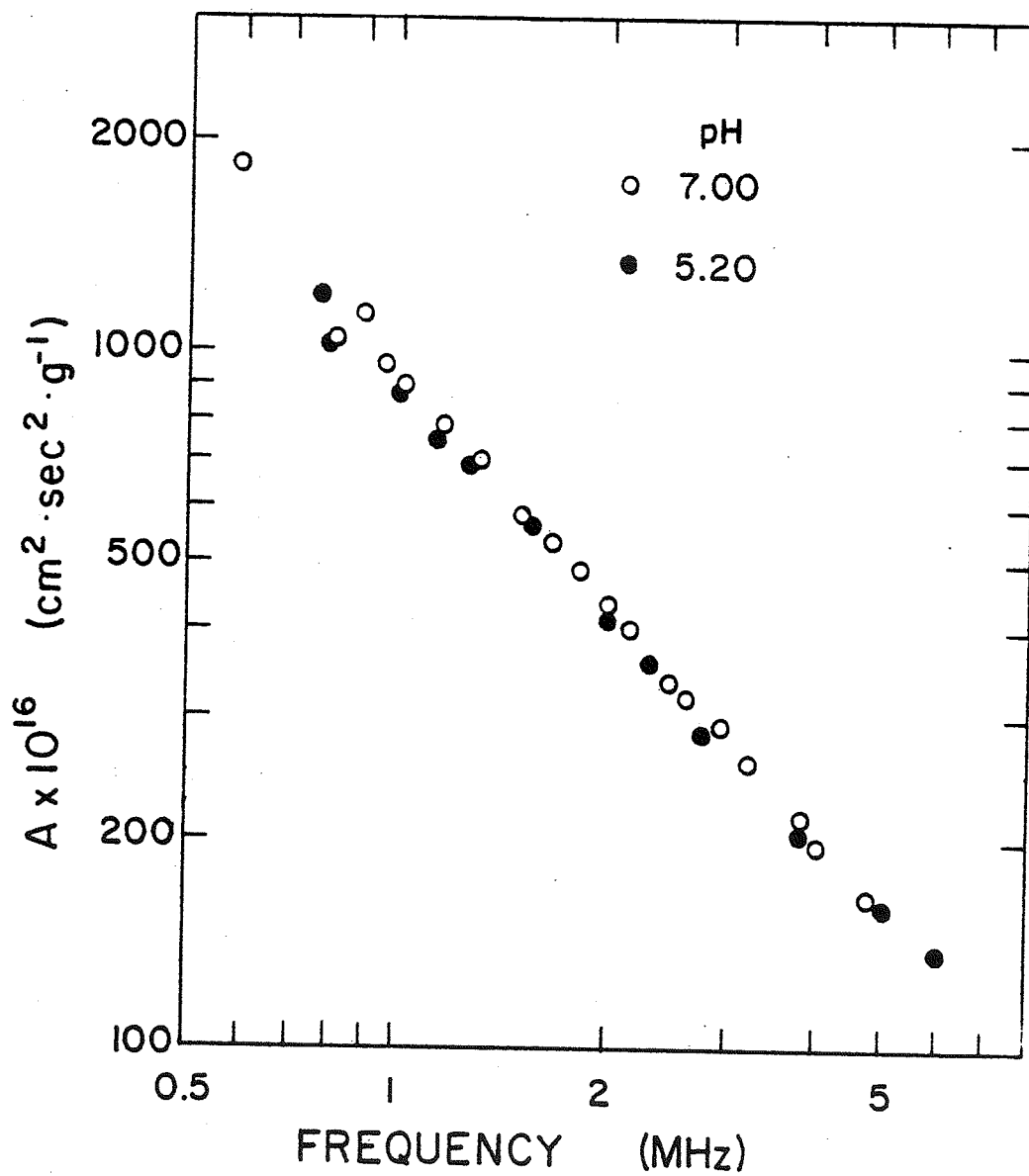


Figure 5.7 Dependence of absorption in solutions of peptide P3 on pH.



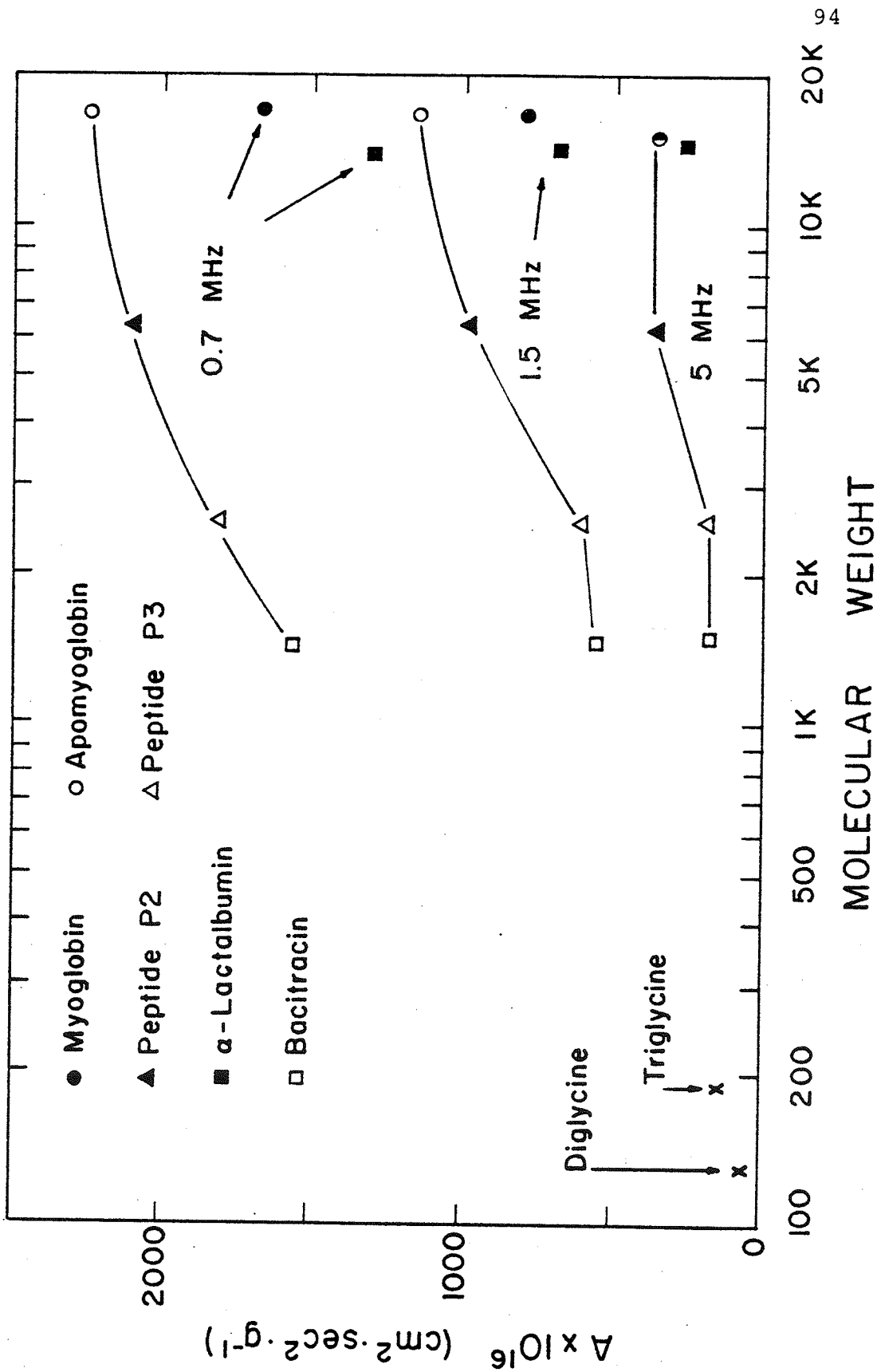


Figure 5.8 Dependence of absorption in solutions of proteins and peptides on molecular weight.

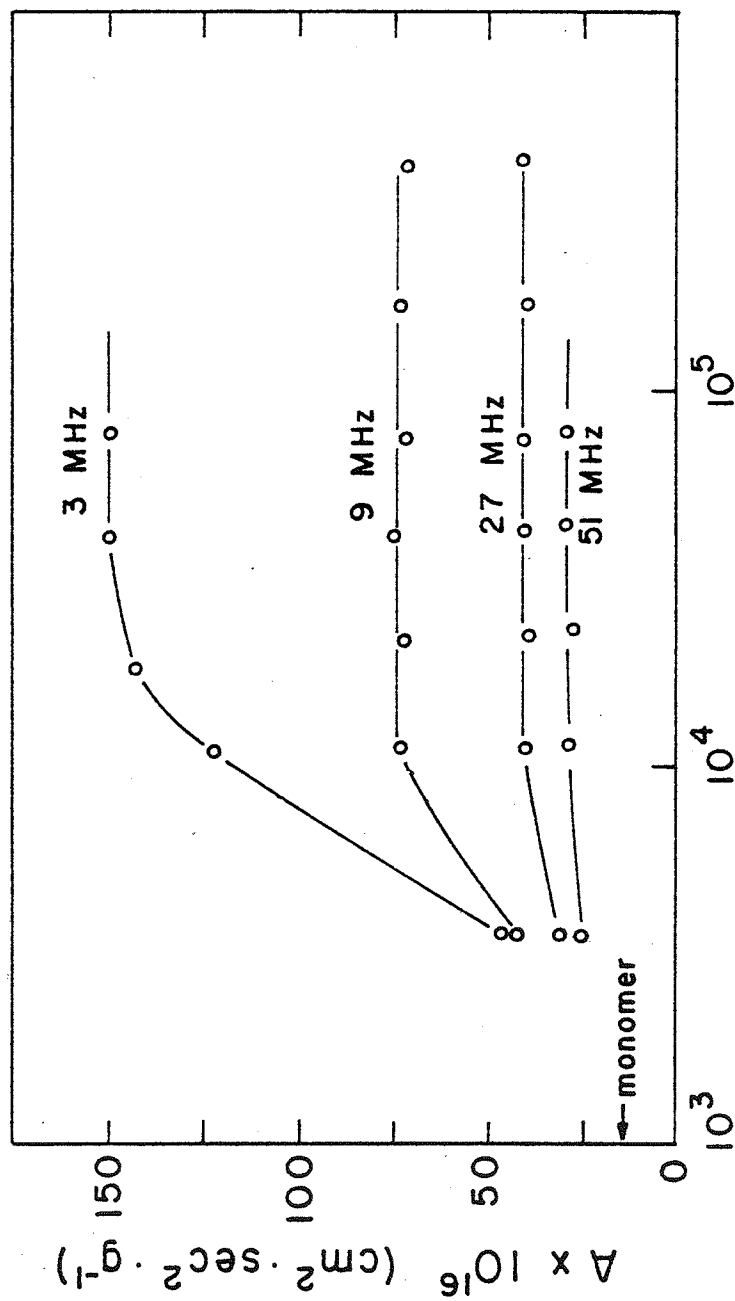


Figure 5.9 Absorption in solutions of dextran (after Hawley and Dunn, 1969).

### MOLECULAR WEIGHT

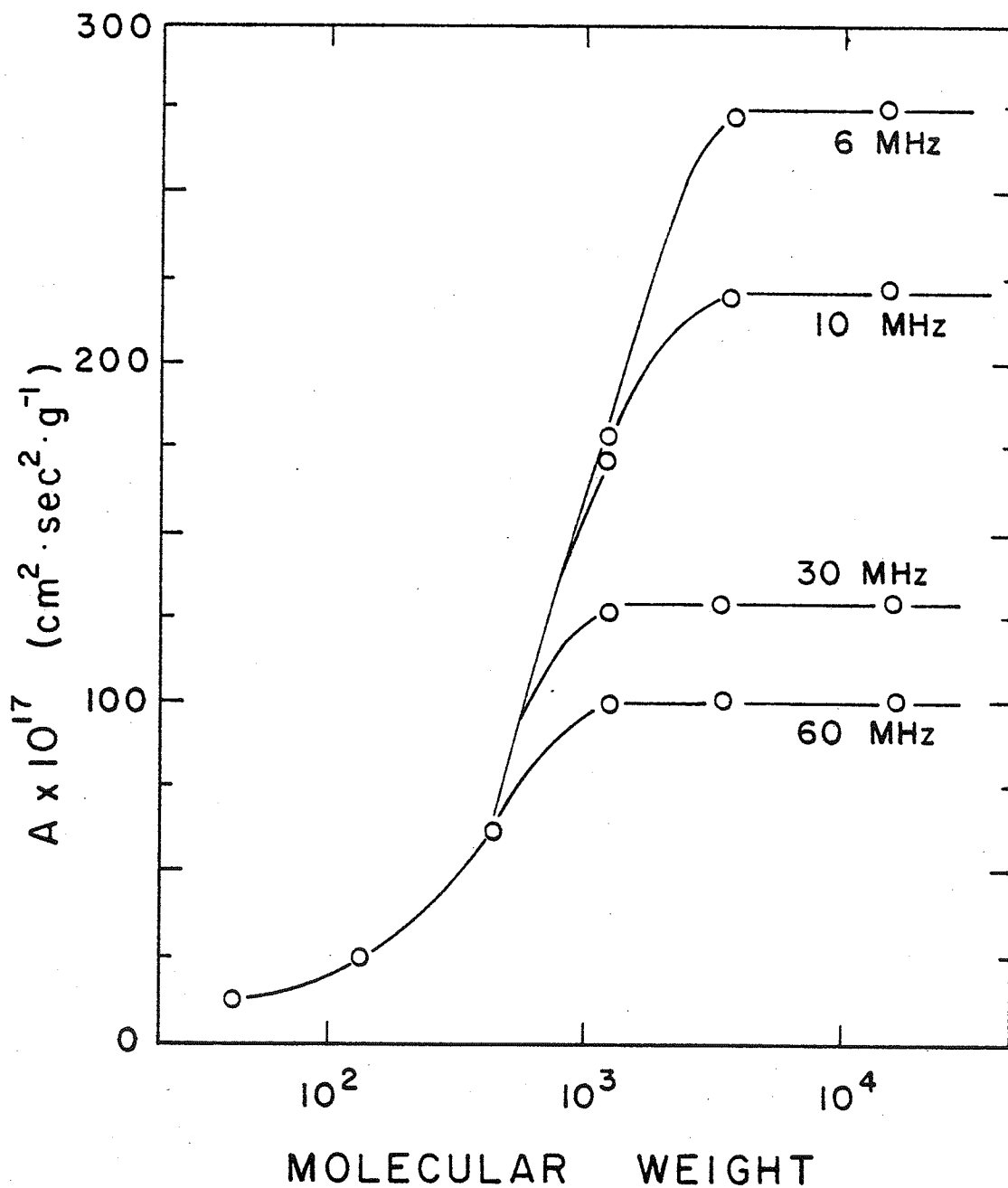


Figure 5.10 Absorption in solutions of polyethylene glycol (after Kessler *et al.*, 1970).

also consistently more pronounced at the lower frequencies. The points corresponding to myoglobin and  $\alpha$ -lactalbumin fall below the smooth curves drawn through the other points. An explanation for this discrepancy will be advanced later.

The similarity of the curves in Figs. 5.8-5.10 suggests that the same mechanism may be responsible for the absorption in each case. Hawley and Dunn (1969) have analysed the data for dextran, treating the polymer as a free-draining coil and attributing the absorption to the viscoelastic properties of the polymer solution. The resulting model agreed qualitatively with the experimental observations but predicted a magnitude of absorption much less than that observed. The suggestion was made by these investigators that the normal modes of the polymer involved in shear viscoelastic behavior may be coupled to another relaxation process involving the solvent. In this process rearrangement of the water molecules along the polymer chain may occur as a result of its interaction with the ultrasound.

This theory has been given support by the results of another study of dextran (Kato *et al.*, 1980). Measurements were made by these investigators on dextrans of various molecular weights as well as on the saccharides maltose, glucose and raffinose. No relaxational absorption was observed for the saccharides while all the dextrans produced absorption spectra which could be fit with two relaxations occurring at about 1 and 15 MHz. Variation in temperature has also been used to affect the degree of hydration (Gekko and

Noguchi, 1971). The relaxation frequencies showed little dependence on the temperature, and so the relaxations were thought to be due primarily to volume changes (as opposed to enthalpy changes). The relaxation amplitudes, however, showed an excellent correlation with the degree of hydration. This was the case for both the 1 and the 15 MHz relaxations. As before, the conclusion was drawn that the acoustic wave perturbs the segmental motion of the polymer chain in such a way as to cause a rearrangement of the water molecules which interact weakly with the chain.

Perturbation of solvent structure is also a possible mechanism of absorption in solutions of PEG. In an investigation by Hammes and Schimmel (1967) the effect of urea on absorption in PEG solutions was examined. The presence of urea in distilled water significantly decreases absorption by water. The most likely cause is a change in the water structure, more closely packing the water molecules. This hypothesis is supported by evidence of a decrease in the adiabatic compressibility and an increase in the density. The results of measurements on solutions of PEG-urea indicate that the absorption due to the PEG is intimately related to the nature of the solvation around the polymer.

Another mechanism has been suggested for this polymer by Kessler *et al.* (1970). Measurements by these investigators over the frequency range 1.5 to 163 MHz showed that the absorption spectrum for PEG cannot be satisfactorily fit by a single relaxation as had previously been supposed (Hammes and

Lewis, 1969). Calculations by Kessler and co-workers showed that dynamic shear viscosity alone could not account for the absorption observed. They proposed two possible mechanisms. One, mentioned above, was perturbation of the hydration structure surrounding the polymer. The other was a structural perturbation of the polymer's short-range configuration. A case was made for involvement of a structural equilibrium between zig-zag and meandering forms of PEG, and was able to explain the molecular weight dependence shown in Fig. 5.10.

With regard to the molecular species of the present investigation, it is reasonable to suggest that for those molecules whose absorption values fall along the smooth curves of Fig. 5.8, a significant amount of the absorption is due to perturbation of the hydration equilibrium. As in the case of dextran, this may be coupled to the ultrasound through motions of the peptide chain itself. This claim is made only for the molecules which exist to some extent as random coils without appreciable tertiary, globular structure.

In the cases of myoglobin and  $\alpha$ -lactalbumin, each having extensive helical secondary and globular tertiary structure, the absorption falls below that of the other materials. This discrepancy is more pronounced at the lower frequencies. The absorption associated with the solvent around the globular molecules is lower, perhaps due to the difference in the surface exposed. Estimates of protein surface area can be made using empirical formulas based on data from twelve different globular proteins (Richards, 1977). The surface

area of a native globular protein is given, in  $\text{Å}^2$ , approximately by  $A_n = 11.12 M^{2/3}$ , where  $M$  is the molecular weight, and the area of an unfolded protein is given by  $A_u = 1.45 M$ . Plots of these two functions are shown in Fig. 5.11. If the rather crude assumption is made that the molecules whose absorption falls on the curves in Fig. 5.8 are unfolded, the low absorption in myoglobin and  $\alpha$ -lactalbumin can be partially explained. If, for example, the  $A$  values for myoglobin and  $\alpha$ -lactalbumin at 1.5 MHz were to fall on the smooth curve they would be expected to correspond to molecular weights of 4000 and 3100, respectively. These molecular weights correspond to areas of unfolded proteins of 5800 and  $4495 \text{ Å}^2$ . These areas then correspond to folded molecular weights of 11,912 and 8127, which are 60-70% below the actual molecular weights of myoglobin and  $\alpha$ -lactalbumin. Thus, the difference in surface areas accounts for most, but not all, of the anomalously low absorption in these two globular proteins. However, both the area and the chemical nature (polar, charged, non-polar) of the residues exposed are different for the two types of materials. The somewhat unfolded molecules which fall along the smooth curves in Fig. 5.8 probably expose a greater percentage of non-polar amino acids to contact with the water. This could account for the additional discrepancy between absorption by these materials and myoglobin and  $\alpha$ -lactalbumin.

Involvement of bound solvent in absorption mechanisms has also been indicated in solutions of diglycine, triglycine

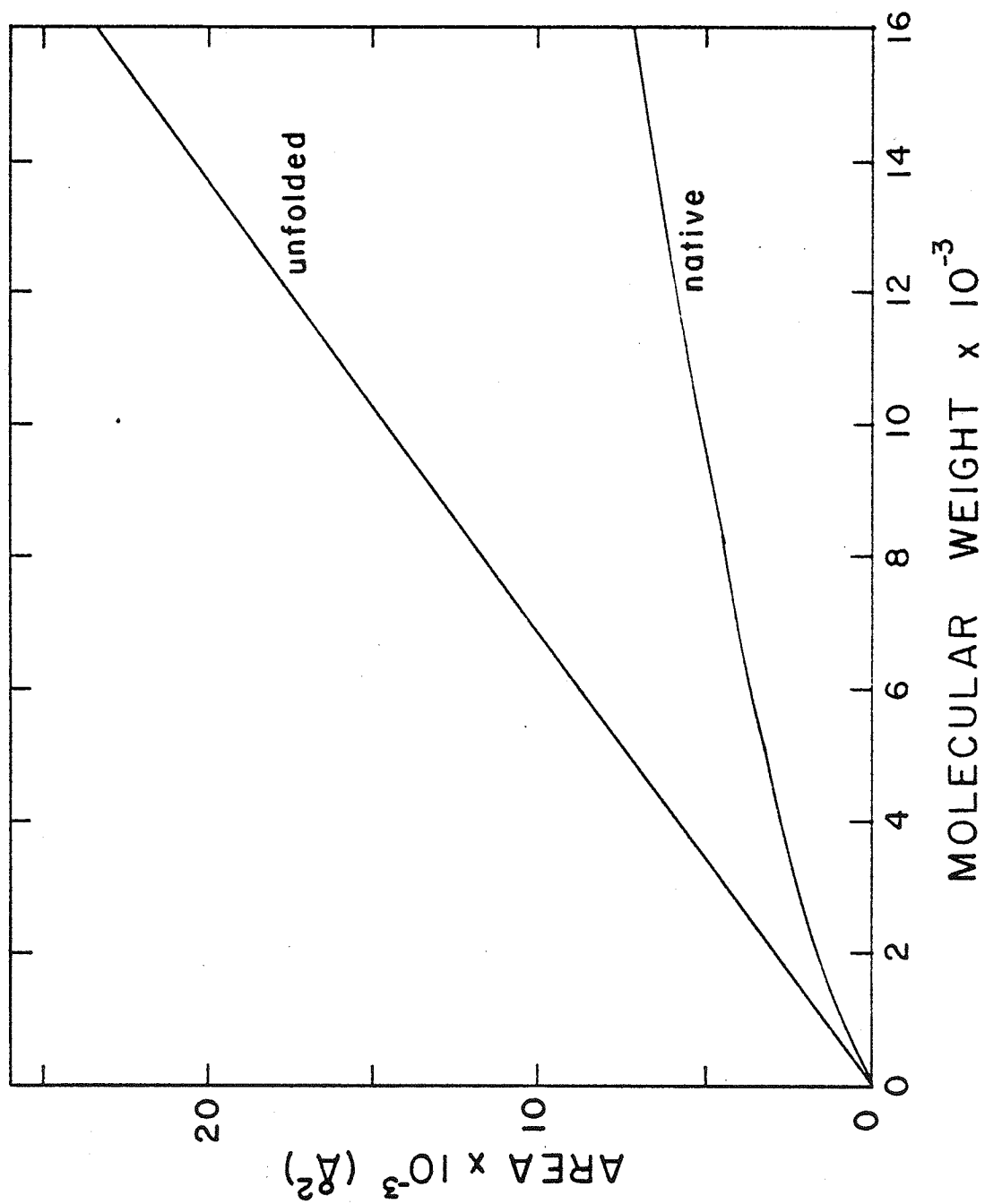


Figure 5.11 Dependence of protein surface area on molecular weight (after Richards, 1977).



(Hammes and Pace, 1968), polyglutamic acid (Burke *et al.*, 1965) and gelatin (Wada *et al.*, 1967). In addition, the amount of hydrating water around the polymer polyvinyl pyrrolidone greatly affects its absorption (Nomura *et al.*, 1975). This polymer has been used as a model for proteins since it has side chains of  $-\text{N}-\overset{\text{O}}{\parallel}{\text{C}}-$  groups. Absorption in a solution of this material decreases significantly as the temperature is increased. Since the degree of hydration around this molecule has been independently found to decrease with increasing temperature, the solvent must be involved in the absorption process.

5.1.4 Effect of Phosphate. Slutsky *et al.* (1977, 1980) have studied the absorption characteristics of the antibiotic bacitracin. In the later study, these investigators examined the effect of phosphate buffered solution on the absorption by bacitracin. The pK of the single histidine residue of bacitracin (6.9 at room temperature) is such that significant proton exchange may occur between this moiety and a phosphate ion. The difference between the absorption by bacitracin in the presence and absence of phosphate was measured as a function of frequency. In the case of a solution 0.01M in bacitracin and 0.1M in phosphate, this difference yielded a curve which was fit extremely well by a single relaxation at 1.2 MHz. This was modeled as a proton transfer relaxation and reasonable kinetic and thermodynamic parameters were obtained for the reaction. Such a mechanism was proposed by these

investigators as a significant contributor to in situ absorption in tissue.

Based on these studies it appeared appropriate to test the effect of phosphate on the materials of the present investigation. Measurements were made with myoglobin and peptide P3, though not with peptide P2 due to its insolubility at pH 7. The results of absorption measurements in 0.1M phosphate solution at pH 7.0 are shown for myoglobin and peptide P3 in Figs. 5.12 and 5.13, respectively. The absorption increases dramatically in the presence of phosphate for both myoglobin and peptide P3.

The algebraic difference between absorption with and without phosphate was calculated for these materials and is shown in Fig. 5.14. The behavior observed in myoglobin may well be due to proton transfer between the phosphate ions and residues (presumably histidines) of the protein with pK values near 7. A single relaxation curve, based on eqn. 2.54 is employed to fit the data for myoglobin using the parameters  $f_R=1.65$  MHz,  $B'/c=200$  cm<sup>2</sup> sec<sup>2</sup> g<sup>-1</sup>, and  $A'\tau/c=2220$  cm<sup>2</sup> sec<sup>2</sup> g<sup>-1</sup>, where c now denotes the myoglobin concentration in g/ml. Despite the good fit by this theory, the limited frequency range of the data prevents conclusive proof of single relaxation behavior. The presence of more than one relaxing element would not be surprising since myoglobin, as a complex protein, has more than one site at which proton transfer might occur under these circumstances. However, the nearness of fit suggests that any multiple relaxations are occurring close to

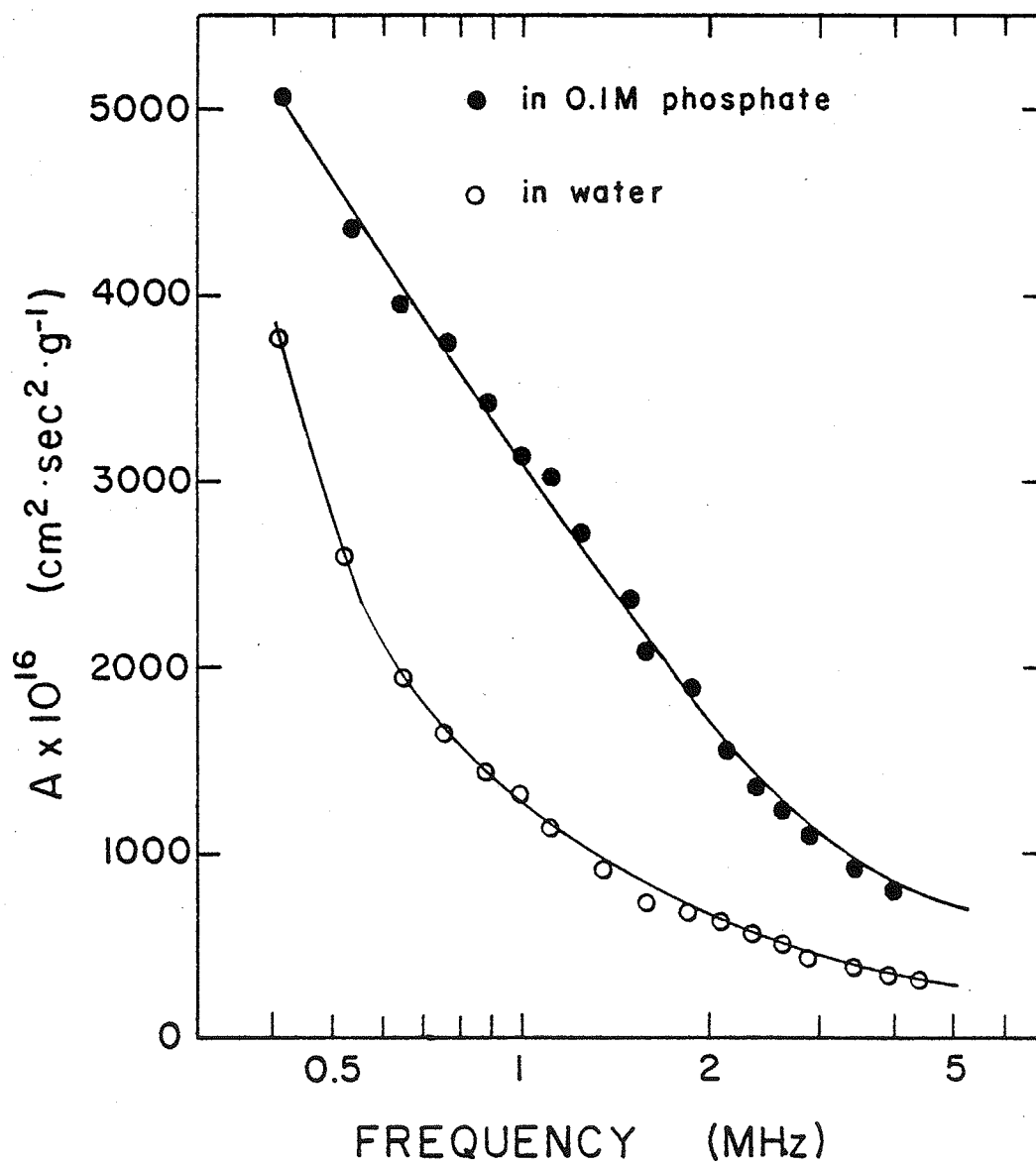


Figure 5.12 Effect of phosphate on absorption in solutions of myoglobin.

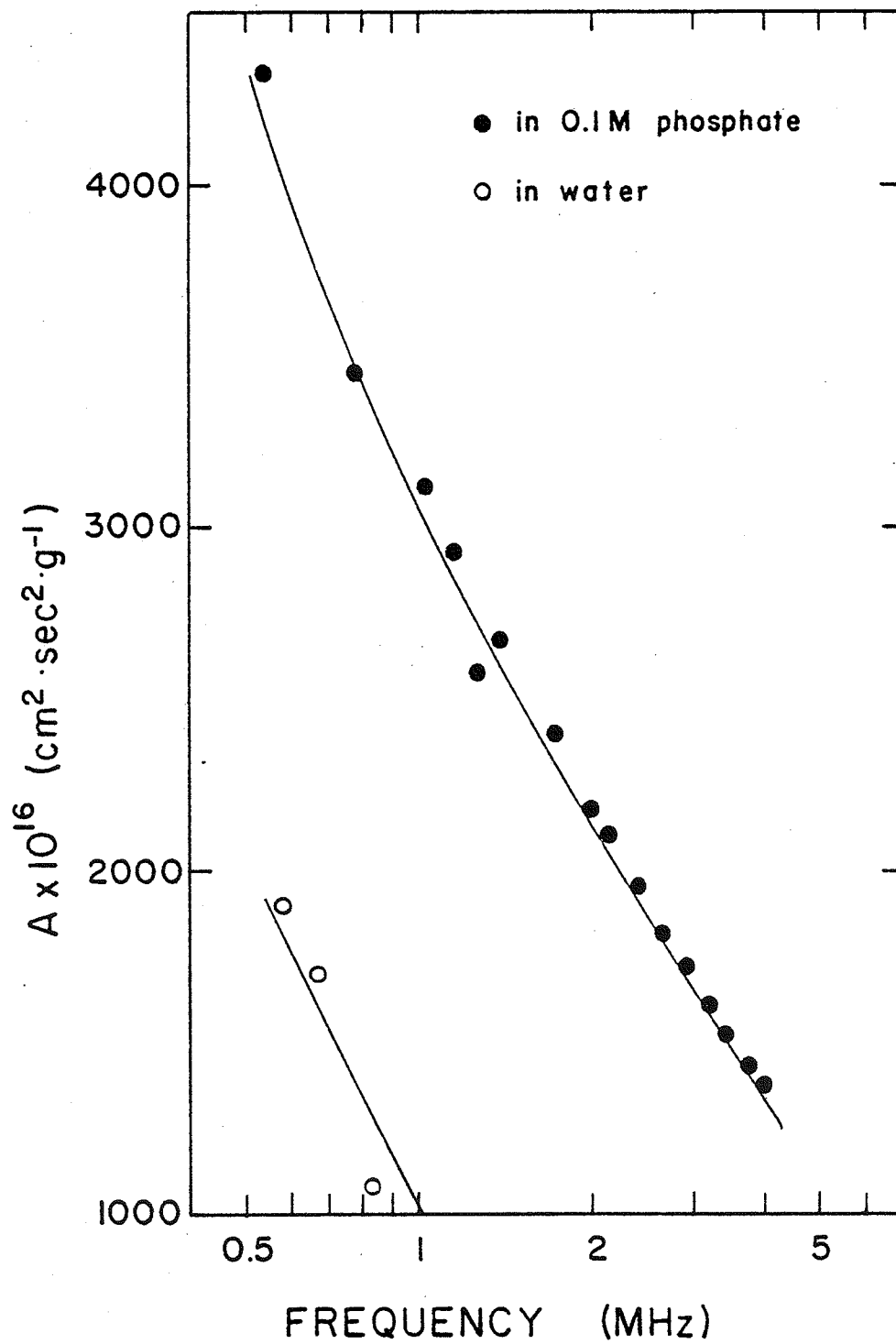


Figure 5.13 Effect of phosphate on absorption in solutions of peptide P3.

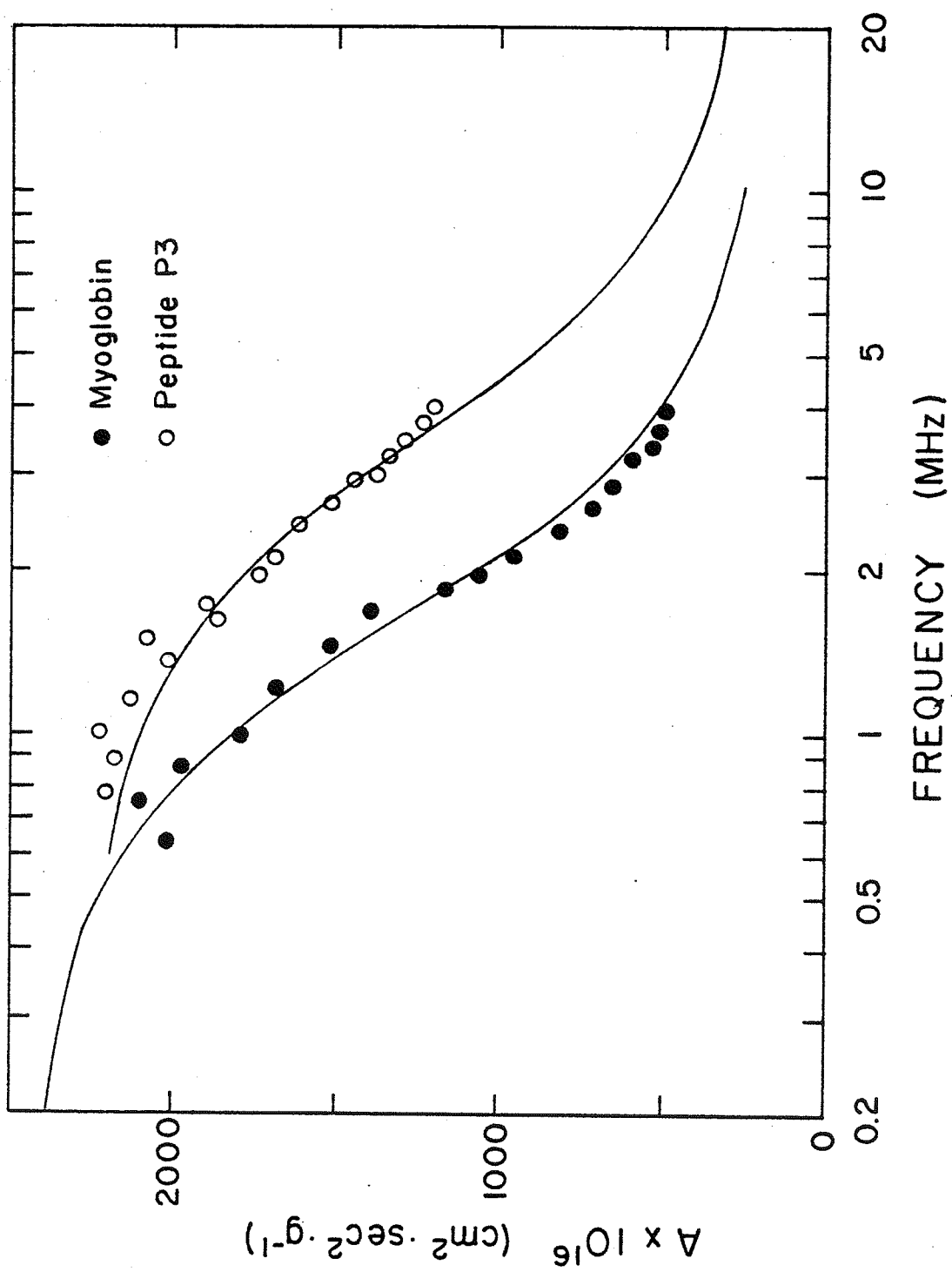


Figure 5.14 Phosphate induced absorption in solutions of myoglobin and peptide P3.

the same frequency. In addition, the relaxation frequency of 1.65 MHz is close to the value of 1.2 MHz obtained by Slutsky for the histidine of bacitracin.

Although a large increase in absorption by peptide P3 was caused by phosphate, this cannot be accounted for on the basis of proton transfer. Peptide P3 contains no histidine residues, and any other ionizable residues (lysine, arginine, and glutamic and aspartic acids) should reasonably have pK values at least two pH units away from 7. Again a single relaxation curve is shown for purpose of comparison to the data for peptide P3 using the values  $f_r=3.5$  MHz,  $B'/c=250$  cm<sup>2</sup>sec<sup>2</sup>g<sup>-1</sup>, and  $A'\tau/c=2000$  cm<sup>2</sup>sec<sup>2</sup>gm<sup>-1</sup>. Alternatively, the action of the phosphate ion may be through its effect on the structure of water. Various "chaotropic" anions have been ranked according to their relative effect on water structure in what is known as the Hofmeister series (Dandliker and de Saussure, 1971). The ions at the extremes of this series can be thought of as structure makers or structure breakers. By all criteria, the phosphate ion is near the extreme of structure makers which tend, apparently, to increase the degree of structure when dissolved in water. For example, shifts of NMR peaks toward higher fields have been observed in sodium salts of  $\text{ClO}_4^-$  and  $\text{I}^-$ , indicating hydrogen bond breaking, whereas shifts toward lower fields have been seen for sodium salts of  $\text{PO}_4^{3-}$ . Thus, it is likely that the structure of the water hydrating the peptide P3 molecule is altered in the presence of phosphate. This difference in

structure manifests itself in a relaxational absorption as seen in Fig. 5.14. This mechanism could also be responsible for part of the phosphate induced absorption in myoglobin. As with myoglobin, the frequency range of the data does not allow verification of only a single relaxation process. The presence of multiple relaxations or a continuous distribution of relaxations with a mean relaxation frequency near 3.5 MHz is also possible. Such behavior is expected from a structural relaxation such as the solvent mechanism.

5.1.5 Conclusions. The results presented above indicate that perturbation of solvent structure around proteins and peptides makes a significant contribution to the absorption of ultrasound. This hypothesis is supported by the molecular weight dependence (Fig. 5.8) of the absorption as well as the effect of phosphate on peptide P3 (Fig. 5.14). This solvent related absorption makes a greater contribution to the absorption of proteins and peptides with significant random coil structure than it does to proteins which are predominantly globular. This may be due to the smaller surface area per unit weight of the globular molecules or to a different chemical nature (amino acids) of the surface.

The molecular weight dependence of the absorption may be related to a cooperative phenomenon occurring in the solvent. Such a mechanism has been proposed by Hammes and Schimmel (1967) to account for the molecular weight dependence of relaxation times observed in solutions of PEG. As the size of the polymers increases, so might the number of water molecules

which participate as a unit in the equilibrium between free and bound water. As the size of the cooperative unit increases, so will the absorption associated with this equilibrium, until some upper limit on the size of the cooperative unit is reached. Such an upper limit may be imposed by the period of the wave as compared to the time required to "communicate" a cooperative change among neighboring water molecules. This would account for the plateau in absorption at high molecular weight characteristic of the polymers discussed above. A cooperative model also provides an explanation for the frequency dependence of the molecular weight effect seen in Fig. 5.8. If the maximum cooperative unit size is directly related to the period of the ultrasonic wave, then a smaller maximum would be expected at higher frequencies. This is indeed the case for the data presented in Fig. 5.8.

Although solvent-structure mechanisms have been indicated here, other mechanisms probably also play an important role in determining the overall absorption by proteins. Slutsky's calculations (Slutsky *et al.*, 1980) show that proton exchange with phosphate may account for a large part of absorption in soft tissues. Also, internal motions of side chains, as suggested by Kanda *et al.* (1976) probably are, in part, responsible for the absorption characteristics of globular proteins. A complete model for absorption by proteins would include, at least, all of these mechanisms.



## 5.2 ULTRASONIC PROPERTIES OF LIPOSOMES

5.2.1 Lipid Bilayers. Measurements of absorption were first made on liposomes, prepared as described in chapter 3, composed of DPPC:DPPG in the ratio 4:1. The results of these measurements are shown in Fig. 5.15 as the difference in absorption per wavelength between the suspension and the solvent at 4 MHz, divided by the lipid concentration. The absorption values at temperatures distant from the transition temperature ( $T_c = 42.5^\circ\text{C}$ , Papahadjopoulos *et al.*, 1975) were only slightly greater than those of the solvent. As the transition is approached, the absorption increases and then reaches a sharp maximum near  $T_c$ .

Also plotted in this figure is the release of an encapsulated drug, cytosine 1- $\beta$ -D-arabino furanoside, as a measure of membrane permeability. A sharp increase in this parameter is seen to occur over the temperature range  $39^\circ\text{C}$  to  $40^\circ\text{C}$ . The release was induced by heating a bulk sample to successively higher temperatures and assaying for released drug after 5 min at each temperature. From Fig. 5.15 it is clear that all of the release occurred when the liposomes were between  $39^\circ\text{C}$  and  $40^\circ\text{C}$  and no more was released at higher temperatures. This release occurred about  $2^\circ\text{C}$  below  $T_c$ .

Measurements on liposomes containing cholesterol support the hypothesis that the ultrasonic absorption maximum is due to the phase transition of the lipids from a crystalline to a liquid-crystalline state. Figure 5.16 shows absorption per wavelength and heat release values for liposomes containing 20

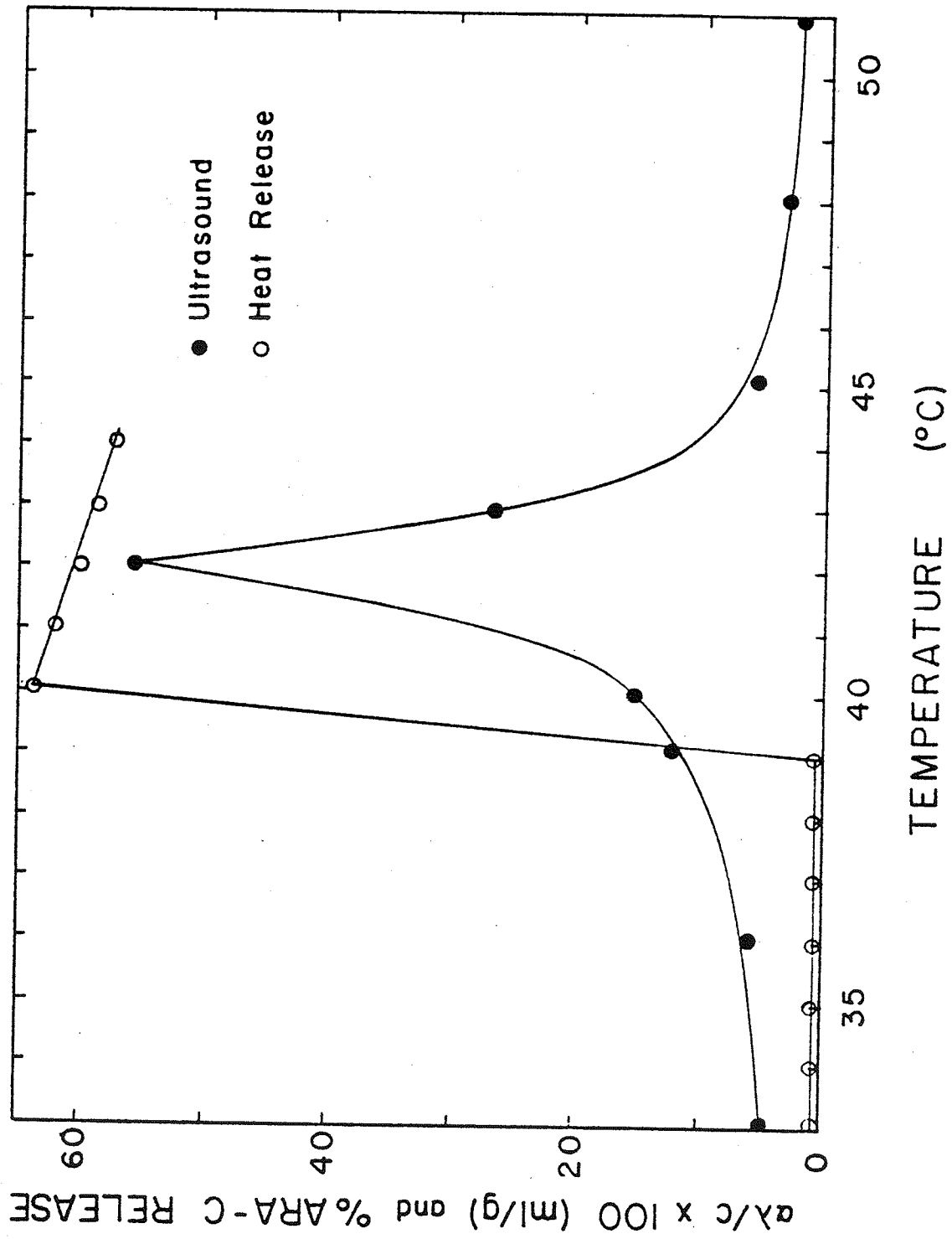


Figure 5.15 Ultrasonic absorption and heat release in pure lipid LUV suspensions.

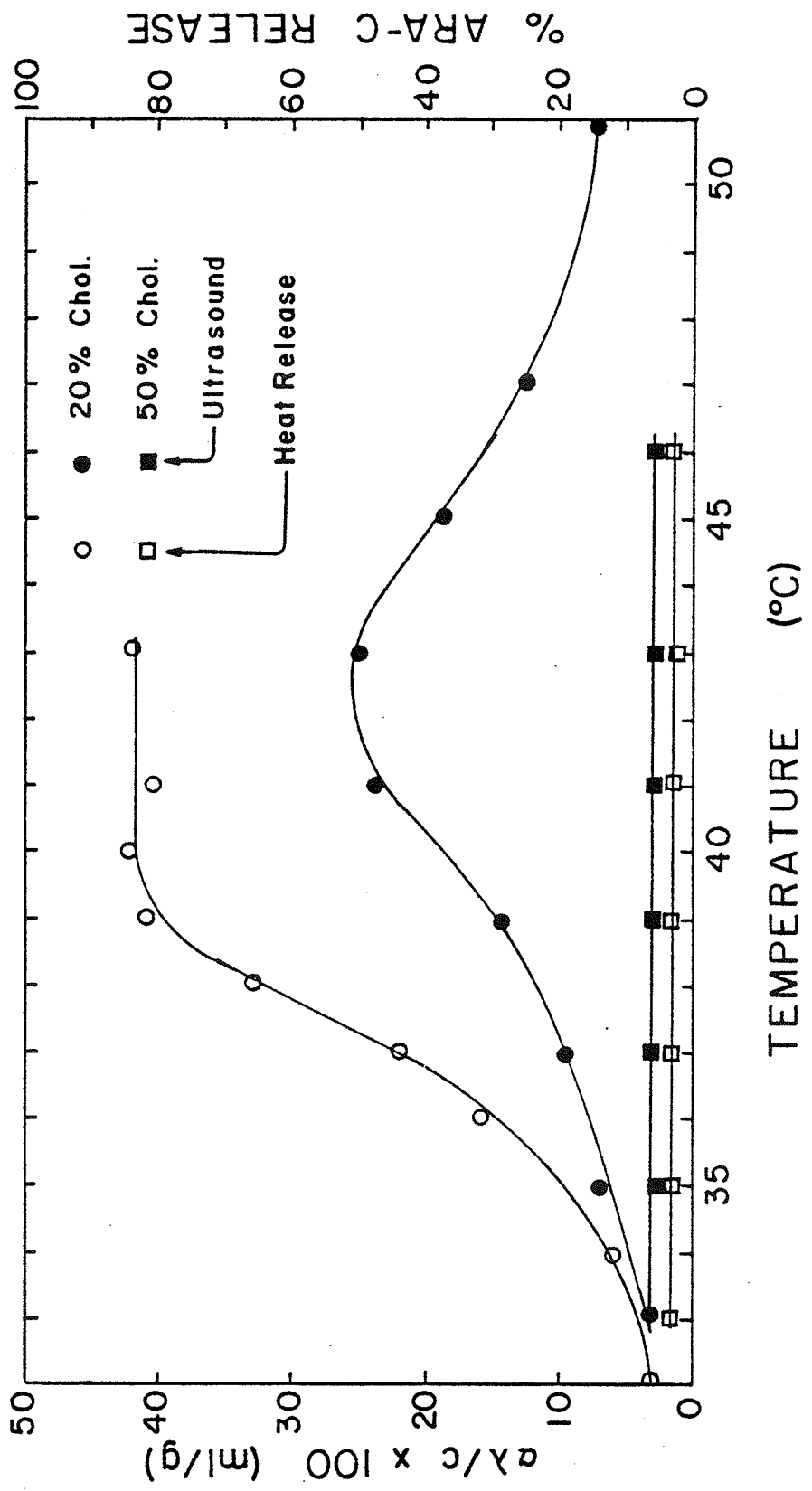


Figure 5.16 Effect of cholesterol on ultrasonic absorption and heat release in LUV suspensions.

and 50 mole percent cholesterol. Comparison to the curves of Fig. 5.15 reveals a broadening of the transition for 20 percent cholesterol and an elimination of the transition by 50 percent cholesterol.

This is expected behavior based on results of calorimetry (Hinz and Sturtevant, 1972). The addition of cholesterol to lipid membranes reduces the latent heat of the transition in a nearly linear fashion until, at 33 mole percent, no transition can be observed calorimetrically. This relation is shown in Fig. 5.17. Evidently, each cholesterol molecule is capable of association with two lipid molecules. In so doing, cholesterol acts as a plasticizer and allows the associated lipids to exist in a semi-fluid state over a wide temperature range (Melchior and Steim, 1976). Thus, at 50 mole percent cholesterol, no ultrasonic absorption maximum was observed, in agreement with calorimetric and heat release measurements.

Having attributed the ultrasonic absorption maximum to the crystalline to liquid-crystalline phase transition, it is appropriate to inquire of mechanisms for this absorption process. As before, it is assumed that some relaxational event is taking place which would account for the absorption. However, the simplification in which a relaxation is assumed to be either primarily structural or primarily thermal cannot be applied to phase transitions (Edmonds and Orr, 1966) due to the fact that oscillations in temperature caused by the ultrasonic wave can perturb structural equilibria associated with the phase transition, as well as interact thermally

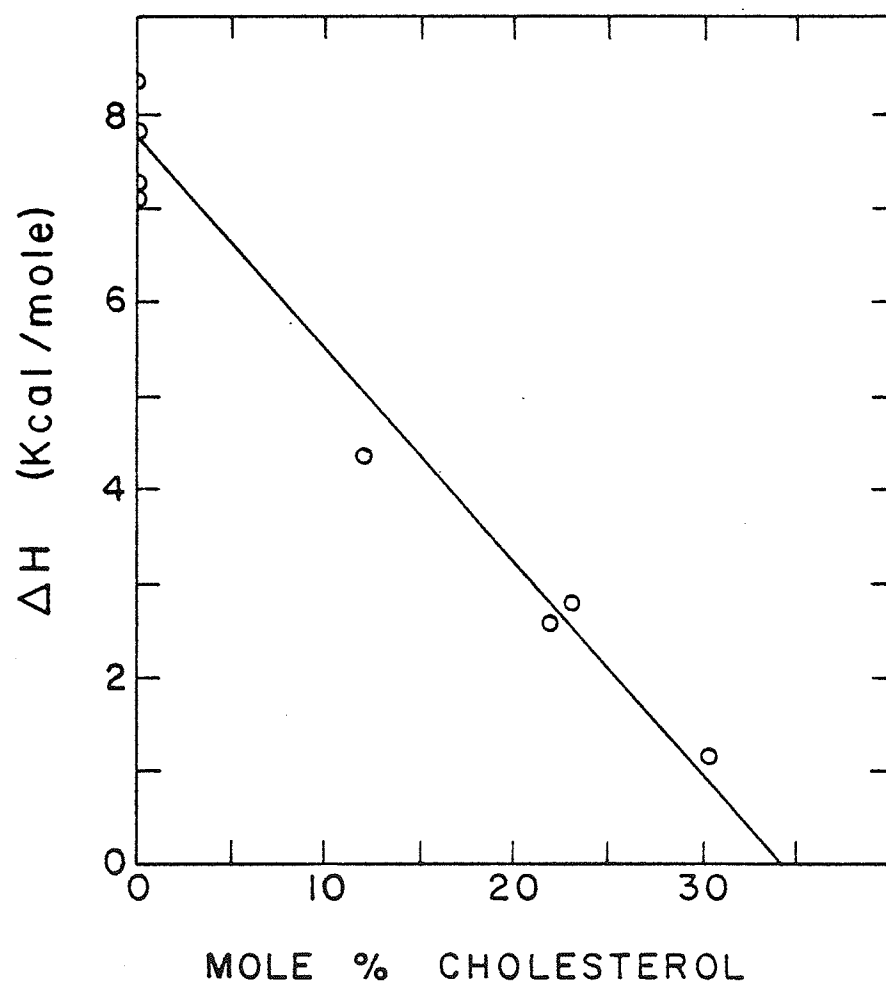
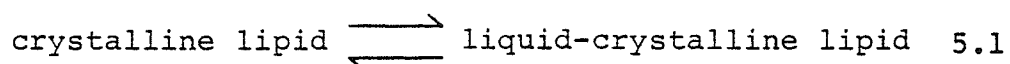


Figure 5.17 Effect of cholesterol on lipid transition enthalpy (after Hinz and Sturtevant, 1972).

through the change in enthalpy. This is not to imply that the absorption maximum may not be due primarily to one type of relaxation or the other, but that such assignment is not possible a priori.

The general equilibrium which the ultrasound has been presumed to perturb is



During the phase change in a liposome, the lipid molecules undergo the transition in state not as independent molecules, but as specific sized cooperative units. The size of a cooperative unit can be estimated from the enthalpy of transition (Papahadjopoulos et al., 1975). In the presence of low concentrations of cholesterol, the enthalpy of transition is decreased due to a reduction in the cooperative unit size caused by the disruptive effect of cholesterol insertion. Thus, it is likely that the high cooperativity in pure lipids results in the large ultrasonic absorption observed in these materials.

It is believed that ultrasonic measurements have not previously been made on LUVs such as employed here. Thus, comparison of these ultrasonic measurements can only be made to studies of SUVs and MLVs. Both of these systems exhibit maxima in ultrasonic absorption as the temperature is raised through the point of transition. Measurements on MLVs agree well with the data in this investigation, both in peak height and width (Mitaku and Okano, 1981). The transition peaks

observed in SUVs, however, were much broader and about one half as great in maximum amplitude (Eggers and Funck, 1976; Harkness and White, 1979). Comparison is made between the various liposome types in Table 5.3. Such discrepancy of absorption by SUVs is expected, based on calorimetric studies. Disruptive sonication, used to prepare SUVs, has been shown to decrease the transition temperature and enthalpy as compared to that in MLVs. This is probably due to the increased mechanical tension present in SUVs, with their small radius of curvature. LUVs, on the other hand, have been found to be calorimetrically equivalent to MLVs (Melchior and Steim, 1976).

Since the heat release transition occurs at a lower temperature than the ultrasonically observed transition, somewhat different phenomena must be involved for each. It has been suggested (Marsh *et al.*, 1976) that the increased permeability results from a poor structural fit occurring between domains of the two different phases which coexist near the transition. If this is the case, then maximum permeability would be expected at the temperature of maximum domain perimeter. The maximum in ultrasonic absorption, based on the previous discussion, should occur at the midpoint of the transition, where equal numbers of lipid molecules are in each state. Marsh and co-workers conclude that these two conditions occur at the same temperature in SUVs but such is not the case in the LUVs of the present investigation.

Table 5.3

## Summary of liposome properties

Type	Diameter Range ( $\mu\text{m}$ )	$\alpha\lambda/c$ (ml/g) @ 4 MHz	$\Delta T_{1/2}$ ( $^{\circ}\text{C}$ ) [d]	Relaxation time at transition temperature (nsec)
MLV [a]	1 - 10	0.45	1.3	79
LUV [b]	0.1 - 0.4	0.56	1.7	76
SUV [a,c]	0.02 - 0.05	0.25	6.8	10

[a] R. White, personal communication

[b] This investigation

[c] Gamble and Schimmel, 1978

[d] Width of ultrasonic peak at half maximum



5.2.2 Lipid-Protein Bilayers. In an effort to understand the ultrasonic characteristics of protein-lipid interactions, the effect of incorporating the antibiotic gramicidin in liposome membranes has also been explored. The effect on absorption at 4 MHz is shown in Fig. 5.18. At gramicidin mole percentages of 5 and 10, the effect is similar to that of cholesterol. In fact, the general effects of this peptide on lipid transitions have been compared to those of cholesterol (Chapman et al., 1977; Papahadjopoulos et al., 1975). In both cases, a low concentration of cholesterol or gramicidin removes the pre-transition calorimetric endotherm characteristic of lecithins and decreases the transition enthalpy. Chapman et al. (1974) measured the enthalpy of transition in DPPC as a function of gramicidin content. Their results are reproduced in Fig. 5.19, which may be compared to the similar plot for cholesterol in Fig. 5.17.

Gramicidin is also known to act as an ionophore for certain small cations. This transport ability is due to the formation of a pore through the membrane, constructed by two gramicidin molecules. These two molecules stack with their formyl ends together to span the bilayer (Urry et al., 1971; Bamberg and Lauger, 1973). Since the combined length of two gramicidin molecules is 25-30 Å, the bilayer must be distorted in the region of a dimer for its operation as a pore. In the membrane, an equilibrium exists between the monomer and the stacked dimer of gramicidin. The time constant of this

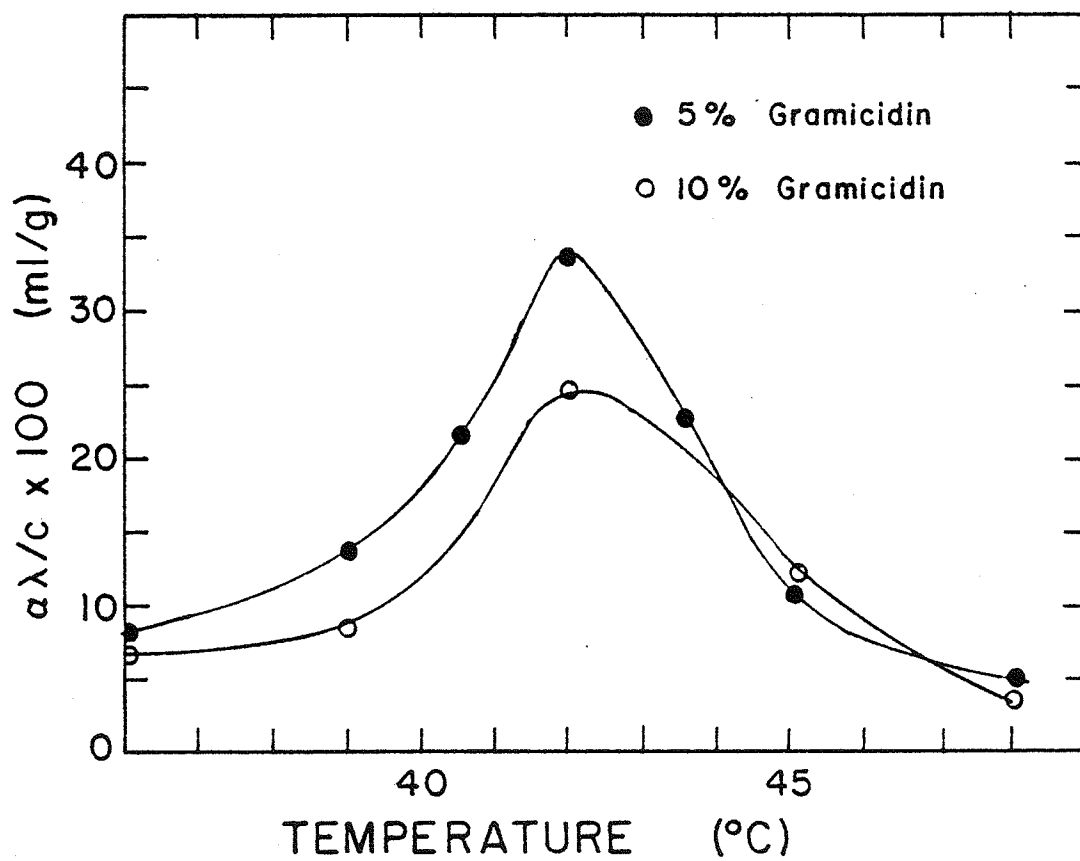


Figure 5.18 Effect of gramicidin on ultrasonic absorption in LUV suspensions.

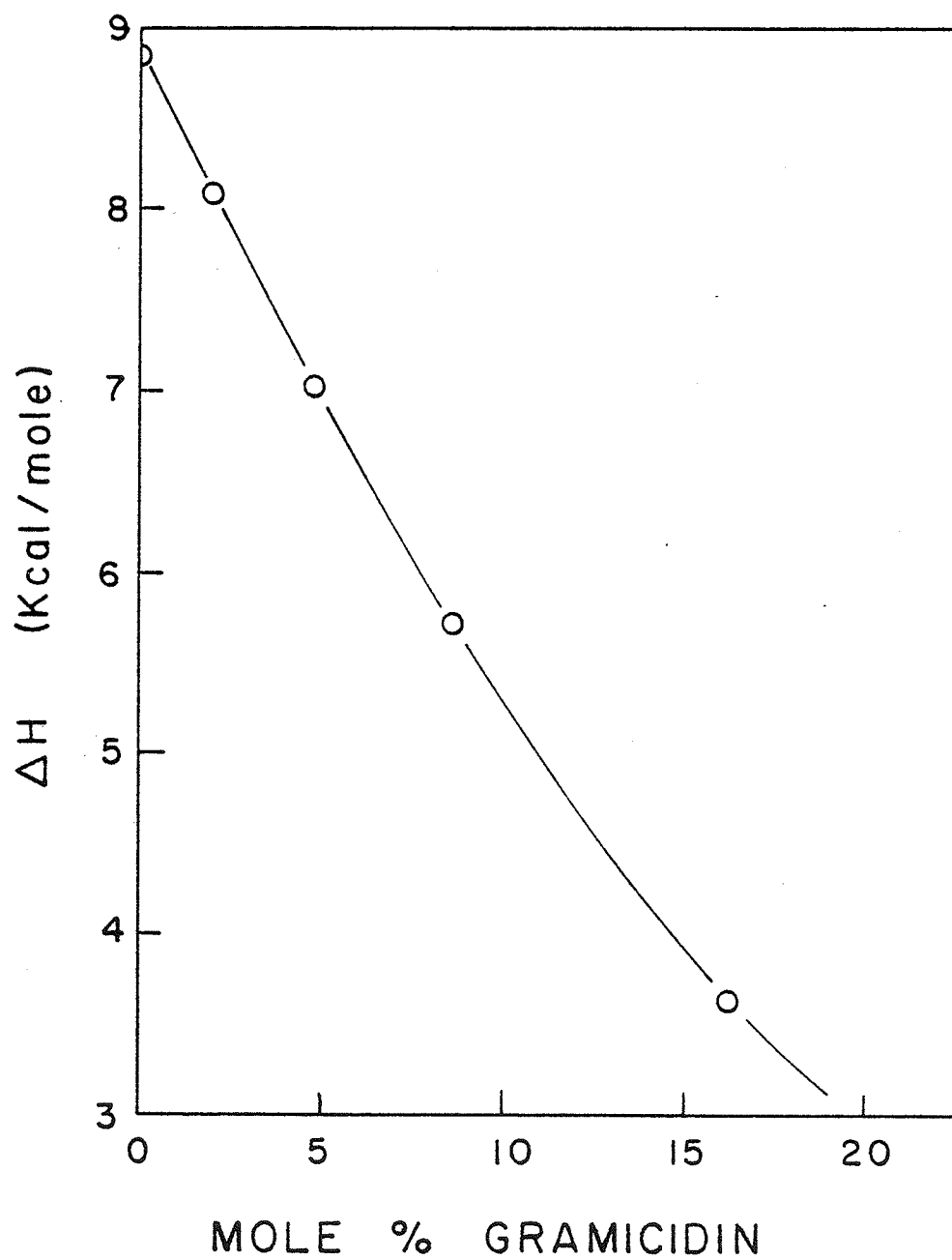


Figure 5.19 Effect of gramicidin on lipid transition enthalpy (after Chapman et al., 1974).

equilibrium is between 0.1 and 0.5 second (Bamberg and Lauger, 1973).

The explanation of the effect of gramicidin seen in Fig. 5.18 is essentially the same as that for cholesterol. When gramicidin is inserted into the bilayer, it is stabilized in this location by hydrophobic interactions with the hydrocarbon chains of the phospholipids. Through associations with adjacent lipids, gramicidin reduces the size of the cooperative unit undergoing the transition and prevents completely some lipids from exhibiting a transition (Papahadjopoulos *et al.*, 1975; Chapman *et al.*, 1977), thus reducing the magnitude of the ultrasonic absorption associated with the transition.

Phase transitions are also characterized by a discontinuity in the propagation velocity (Edmonds and Orr, 1966). This behavior has been observed in previous investigations of liposomes (Mitaku *et al.*, 1978; Mitaku and Okano, 1981). Since liposomes are used here in suspension, the extraction of velocity data is not as simple as in a pure system. The velocity changes which occur as a function of temperature are accompanied by changes in the velocity characteristic of the solvent, water. The velocity due to the liposomes, shown in Fig. 5.20, is the algebraic difference between the velocity in the suspension and that in the solvent at each temperature. Values are given for specimens of 5 and 10 percent gramicidin. As in the case of the absorption curves, the transition is sharper for 5 than for 10 percent.

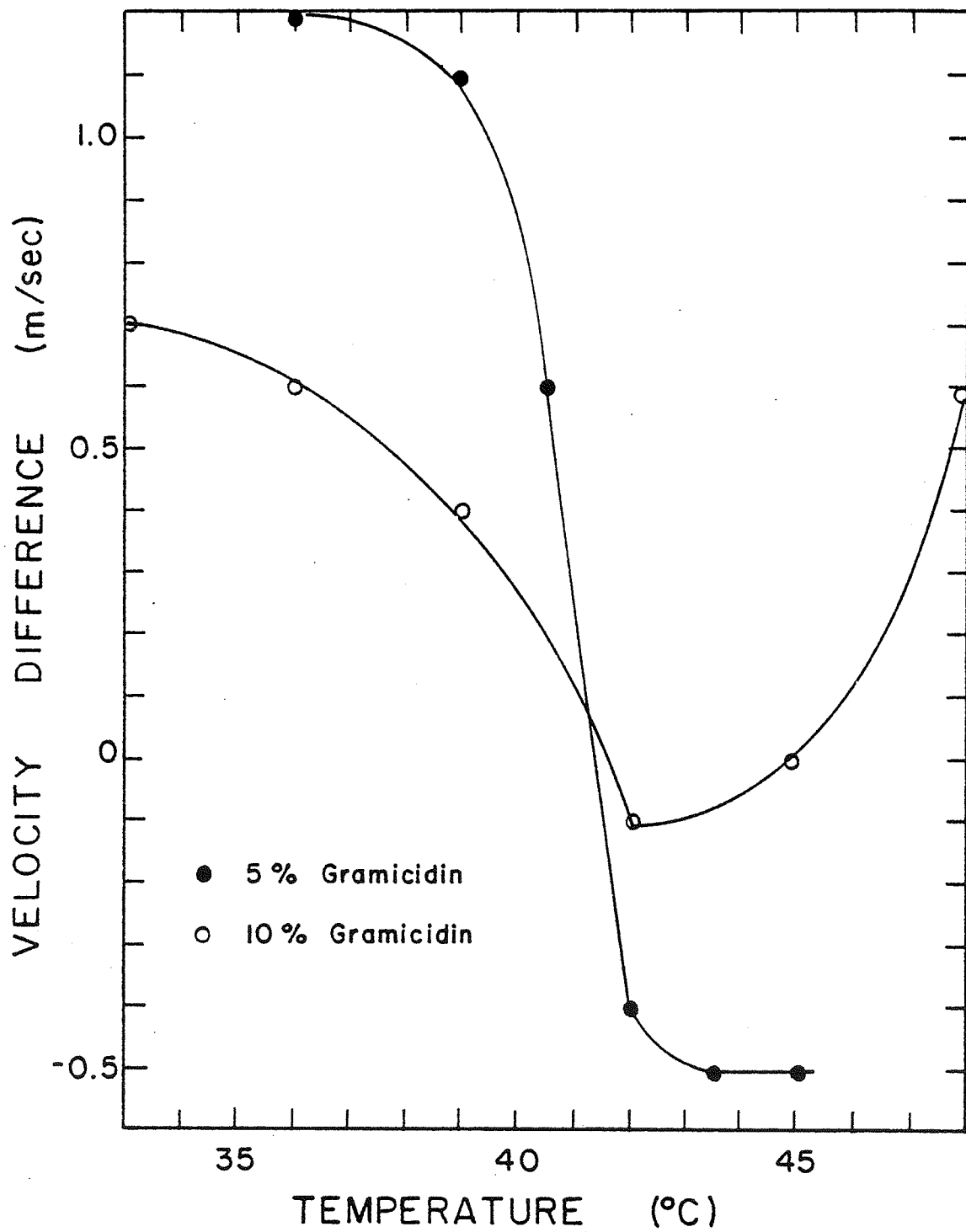


Figure 5.20 Ultrasonic velocity change due to LUVs.

This discontinuity can be understood by recalling eqn. 2.16 and noting that the velocity is inversely related to the adiabatic compressibility. During the transition in the liposomes, liquid-like and solid-like regions coexist and the large density fluctuations result in "gaps" causing an increase in the lateral compressibility of the bilayers (Gennis and Jonas, 1977).

5.2.3 Dependence on Frequency. Further understanding of ultrasonic interactions with liposomes may be gained by examining the frequency dependence of the absorption. The absorption per wavelength, as a function of frequency and temperature, is plotted in Figs. 5.21, 5.22, 5.23, and 5.24 for liposomes composed of lipid only, 20 percent cholesterol, 5 percent gramicidin, and 10 percent gramicidin, respectively. Generally, measurements were made in increments of 0.5 MHz over as much of the range from 1 to 7 MHz as possible. Away from the transition temperature, the curves are generally featureless with some indication of a slight increase in absorption with frequency. Near the transition, however, there is always a strong increase in absorption per wavelength values at the lower frequencies.

Since this tendency is indicative of some relaxation process, the frequency range of the measurements was extended for samples of pure lipids and 5 percent gramicidin at 42°C. The results are shown in Fig. 5.25. The trend of the data indicates the existence of relaxation processes occurring at rates amenable to study in this frequency range. These

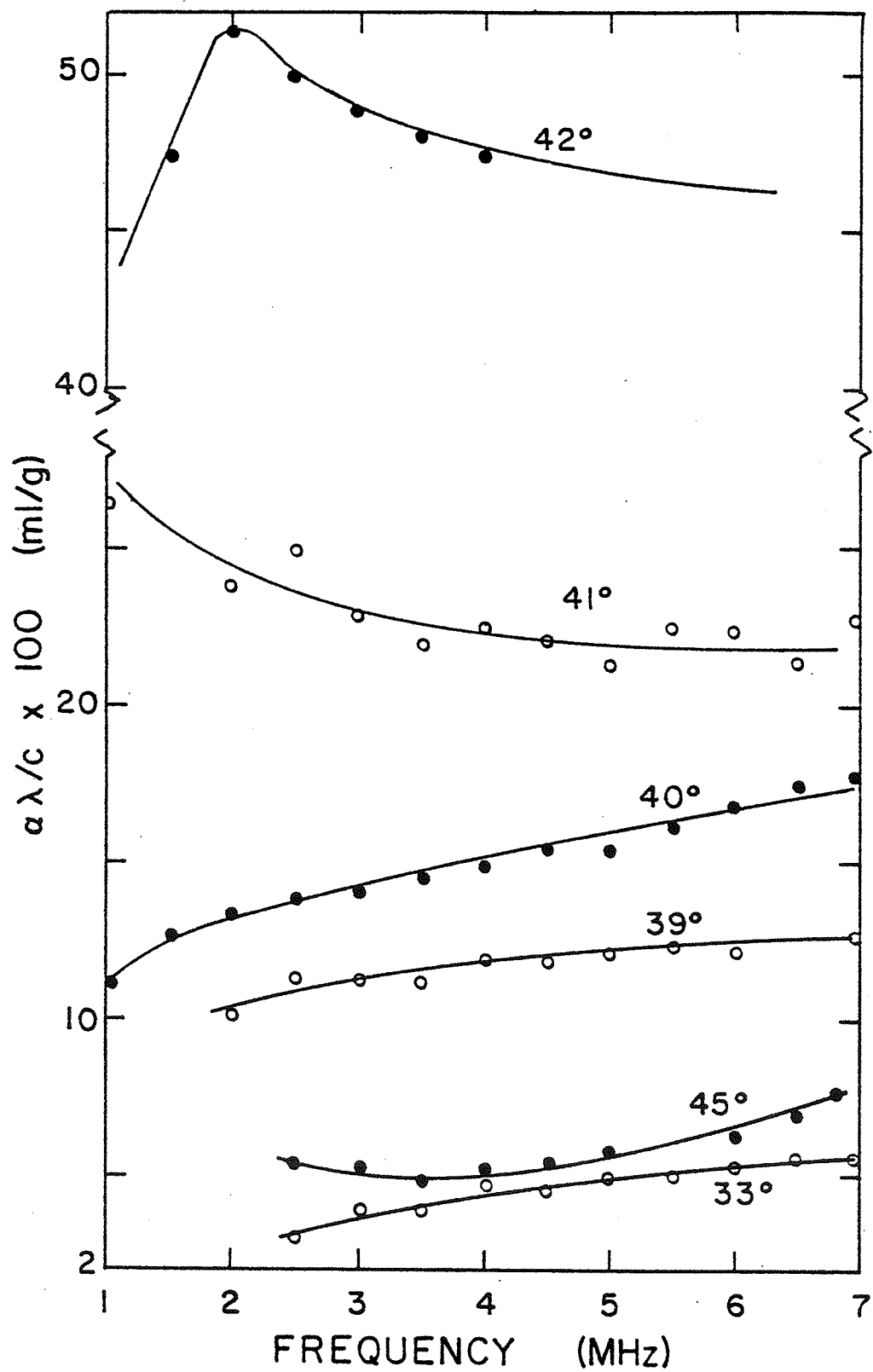


Figure 5.21 Dependence of absorption in pure lipid LUV suspensions on frequency. Temperature is indicated in degrees Celsius.

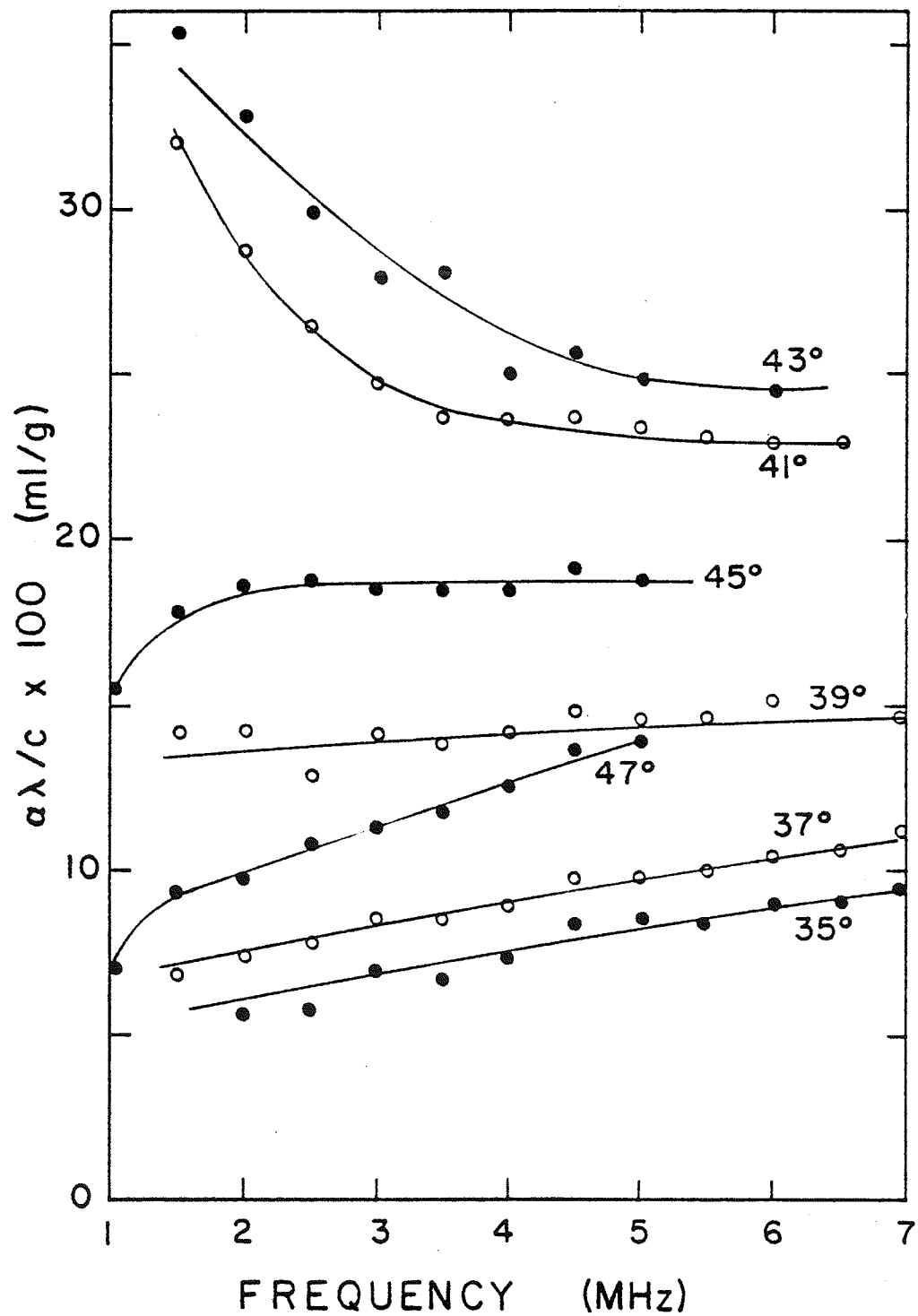


Figure 5.22 Dependence of absorption in 20 mole percent cholesterol LUV suspensions on frequency. Temperature is indicated in degrees Celsius.



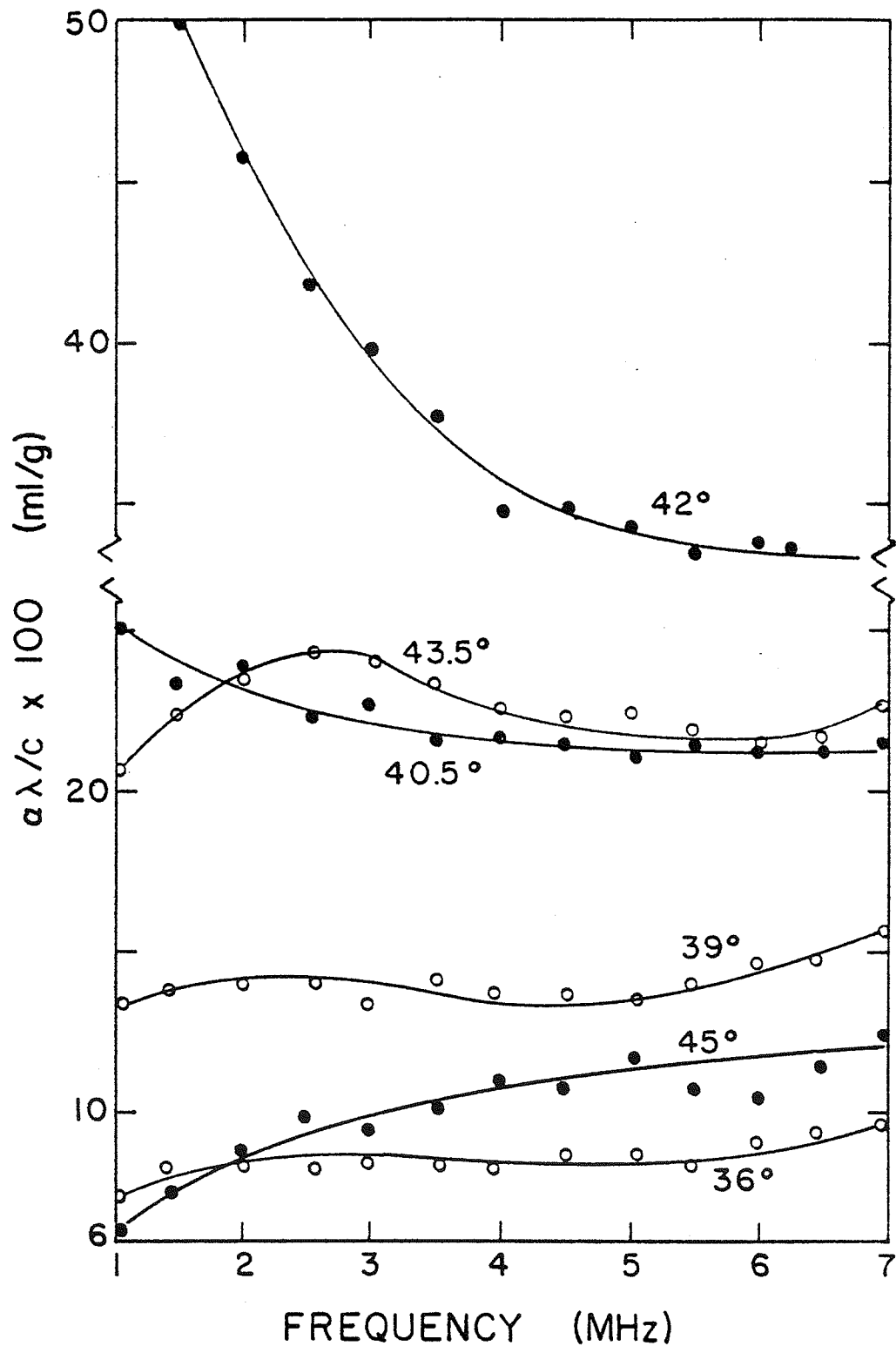


Figure 5.23 Dependence of absorption in 5 mole percent gramicidin LUV suspensions on frequency. Temperature is indicated in degrees Celsius.

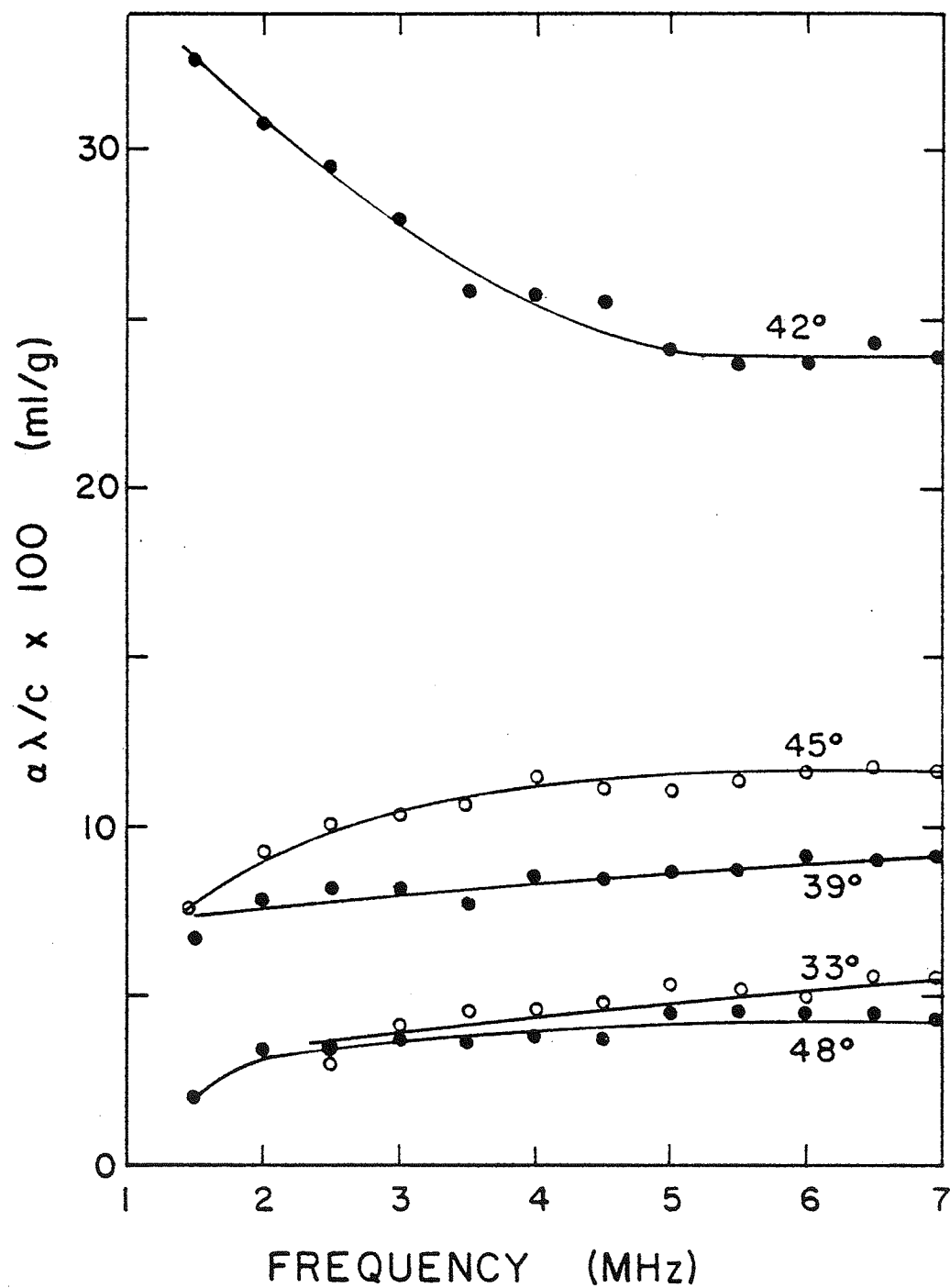


Figure 5.24 Dependence of absorption in 10 mole percent gramicidin LUV suspensions on frequency. Temperature is indicated in degrees Celsius.

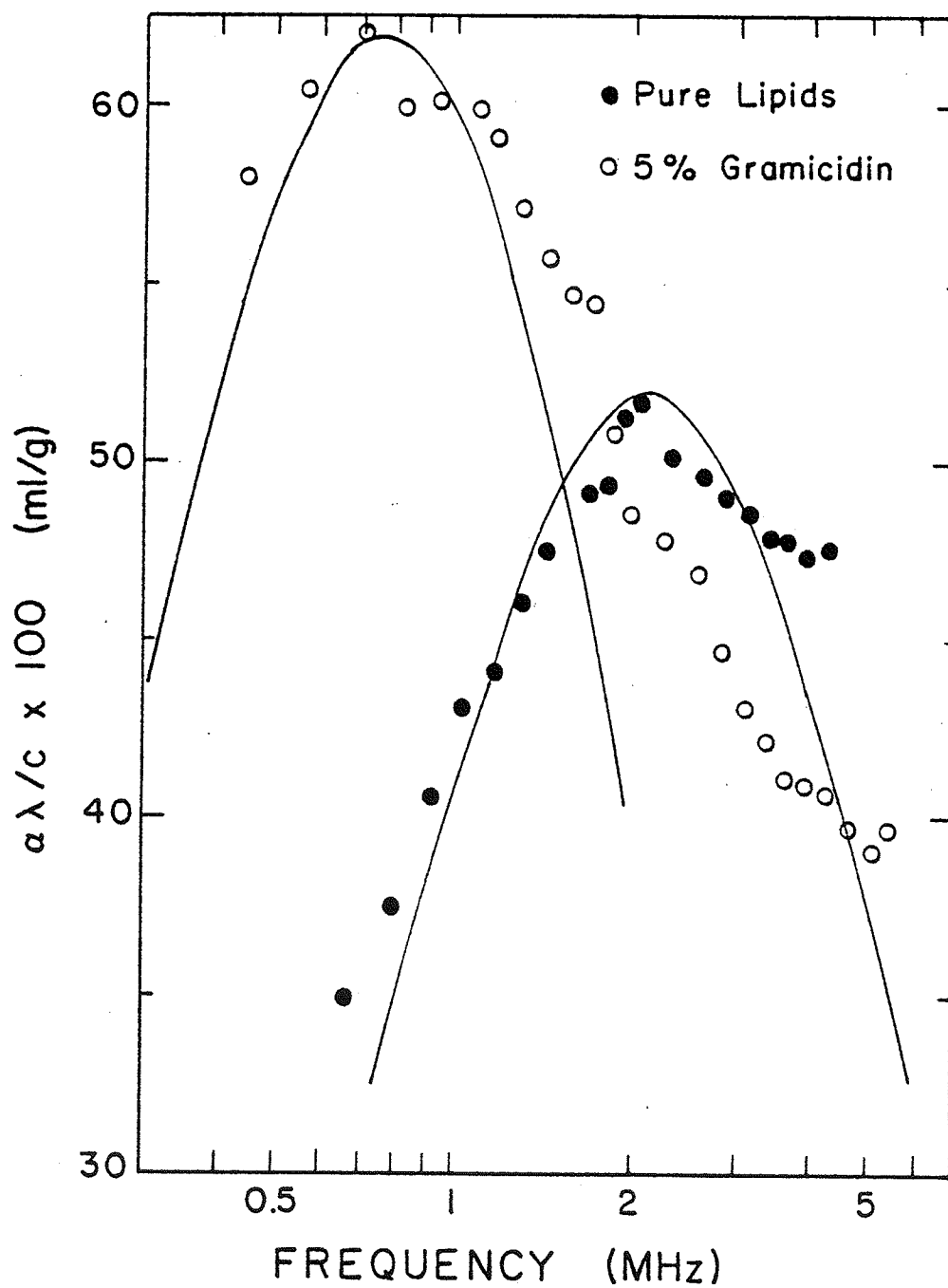


Figure 5.25 Dependence of absorption in pure lipid and 5 mole percent gramicidin LUV suspensions at 42°C.

relaxations, since they are not present at much lower and much higher temperatures, must be associated with processes occurring only at or near the transition. Shown also in Fig. 5.25, for sake of comparison, are solid curves calculated from the expression for a single relaxation process given by eqn. 2.53. The parameters used for calculation are  $\tau=212$  nsec ( $f_r=0.75$  MHz),  $A\tau=124$  ml/g for 5 mole percent gramicidin and  $\tau=76$  nsec ( $f_r=2.1$  MHz),  $A\tau=104$  ml/g for pure lipids, with  $B=0$  in both cases. Both sets of data are somewhat broader than expected assuming a single relaxation process. This implies that multiple relaxations are occurring, which broaden the frequency peak in absorption. However, since the empirical distribution is only slightly broader than a single relaxation, the multiple relaxations probably occur fairly close together in frequency.

What specific equilibrium is responsible for the observed relaxations? Several changes take place during the phase transition which could be involved. The transition involves a change in the planar bilayer packing of the lipids and the polar headgroup organization as well as a type of melting of the hydrocarbon chains. During the melting, the all-trans, low temperature structure of the fatty acyl chains is replaced by one with several gauche bonds; this is the primary event occurring at  $42^\circ\text{C}$  in DPPC (Melchior and Steim, 1976). The trans-gauche isomerization, as part of the equilibrium of eqn. 5.1, is most likely the specific cause of the observed relaxational absorption. A theory developed by Landau and

Khalatnikov (1954) and extended by Mitaku and Okano (1981) can be used to explain the temperature dependence of such a relaxation process. In this theory, the relaxation time increases sharply in the vicinity of the transition point, e.g., the rate of conversion between trans and gauche bonds in the lipids slows as the transition is approached. This effect, combined with a much greater probability of such conversions near the transition temperature, accounts for the frequency and temperature dependence of the specific absorption per wavelength. At temperatures well away from the transition, relaxation processes that do exist, would occur at frequencies too high for observation in the present system.

Curves similar to those in Fig. 5.21 were reported by Harkness and White (1979) for MLVs and SUVs. However, no relaxation was found by these investigators within the frequency range 0.4 MHz to 4 MHz. In another ultrasonic study of SUVs (Gamble and Schimmel, 1978) a relaxation centered at 16 MHz was postulated to model absorption at the transition temperature. Present results suggest a much greater similarity of the ultrasonic absorption of LUVs to MLVs than to SUVs. This is in agreement with calorimetric results. In addition, Nagle (1973) has listed results of NMR correlation times for the hydrocarbon chains in MLVs of  $10^{-6}$  to  $10^{-8}$  sec for the methylene groups nearest and furthest from the headgroup, respectively. Similar NMR measurements on SUVs indicate shorter correlation times. These properties of SUVs are probably due to their small radius, which leads to less

efficient hydrocarbon packing and greater fluidity. It is expected, therefore, that a structural relaxation process should occur at different rates in LUVs and SUVs. Based on the results of this investigation, the relaxation process in LUVs occurs about seven times slower than that in SUVs.

Finally, it is clear from Fig. 5.25 that gramicidin has a significant effect on the relaxation characteristics of LUVs at their transition temperature. The most noticeable change from the pure lipid specimen is a decrease in the average relaxation frequency from 2.1 MHz to 0.75 MHz. This represents a slowing of the reaction responsible for the relaxational absorption. Such an effect by gramicidin might be expected on the basis of its largely hydrophobic interaction with the bilayer (Papahadjopoulos *et al.*, 1975). Through these interactions the gramicidin will restrict the motion of hydrocarbon chains of nearby phospholipids. The result of this restriction is an increase in the relaxation time (decrease in the relaxation frequency) as observed by ultrasonic absorption.

5.2.4 Conclusions. Under certain conditions, e.g., near the phase transition, lipid membranes have been shown to possess a large specific absorption. Whether any conditions exist for natural membranes *in vivo* which would create similar absorption characteristics is still a matter of speculation. Most mammalian membranes are heterogeneous mixtures of lipids such that no sharp phase transition occurs. Factors other than temperature, however, may be able to affect the magnitude

of absorption by membranes. For example, Hammes and Roberts (1970) found that absorption by liposomes increased in the presence of divalent cations. Many solvent variables, which have yet to be investigated, may play an important role in absorption by natural membranes.

Measurements in this investigation have shown clearly that the presence of proteins in lipid membranes can have profound effects on their ultrasonic absorption. In the case of the peptide gramicidin, strong hydrophobic interactions take place which alter the behavior of adjacent phospholipids, and thus the frequency dependence of the ultrasonic absorption. This may be a result of the presence of a boundary lipid region believed to exist around many integral membrane proteins (Gennis and Jonas, 1977). This is an annulus of lipid adjacent to the protein which is less mobile than the bulk lipid, somewhat analogous to the water hydrating a soluble protein. It is likely, therefore, that the concentration of proteins within natural membranes, and the nature of their interaction with the membranes, play key roles in determining the resultant ultrasonic properties of the membrane.

CHAPTER 6  
CONCLUDING REMARKS

The studies here undertaken have shown the importance of the material surrounding proteinaceous molecules in determining their ultrasonic properties. In the case of soluble proteins, the water of hydration, which stabilizes native structures, also contributes to the ultrasonic absorption through a relaxation of its equilibrium with the bulk water. Such has been the suggestion in several previous studies on soluble proteins and it is largely verified in the present investigation. Absorption associated with this mechanism is characterized by relaxation frequencies in the range 0.5 to 5 MHz and possibly lower. Its magnitude varies with the molecular weight and surface area of the solute, probably through a cooperative effect between water molecules.

A complete explanation of ultrasonic absorption by soluble proteins should also include other mechanisms. In particular, processes associated with the folded, globular nature of some specimens in this investigation are indicated. While the proteins myoglobin and  $\alpha$ -lactalbumin had lower specific absorption than the other materials over most of the present frequency range, they exhibited other behavior indicating a significant relaxation process occurring at higher frequencies. Since this behavior was absent in the smaller and less folded peptides, it is most likely related to a process requiring globular structure. Intra-residue proton



exchange and internal side chain motion have been mentioned as candidates for this type of mechanism.

The picture of protein absorption mechanisms that emerges is a complex one in which proteinaceous molecules of all sizes may exhibit each of the above mechanisms to a greater or lesser extent. In small or predominantly unfolded peptides, the effects of perturbation of the hydrating water are dominant and this contribution to the ultrasonic absorption grows noticeably with the size of the molecule. In globular proteins, the hydration mechanism makes a smaller contribution, and internal mechanisms become relatively more important in determining the total absorption. These internal mechanisms probably occur with relaxation frequencies above 5 MHz.

Ultrasonic absorption by liposomes has been shown to be highly dependent upon their physical state. Absorption at the phase transition temperature of pure dipalmitoyl liposomes is characterized by a mean relaxation time of 76 nsec, which has been attributed to the equilibrium between trans and gauche isomers in the phospholipid hydrocarbon chains. The presence of gramicidin in the bilayer slows this isomerization, resulting in a mean relaxation time of 212 nsec. This result agrees with current understanding of gramicidin behavior in which strong hydrophobic interactions take place between the gramicidin exterior and nearby lipids. Much more work needs to be done in this area before a complete understanding of ultrasonic absorption by lipid membranes is obtained.

However, the results of this investigation suggest that the presence of proteins in membranes, and the nature of their interactions with those membranes, can greatly affect the ultrasonic absorption, and in particular, its frequency dependence.

Further work in these areas might profitably proceed in several directions. More low molecular weight peptides might be found for study or the frequency range of measurement extended at the low end. Both of these tasks present formidable difficulties. Obtaining small peptides is a challenge in itself and the products often have limited solubility. Extension of the frequency range below 0.2 MHz would, at present, entail the use of such large volumes as to render examination of most biochemicals impractical.

It may be possible to examine the hydration dependence of absorption in solutions of the enzyme chymotrypsin. Luscher *et al.* (1979) have shown that chemical modification at a single amino acid by tosylation can dramatically increase the amount of bound water around the chymotrypsin molecule. Comparison between the absorption by the native and modified enzymes may further elucidate the nature of absorption involving solute-solvent interactions.

Another possible subject of study is the protein cytochrome  $b_5$ . This molecule, which can be isolated from liver, has the attractive property of being both water soluble (as an octamer aggregate) and lipid soluble (i.e., it can be incorporated into liposome bilayers). Thus, it might be

possible to measure its ultrasonic properties in both environments.

Finally, there are many properties of liposomes which can be easily varied and could affect their ultrasonic behavior. One of the most interesting is liposome diameter. The LUVs in this investigation (approx. mean diameter, 0.2  $\mu\text{m}$ ) exhibit a transition point relaxation time of 76 nsec while SUVs (approx. diameter, 0.05  $\mu\text{m}$ ) show a corresponding relaxation time of 10 nsec. Dependence of the relaxation time on liposome diameter may contribute to an understanding of the way in which this diameter affects lipid packing and thereby lipid motion.

## REFERENCES

- Applegate, K., L.J.Slutsky and R.C.Parker (1968). "Kinetics of Proton-Transfer Reactions of Amino Acids and Simple Polypeptides," J.Am.Chem.Soc., 90: 6909-6913.
- Bamberg, E. and P.Lauger (1973). "Channel Formation Kinetics of Gramicidin A in Lipid Bilayer Membranes," J.Molec.Biol., 11: 177-194.
- Barksdale, A.K. and J.E.Stuehr (1972). "Kinetics of the Helix-Coil Transition in Aqueous Poly (L-glutamic acid)," J.Am.Chem.Soc., 94: 3334-3338.
- Blandamer, M.J., M.J.Foster, N.J.Hidden, and M.C.R.Symons (1968). "Ultrasonic Absorption Properties of Solutions, Part 6," Trans.Far.Soc., 64: 3247-3254.
- Botelho, L.H. and F.R.N.Gurd (1976). "pKs of Proteins," in Handbook of Biochemistry and Molecular Biology, 3rd ed. Vol. II, G.D.Fasman, ed., CRC Press, Cleveland.
- Burke, J.J., G.G.Hammes, and T.B.Lewis (1965). "Ultrasonic Attenuation Measurements in Poly-L-Glutamic Acid Solutions," J.Chem.Phys., 42: 3520-3525.
- Carstensen, E.L. (1979). "Absorption of Sound in Tissues," in Ultrasonic Tissue Characterization II, M.Linzer, ed., National Bureau of Standards, Spec. Publ. 525, U.S. Govt. Printing Office, Washington, D.C.
- Carstensen, E.L., K.Li, and H.P.Schwan (1953). "Determination of the Acoustic Properties of Blood and its Components," J.Acoust.Soc.Am., 25: 286-289.

- Carstensen, E.L. and H.P.Schwan (1959a). "Absorption of Sound Arising from the Presence of Intact Cells in Blood," J.Acoust.Soc.Am., 81: 185-189.
- Carstensen, E.L. and H.P.Schwan (1959b). "Acoustic Properties of Hemoglobin Solutions," J.Acoust.Soc.Am., 31: 305-311.
- Chapman, D., B.A.Cornell, A.W.Eliasz, and A.Perry (1977). "Interactions of Helical Polypeptide Segments which Span the Hydrocarbon Region of Lipid Bilayers. Studies of the Gramicidin A Lipid - Water System," J.Mol.Biol., 113: 517-538.
- Chapman, D., J.Urbina, and K.Keough (1974). "Biomembrane Phase Transitions. Studies of Lipid-Water Systems Using Differential Scanning Calorimetry," J.Biol.Chem., 249: 2512-2521.
- Cochran, M.A., P.B.Jones, A.M.North, and R.A.Pethrick (1972). "Ultrasonic Relaxation in Liquid C<sub>5</sub>-C<sub>10</sub>, C<sub>12</sub> and C<sub>14</sub> n-alkanes," J.Chem.Soc.Lond.Faraday Trans.II, 68: 1719-1728.
- Dandliker, W.B. and V.A.deSaussure (1971). "Stabilization of Macromolecules by Hydrophobic Bonding: Role of Water Structure and of Chaotropic Ions," in The Chemistry of Biosurfaces, Vol, 1, M.L.Hair, ed., Marcel Dekker, Inc., New York.
- Dayhoff, M. and R.Eck, eds. (1965). Atlas of Protein Sequence and Structure, National Biomedical Research Foundation, Silver Spring.

- Dunn, F. (1975). "Acoustic Properties of Biological Materials," in Fundamental and Applied Aspects of Nonionizing Radiation, S.M. Michaelson and M.W. Miller, eds., Plenum Publishing Corp., New York.
- Dunn, F., P.D. Edmonds, and W.J. Fry (1969). "Absorption and Dispersion of Ultrasound in Biological Media," in Biological Engineering, H.P. Schwan, ed., McGraw-Hill, Inc., New York.
- Dunn, F. and L.W. Kessler (1970). "Further Remarks on Ultrasonic Properties of Bovine Serum Albumin Solutions," J. Phys. Chem., 74: 2736.
- Dunn, F. and W.D. O'Brien, Jr. (1978). "Ultrasonic Absorption and Dispersion," in Ultrasound: Its Applications in Medicine and Biology, F.J. Fry, ed., Elsevier Scientific Publishing Co., Amsterdam.
- Edmonds, P.D., T.J. Bauld III, J.F. Dyro, and M. Hussey (1970). "Ultrasonic Absorption of Aqueous Hemoglobin Solutions," Biochim. Biophys. Acta, 200: 174-177.
- Edmonds, P.D. and D.A. Orr (1966). "Ultrasonic Absorption and Dispersion at Phase Transition in Liquid Crystalline Compounds," Mol. Cryst., 2: 135-166.
- Edmundson, A.B. (1963). "Cleavage of Sperm Whale Myoglobin with Cyanogen Bromide," Nature, 198: 354-357.
- Eggers, F. and Th. Funck (1973). "Ultrasonic Measurements with Milliliter Liquid Samples in the 0.5-100 MHz Range," Rev. Sci. Instrum., 44: 969-977.

- Eggers, F. and Th.Funck (1976). "Ultrasonic Relaxation Spectroscopy in Liquids," Naturwissenschaften, 63: 280-285.
- Eggers, F., Th.Funck, and K.H.Richmann (1976). "High Q Ultrasonic Liquid Resonators with Concave Transducers," Rev.Sci.Instr., 47: 361-367.
- Eggers, F., Th.Funck, and K.H.Richmann (1978). "Improved Ultrasonic Resonator Cell for Liquid Samples," Acustica, 40: 273-275.
- Eigen, M. and L.deMaeyer (1963). "Relaxation Methods," in Technique of Organic Chemistry, Vol. VIII pt.2, A.Weissberger, ed., Interscience, New York.
- Fry, W.J. and F.Dunn (1962). "Ultrasound: Analysis and Experimental Methods in Biological Research," in Physical Techniques in Biological Research vol. 4, Academic Press, New York.
- Galardy, R.E., M.P.Printz, and L.C.Craig (1971). "Tritium-Hydrogen Exchange of Bacitracin A. Evidence for an Intramolecular Hydrogen Bond," Biochemistry, 10: 2429-2436.
- Gamble, R.C. and P.R.Schimmel (1978). "Nanosecond Relaxation Processes of Phospholipid Bilayers in the Transition Zone," Proc.Nat.Acad.Sci., 75: 3011-3014.
- Gekko, N. and H.Noguchi (1971). "Physicochemical Studies of Oligodextran. I. Molecular Weight Dependence of Intrinsic Viscosity, Partial Specific Compressibility and Hydrated Water," Biopolymers, 10: 1513-1524.

- Gennis, R.B. and A.Jonas (1977). "Protein-Lipid Interactions," Ann.Rev.Biophys.Bioeng., 6: 195-238.
- Goss, S.A. and F.Dunn (1974). "Concentration Dependence of Ultrasonic Absorption in Aqueous Solutions of Bovine Serum Albumin," 1974 Ultrasonic Symposium Proceedings, IEEE Cat. # 74 CHO 896-1SU, pp. 65-68.
- Grimshaw, D., P.J.Heywood, and E.Wyn-Jones (1973). "Proton Transfer in some Amino-acids Studied by the Ultrasonic Method," J.Chem.Soc.Lon.Faraday Trans. II, 69: 756-762.
- Hammes, G.G., and T.B.Lewis (1966). "Ultrasonic Absorption in Aqueous Polyethylene Glycol Solutions," J.Phys.Chem., 70: 1610-1613.
- Hammes, G. and C.N.Pace (1968). "Ultrasonic Absorption Measurements in Aqueous Solutions of Glycine, Diglycine, and Triglycine," J.Phys.Chem., 72: 2227-2230.
- Hammes, G.G. and P.B.Roberts (1970). "Ultrasonic Attenuation Measurements in Phospholipid Dispersions," Biochim.Biophys.Acta, 203: 220-227.
- Hammes, G.G. and P.B.Roberts (1969). "Dynamics of the Helix-Coil Transition in Poly-L-Ornithine," J.Am.Chem.Soc., 91: 1812-1816.
- Hammes, G.G. and P.R.Schimmel (1967). "An Investigation of Water-Urea and Water-Urea-Polyethylene Glycol Interactions," J.Am.Chem.Soc., 89: 442-446.
- Hammes, G.G. and J.C.Swann (1967). "Influence of Denaturing Agents on Solvent Structure," Biochemistry, 6: 1591-1596.



- Hawley, S.A. and F.Dunn (1969). "Ultrasonic Absorption in Aqueous Solutions of Dextran," J.Chem.Phys., 50: 3523-3526.
- Hawley, S.A., L.W.Kessler, and F.Dunn (1965). "Ultrasonic Absorption in Aqueous Solutions of High-Molecular-Weight Polysaccharides," J.Acoust.Soc.Am., 38: 521-523.
- Harkness, J.E. and R.D.White (1979). "An Ultrasonic Study of the Thermotropic Transition of Dipalmitoyl Phosphatidylcholine," Biochim.Biophys.Acta, 552: 450-456.
- Hermans J.Jr. and D.Puett (1971). "Relative Effects of Primary and Tertiary Structure on Helix Formation in Myoglobin and  $\alpha$ -Lactalbumin," Biopolymers, 10: 895-914.
- Herzfield, K.F. and T.A.Litovitz (1959). Absorption and Dispersion of Ultrasonic Waves, Academic Press, New York.
- Hinz, H-J. and J.M.Sturtevant (1972). "Calorimetric Investigation of the Influence of Cholesterol on the Transition Properties of Bilayers Formed from Synthetic L- $\alpha$ -Lecithins in Aqueous Suspension," J.Biol.Chem., 247: 3697-3700.
- Hunter, F.E. and L.S.Schwartz (1967). "Gramicidins," in Antibiotics I, S.Gottlieb and P.Shaw eds., Springer-Verlag, New York.
- Hussey, M. and P.D.Edmonds (1971a). "Ultrasonic Examination of Proton-Transfer Reactions in Aqueous Solutions of Glycine," J.Acoust.Soc.Am., 49: 1309-1316.

- Hussey, M. and P.D.Edmonds (1971b). "Ultrasonic Examination of Proton-Transfer Reactions at the  $\alpha$ -Amino and Side-Chain groups of Arginine and Lysine in Aqueous Solution," J.Acoust.Soc.Am., 49: 1907-1908.
- Hussey, M. and P.D.Edmonds (1971c). "Proton-Transfer Reactions. A Mechanism for the Absorption of Ultrasound in Aqueous Solutions of Proteins," J.Phys.Chem., 75: 4012-4019.
- Ilgenfritz, G. (1977). "Theory and Simulation of Chemical Relaxation Spectra," in Chemical Relaxation in Molecular Biology, I.Pecht and R.Rigler, eds., Springer-Verlag, Berlin.
- Kato, S., T.Suzuki, H.Nomura, and Y.Miyahara (1980). "Ultrasonic Relaxation in Aqueous Solutions of Dextran," Macromolecules, 13: 889-892.
- Kanda, H., N.Olkubo, H.Nakajima, Y.Suzuki, M.Minato, T.Ihara, and Y.Wada (1976). "Ultrasonic Absorption in Aqueous Solution of Lysozyme," Biopolymers, 15: 785-795.
- Kessler, L.W. and F.Dunn (1969). "Ultrasonic Investigation of the Conformational Changes of Bovine Serum Albumin in Aqueous Solution," J.Phys.Chem., 73: 4256-4263.
- Kessler, L.W., W.D.O'Brien, Jr., and F.Dunn (1970). "Ultrasonic Absorption in Aqueous Solutions of Polyethylene Glycol," J.Phys.Chem., 74: 4096-4102.
- Kinsler, L.E. and A.R.Frey (1962). Fundamentals of Acoustics, 2nd ed., John Wiley & Sons, Inc., New York.

- Kremkau, F.W. (1972). "Macromolecular Interaction in the Absorption of Ultrasound in Biological Material," Ph.D. Thesis, University of Rochester, Rochester, New York.
- Labhardt, A. and G.Schwartz (1976). "A High Resolution and Low Volume Ultrasonic Resonator Method for Fast Chemical Relaxation Measurements," Ber.Bunsenges., 80: 83-92.
- Landau, L.D. and I.M.Khalatnikov (1954). "On the Anomalous Absorption of Sound Near a Second-Order Phase Transition Point," Dokl. Akad. Nauk SSSR 96: 469, in Collected Papers of L.D.Landau, D.ter Haar, ed., Gordon and Breach, Science Publishers, Inc., New York.
- Lang, J., D.Tondre, and R.Zana (1971). "Effect of Urea and Other Organic Substances on the Ultrasonic Absorption of Protein Solutions," J.Phys.Chem., 75: 374-379.
- Luscher, M., P.Schindler, M.Ruegg, and M.Rottenberg (1979). "Effect of Inhibitor Complex Formation on the Hydration Properties of  $\alpha$ -Chymotrypsin. Changes Induced in Protein Hydration by Tosylation of the Native Enzyme," Biopolymers, 18: 1775-1791.
- Marsh, D., A.Watts, and P.F.Knowles (1976). "Evidence for Phase Boundary Lipid. Permeability of Tempo-choline into Dimyristoylphosphatidylcholine Vesicles at the Phase Transition," Biochem., 15: 3570-3578.
- Marshall, R.C., W.C.Jones, Jr., R.A.Vigna and F.R.N.Gurd (1974). "Isolation of Cyanogen Bromide Cleavage Peptides from Myoglobins," Zeit.f.Naturfors., part C, 29: 90-91.

- Melchior, D.L. and J.M.Steim (1976). "Thermotropic Transitions in Biomembranes," Ann.Rev.Biophys.Bioeng., 5: 205-238.
- Mitaku, S., A.Ikegami, and A.Sakanishi (1978). "Ultrasonic Studies of Lipid Bilayer. Phase Transitions in Synthetic Phosphatidylcholine Liposomes," Biophys.Chem., 8: 295-304.
- Mitaku, S. and K.Okano (1981). "Ultrasonic Measurements of Two-Component Lipid Bilayer Suspensions," Biophys.Chem., 14: 147-158.
- Nagle, J.F. (1973). "Theory of Biomembrane Phase Transitions," J.Chem.Phys., 58: 252-264.
- Nomura, H., S.Kato, and Y.Miyahara (1975). "Ultrasonic Absorption in Polymer Solutions," Memoirs of the Faculty of Engineering, Nagoya University, 27: 72-125.
- O'Brien, W.D., Jr. and F.Dunn (1971). Ultrasonic Examination of the Hemoglobin Dissociation Process in Aqueous Solutions of Guanidine Hydrochloride," J.Acoust.Soc.Am., 50: 1213-1215.
- O'Brien, W.D., Jr. and F.Dunn (1972) "Ultrasonic Absorption Mechanisms in Aqueous Solutions of Bovine Hemoglobin," J.Phys.Chem., 76: 528-533.
- Papahadjopoulos, D., M.Moscarello, E.H.Eylar, and T.Isac (1975). "Effects of Proteins on Thermotropic Phase Transitions of Phospholipid Membranes," Biochim.Biophys.Acta, 401: 317-335.

- Pauly, H. and H.P.Schwan (1971). "Mechanism of Absorption of Ultrasound in Liver Tissue," J.Acoust.Soc.Am., 50: 692-699.
- Piercy, J.C. and S.V.Subrahmanyam (1965). "Ultrasonic Relaxation and Axial-Equatorial Isomerization in Methylcyclohexane. II," J.Chem.Phys., 42: 4011-4017.
- Richards, F.M. (1977). "Areas, Volumes, Packing and Protein Structure," Ann.Rev.Biophys.Bioeng., 6: 151-176.
- Robbins, F.M. and M.J.Kronman (1964). "A Simplified Method for Preparing  $\alpha$ -Lactalbumin and  $\beta$ -Lactoglobulin from Cow's Milk," Biocim.Biophys.Acta, 82: 186-188.
- Schneider, F., F.Muller-Landau, and A.Mayer (1969). "Acoustical Properties of Aqueous Solutions of Oxygenated and Deoxygenated Hemoglobin," Biopolymers, 8: 523-529.
- Slutsky, L.J., L.Madsen, and R.D.White (1977). "Acoustic Absorption in Solutions of Small Peptides and Proteins," 1977 Ultrasonics Symposium Proceedings, IEEE Cat. # 77CH1264-1SU.
- Slutsky, L.J., L.Madsen, R.K.White, and J.Harkness (1980). "Kinetics of the Exchange of Protons between Hydrogen Phosphate Ions and a Histidyl Residue," J.Phys.Chem., 84: 1325-1329.
- Sturm, J., J.Lang, and R.Zana (1972). "Ultrasonic Absorption of DNA Solutions: Influence of pH," Biopolymers, 10: 2639-2643.
- Teale, F.W.J. (1959). "Cleavage of the Haem-Protein Link by Acid Methyleneacetone," Biochim.Biophys.Acta, 35: 543.

- Temkin, S. (1981). Elements of Acoustics, John Wiley & Sons, New York.
- Urry, D.W., M.C. Goodall, J.D. Glickson, and D.F. Mayers (1971). "The Gramicidin A Transmembrane Channel: Characteristics of Head-to-Head Dimerized  $\pi$ (L,D) Helices," Proc. Nat. Acad. Sci., 68: 1907-1911.
- Wada, Y., H. Sasabe, and N. Tomono (1967). "Viscoelastic Relaxations in Solutions of Poly (glutamic Acid) and Gelatin at Ultrasonic Frequencies," Biopolymers, 5: 887-897.
- White, R.D. and L.J. Slutsky (1971). "Ionization Kinetics in Aqueous Solutions of Bovine Hemoglobin," J. Coll. Inter. Sci., 37: 727-730.
- White, R.D. and L.J. Slutsky (1972). "Ultrasonic Absorption and Relaxation Spectra in Aqueous Bovine Hemoglobin," Biopolymers, 11: 1973-1984.
- White, R.D., L.J. Slutsky, and S. Pattison (1971). "Kinetics of the Proton-Transfer Reactions of Serine and Threonine," J. Phys. Chem., 75: 161-163.
- Yamanaka, K., H. Nakajima, and Y. Wada (1978). "Kinetic Study of Denaturation and Subsequent Reduction of Disulfide Bonds of Lysozyme by the Rapid Ultrasonic Absorption Measurement," Biopolymers, 17: 2159-2169.
- Zana, R. (1972). "On the Detection of the Helix-Coil Transition of Polypeptides by Ultrasonic Absorption Measurements in the Megahertz Range," J. Am. Chem. Soc., 94: 3646-3647.

Zana, R. and J. Lang (1970). "Effect of pH on the Ultrasonic Absorption of Aqueous Solutions of Proteins," J. Phys. Chem., 74: 2734-2736.

Zana, R. and C. Tondre (1972a). "Ultrasonic Studies of Proton Transfers in Solutions of Poly(lysine) and Poly(ornithine). Implications for the Kinetics of the Helix-Coil Transition of Polypeptides and for the Ultrasonic Absorption of Proteins," J. Phys. Chem., 76: 1737-1743.

Zana, R. and C. Tondre (1972b). "Ultrasonic Studies in Relation to the Helix-Coil Transition in Aqueous Solutions of Poly-L-Lysine," Biopolymers, 10: 2635-2638.

## VITA

Philip Reed Strom-Jensen was born in Los Angeles, CA on March 19, 1955. After receiving a diploma with highest honors from South Hills High School, Covina, CA, he enrolled in the Physics program at Pomona College, Claremont, CA. Mr. Strom-Jensen graduated, cum laude, from Pomona in 1977 and later that year began graduate study in Biophysics at the University of Illinois at Urbana-Champaign. During this period he held Teaching Assistantships in the Department of Physiology and Biophysics, Research Assistantships in the Department of Electrical Engineering, and a Radiation Oncology Traineeship from the National Institutes of Health. Mr. Strom-Jensen is a member of Sigma Xi, Phi Kappa Phi, and the American Association for the Advancement of Science.